

# **Dimeric metallacycles and coordination polymers: Zn(II), Cd(II) and Hg(II) complexes of two positional isomers of a flexible N,O-hybrid bispyrazole derived ligand.**

Joan Soldevila-Sanmartín<sup>a</sup>, Miguel Guerrero <sup>a</sup>, Duane Choquesillo-Lazarte <sup>b</sup>, José Giner Planas <sup>c</sup>, Josefina Pons<sup>a,\*</sup>.

<sup>a</sup> *Departament de Química, Universitat Autònoma de Barcelona, 08913-Bellaterra, Barcelona, Spain.*

<sup>b</sup> *Laboratorio de Estudios Cristalógraficos, IACT (CSIC-Universidad de Granada), Avda. de las Palmeras 4, Armilla, 18100 Granada, Spain.*

<sup>c</sup> *Institut de Ciència de Materials de Barcelona (ICMAB-CSIC), Campus UAB, 08913-Bellaterra, Barcelona, Spain.*

\* Corresponding Author

*E-mail address:* [josefina.pons@uab.cat](mailto:josefina.pons@uab.cat) (J. Pons)

## Abstract

Reaction of  $MCl_2$  ( $M = Zn(II)$ ,  $Cd(II)$  and  $Hg(II)$ ) with two flexible *N,O*-hybrid arene-linked, bispyrazole derivative ligands (1,2-bis([4-(3,5-dimethyl-1*H*-pyrazol-1-yl)-2-oxabutyl]benzene (**L1**) and 1,4-bis([4-(3,5-dimethyl-1*H*-pyrazol-1-yl)-2-oxabutyl]benzene (**L2**)) in EtOH yields six new compounds. All compounds have been characterized by analytical and spectroscopic techniques. Their crystal structures have been elucidated by single-crystal X-ray diffraction. Compounds containing **L1** are isostructural dimeric metallacycles of general formula  $[M(L1)Cl_2]_2$  ( $M = Zn(II)$  (**1**),  $Cd(II)$  (**2**) and  $Hg(II)$  (**3**)), **L1** bearing a *NN'*-bridged coordination mode. Those containing **L2**, are coordination polymers of general formula  $\{[M(L2)Cl_2] \cdot 1/2 \text{Solvent}\}_n$  ( $M = Zn(II)$ , Solvent =  $H_2O$  (**4**);  $M = Cd(II)$  (**5**) or  $Hg(II)$  (**6**), Solvent = EtOH), **L2** showing two different coordination modes depending on the metal: *NN'*-bridged in **4** and *NON'*-chelated and bridged in isostructural **5** and **6**. Their molecular and extended structures are discussed, with a special focus on the coordination modes and conformations of **L1** and **L2**. Finally, their photoluminescence properties have been analyzed.

**Keywords:** Coordination Polymers /  $d^{10}$  Metals / Metallacycles / *N,O*-ligands / Pyrazole ligands

## 1. Introduction

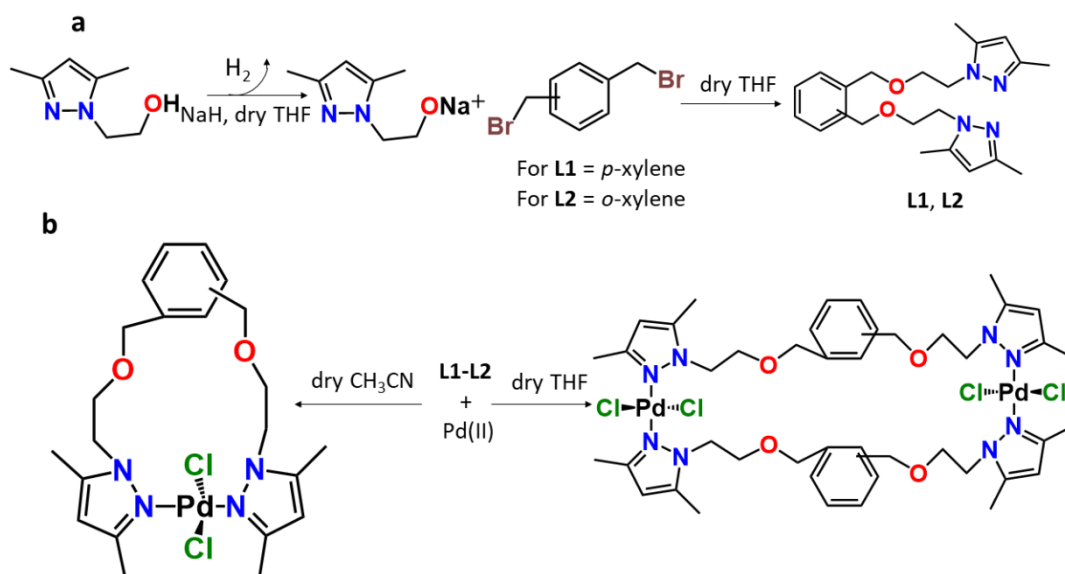
Since the late eighties, the discovery of Metal-Organic Frameworks (MOFs) and porous coordination polymers (PCPs) opened the gate for a whole new field of research in coordination chemistry, and arguably one of the most researched topics of today. Since these days, interest in this field has skyrocketed, leading to the systematization of the principles of ligand design and molecular architecture [1-4]. In the first stages, the research was focused on the synthesis of said materials using rigid organic ligands and their properties in gas absorption and storage. The field evolved towards the search of different applications [5], due to the infinite customization properties that the combination of inorganic (nodes) and organic moieties (linkers) allow. Thus, ligand design became the driving force of many coordination chemists' research. As of today, no longer rigid linkers are considered of interest, but also flexible ones which could lead to stimuli-responsive materials [5-7].

In recent times, *N*-donor ligands appear as great candidates for the synthesis of functional coordination polymers due to their greater resistance to hydrolysis. Among them, azoles appear as better candidates over pyridines due to their stronger and directional *N*-metal bond. Thus, ligand design of new linkers containing azoles is thriving [8,9]. Among them, pyrazole derivative ligands are of great interest, as they can be easily functionalized *via* modification of the parent pyrazole and possess interesting applications in the fields of catalysis [10-12], sensing [13], medicine [14], magnetism [15], and optics [16].

Conformational freedom of the ligand does also have a great impact on the final topology of the coordination polymers. As demonstrated by a plethora of different works, the presence of a flexible moiety, or weak spot, between the *N*-pyrazole coordinating sites greatly increases the possibility of obtaining interesting networks, promotes different types of self-assembly and even enhances the functionality of the new compounds. This has spurred the synthesis of new polypyrazole ligands in the last decades [17-23]. Besides, the inclusion of new functional groups bearing heteroatoms in di-, tri- or tetrapyrazole ligands could also further increase the variability of coordination modes and promote fascinating interactions such as hemilability or selective coordination [24-26].

Previously, our group has synthesized and studied the coordination behavior of several *N,X*-hybrid bispyrazole ligands ( $X = N, O$  and  $S$ ) containing functional groups

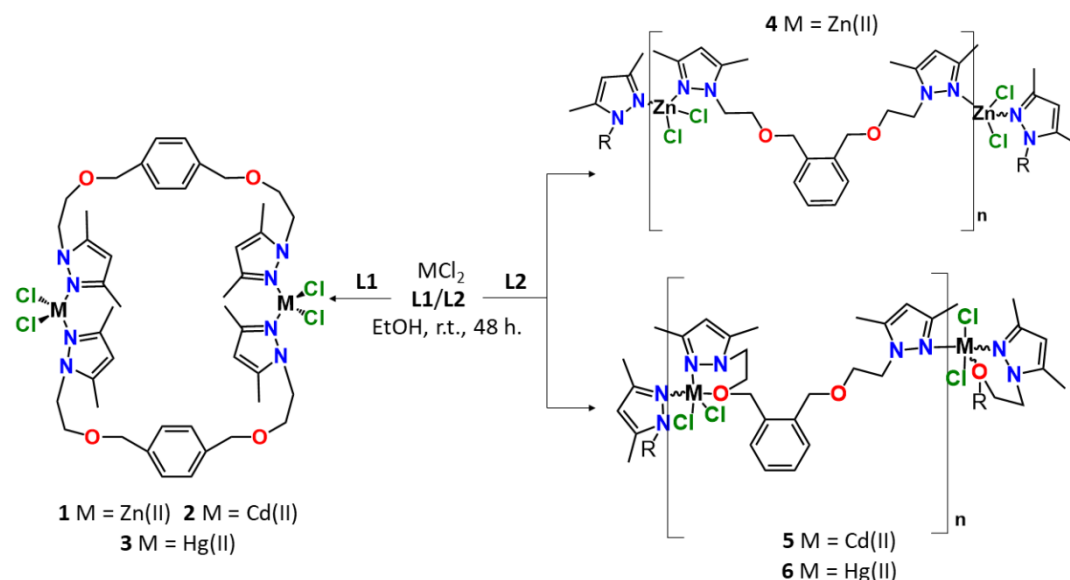
such as amines [27,28], thioethers [29,30], or sulfoxides/sulfones [31]. Furthermore, several bispyrazole ligands bearing ether functional groups have been previously synthesized [32] and their reactivity against different metal centers studied. For instance, an extensive research on the reactivity of the *N,O*-hybrid bispyrazole, diether ligand 1,8-bis(3,5-dimethyl-1*H*-pyrazol-1-yl)-3,6-dioxaoctane (bpdo) against different Zn(II), Cd(II), Hg(II), Pd(II), Pt(II) and Ni(II) salts was conducted, showing that the use of different metal centers resulted in coordination compounds with a wide diversity of nuclearity, coordination geometries and modes [33,34]. Moreover, the reactivity of the title compounds 1,2-bis([4-(3,5-dimethyl-1*H*-pyrazol-1-yl)-2-oxabutyl]benzene (**L1**) and 1,4-bis([4-(3,5-dimethyl-1*H*-pyrazol-1-yl)-2-oxabutyl]benzene (**L2**) against Pd(II) was carried out (Scheme 1) [35]. In the resulting Pd(II) coordination compounds only *syn* conformations were observed, despite the fact that bispyrazolyl ligands can adopt *syn* or *anti* conformations. In the light of these results, new metal centers which allow different coordination geometries such as Zn(II), Cd(II) and Hg(II) were chosen to study their reactivity against **L1** and **L2**.



**Scheme 1.** a. Schematic representation of the synthesis of **L1** and **L2**. b. Previously Synthesized compounds containing **L1** and **L2**.

In this contribution, we present the synthesis, characterization and X-ray crystal structures of six new compounds: three of general formula  $[M(\mathbf{L1})Cl_2]_2$  ( $M = \text{Zn(II)}$  (**1**),  $\text{Cd(II)}$  (**2**) and  $\text{Hg(II)}$  (**3**)), and three of general formula  $\{[M(\mathbf{L2})Cl_2] \cdot 1/2\text{Solvent}\}_n$  ( $M = \text{Zn(II)}$ , Solvent =  $\text{H}_2\text{O}$  (**4**);  $M = \text{Cd(II)}$  (**5**) or  $\text{Hg(II)}$  (**6**), Solvent =  $\text{EtOH}$ ) (Scheme 2).

The molecular and supramolecular structures of these compounds are discussed, with a special focus on the different coordination modes and conformations of **L1** and **L2**. Finally, their behavior in solution has been studied via NMR and photoluminescence measurements.



**Scheme 2.** Synthetic reactions carried out in this work. Compounds are shown with their numbering scheme. Compounds **4-6** occluded solvents have been removed for clarity.

## 2. Results and Discussion

### 2.1 Synthesis and characterization of the complexes

The reaction of **L1** and **L2** with  $MCl_2$  (M = Zn(II), Cd(II) and Hg(II)) in absolute ethanol (EtOH) in a 1M/1L ratio yields compounds **1-6**. Phase purity of the samples has been confirmed by powder X-ray diffraction (PXRD) (S.I.: Figures S1-S6). All compounds have been characterized by elemental analysis (EA), FTIR-ATR,  $^1H$ ,  $^{13}C\{^1H\}$ , HSQC, DOSY NMR and UV-Vis spectroscopies. This data is provided in the experimental section and in the Supporting Information (S.I.). Finally, their photoluminescence properties are studied.

For compounds **1-6** it has been possible to obtain crystals suitable for single-crystal X-ray diffraction. In them, **L1** and **L2** show extremely different coordination behavior. Compounds **1-3** are dimers with general formula  $[M(L1)Cl_2]_2$  (M= Zn(II) (**1**), Cd(II) (**2**) and Hg(II) (**3**)). These compounds are isostructural, showing a  $M_2L_2$  metallacyclic ring motif of thirty-four members. Compounds **4-6** are polymers with

general formula  $\{[M(\mathbf{L2})Cl_2] \cdot 1/2\text{Solvent}\}_n$  ( $M = \text{Zn(II)}$ , Solvent =  $\text{H}_2\text{O}$  (**4**);  $M = \text{Cd(II)}$  (**5**) or  $\text{Hg(II)}$  (**6**), Solvent =  $\text{EtOH}$ ). Despite compounds **4-6** sharing a similar chemical composition, the metal center in **4** is tetracoordinate, whereas in isostructural compounds **5** and **6** is pentacoordinate due the coordination of an oxygen atom from **L2**. Furthermore, in **4** the presence of occluded  $\text{H}_2\text{O}$  molecules can be seen, while in **5** and **6** the occluded solvent is  $\text{EtOH}$  (Scheme 2). For all of them, EA agree with the elucidated crystal structures.

The FTIR-ATR spectra of the six compounds in the range of  $4000\text{-}500\text{ cm}^{-1}$  confirms the coordination of the organic ligand to the metal center. The most characteristic bands of the IR spectra are those attributable to the  $[\nu(\text{C}=\text{C})_{\text{ar}}/\nu(\text{C}=\text{N})_{\text{ar}}]$  ( $1554\text{-}1547\text{ cm}^{-1}$ ) and  $[\delta(\text{C}=\text{C})_{\text{ar}}/\delta(\text{C}=\text{N})_{\text{ar}}]$  ( $1424\text{-}1420\text{ cm}^{-1}$ ) of the pyrazolyl group [36]. Other characteristic bands are attributable to the  $[\nu(\text{C-O-C})]$  ( $1105\text{-}1099\text{ cm}^{-1}$ ) of the ether groups [36]. Moreover, for compounds **4-6**, the presence of solvent molecules allows further identification of some bands. Compound **4** shows a broad band between  $3600\text{-}3200\text{ cm}^{-1}$  attributable to  $[\nu(\text{O-H})]$  of  $\text{H}_2\text{O}$  molecules. For compounds **5** and **6**, bands at  $3496\text{ cm}^{-1}$  and  $3515\text{ cm}^{-1}$  are attributed to  $[\nu(\text{O-H})]$  of  $\text{EtOH}$  molecules (S.I.: Figures S7-S12 and experimental section).

## 2.2 Crystal and Extended Structures of compounds 1-3.

For isostructural compounds **1-3**, two **L1** molecules act as a  $NN'$ -bridged ligand in a *syn* configuration, coordinating to two metal centers forming a closed-loop. Hence, a  $\text{M}_2\text{L}_2$  type metallacyclic motif of thirty-four members is obtained (Figure 1 and S.I: Figure 13).

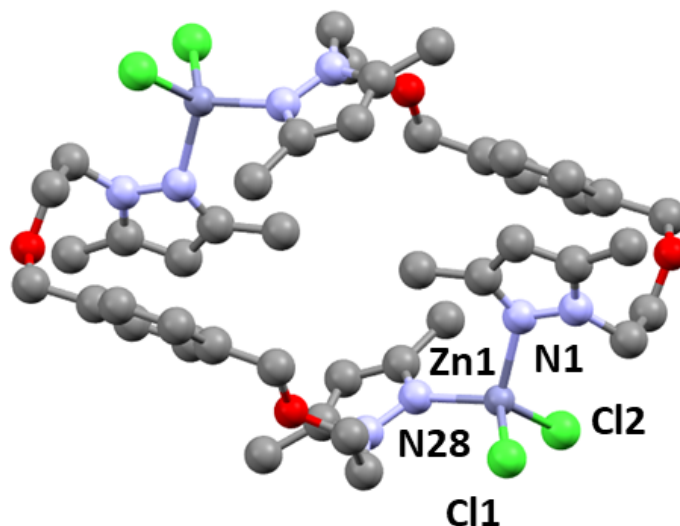


**Figure 1.** Compound **1** showing all its non-hydrogen atoms and their corresponding numbering scheme.

The metal centers have the same distorted tetrahedral ( $\tau_4 = 0.88$  to  $0.92$  [37])  $[M(N_{Pz})_2Cl_2]$  core (M = Zn(II) (**1**), Cd(II) (**2**) Hg(II) (**3**)), with angles ranging from  $98.52(15)^\circ$  to  $122.45(6)^\circ$ . A search in the CCDC database [38] reveals that this core is present in up to sixty-one reported crystal structures containing Zn(II), four containing Hg(II) and none containing Cd(II). Of them, only one is a Zn(II) metallacycle [20]. Similar macrocyclic architectures are reported with monopyrazolyl [39] and tetrapyrzolyl derivative ligands [40,41]. Remarkably, coordination compounds of the bis(dipyrzolyl) analogue of **L1** containing Ag(I) are mononuclear metallacycles [42], in stark contrast to the dimeric metallacycles reported in this work. Selected bond lengths and bond angles are reported on Table 1. All these values agree with similar compounds reported in the literature [20,33,34,43].

**Table 1.** Selected bond lengths and angles for compounds **1-3**

<b>1</b>		<b>2</b>		<b>3</b>	
Bond lengths (Å)					
Zn(1)-Cl(1)	2.2485(7)	Cd(1)-Cl(1)	2.4277(12)	Hg(1)-Cl(1)	2.4216(16)
Zn(1)-Cl(2)	2.2563(7)	Cd(1)-Cl(2)	2.4236(12)	Hg(1)-Cl(2)	2.4403(16)
Zn(1)-N(1)	2.062(2)	Cd(1)-N(1)	2.258(4)	Hg(1)-N(1)	2.270(6)
Zn(1)-N(28)#1	2.035(2)	Cd(1)-N(3)#1	2.234(4)	Hg(1)-N(3)#1	2.331(6)
Zn(1)⋯Zn(1)	9.3697(6)	Cd(1)⋯Cd(1)	9.5206(7)	Hg(1)⋯Hg(1)	9.6636(5)
Bond angles (°)					
Cl(1)-Zn(1)-Cl(2)	113.09(2)	Cl(1)-Cd(1)-Cl(2)	116.75(4)	Cl(1)-Hg(1)-Cl(2)	122.45(6)
N(28)#1-Zn(1)-Cl(1)	115.23(7)	N(1)-Cd(1)-Cl(1)	112.48(11)	N(1)-Hg(1)-Cl(1)	114.16(16)
N(28)#1-Zn(1)-Cl(2)	104.59(6)	N(1)-Cd(1)-Cl(2)	100.31(11)	N(1)-Hg(1)-Cl(2)	102.93(15)
N(1)-Zn(1)-Cl(2)	114.57(6)	N(1)-Cd(1)-N(3)#1	109.88(15)	N(1)-Hg(1)-N(3)#1	107.8(2)
N(1)-Zn(1)-Cl(1)	100.45(6)	N(3)#1-Cd(1)-Cl(1)	104.50(10)	N(3)#1-Hg(1)-Cl(1)	98.52(15)
N(1)-Zn(1)-N(28)#1	109.23(8)	N(3)#1-Cd(1)-Cl(2)	113.04(12)	N(3)#1-Hg(1)-Cl(2)	110.47(15)
#1: -x+1, -y+1, -z+1					

The metallacyclic ring can be defined by its intramolecular M⋯M distance, the distance between two methyl groups and the distance between the centroids of pyrazolyl rings (S.I.: Figure S14). Compounds **1-3** show intramolecular C-H⋯ $\pi$  interactions between the methyl groups and the phenyl rings (Table 2). The angle between the mean planes of **L1** pyrazolyl rings in the same ligand is 89.13° (**1**), 87.78° (**2**) and 87.11° (**3**), whereas phenyl rings are parallel to each other in all three compounds. This metallacycle highly reminds of the previously reported [Pd(**L2**)Cl<sub>2</sub>]<sub>2</sub> compound [35]. However, in this compound the ring is not folded, which allows for the above-mentioned compound to be nanoporous.

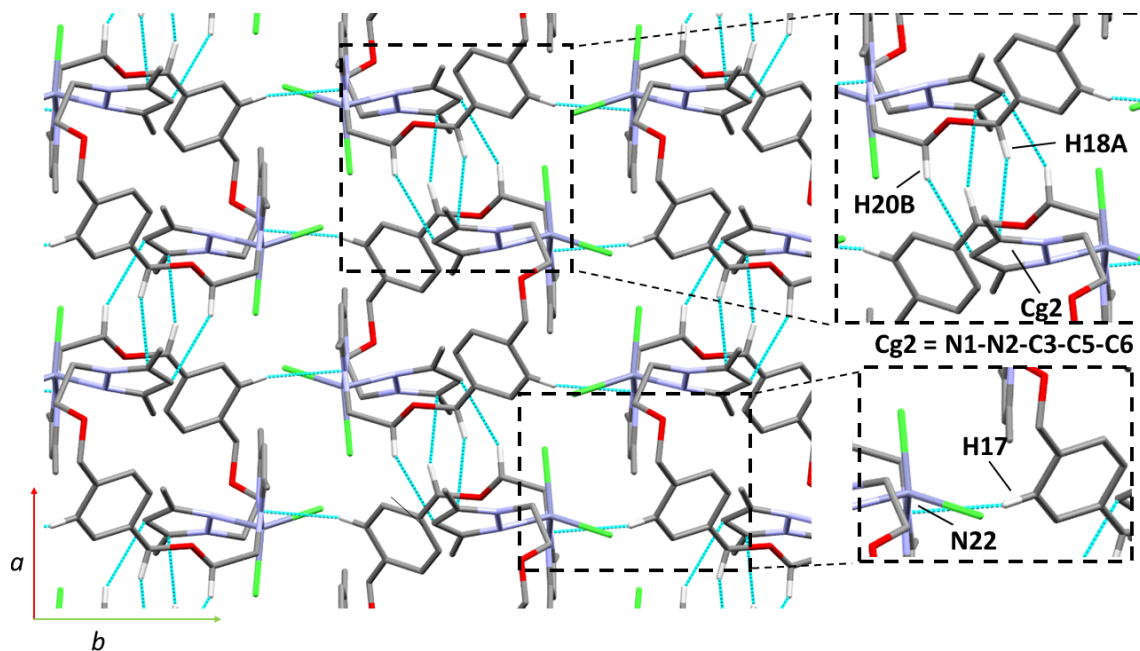
As isostructural compounds, the extended structures of **1-3** are alike. They could be described as a close-packing of M<sub>2</sub>L<sub>2</sub> rings, where each ring is connected to six other rings *via* hydrogen interactions, forming a three-dimensional lattice. This net is sustained thanks to interactions between the pyrazolyl rings and hydrogens from the phenyl rings as well as between hydrogens from the ether chains and pyrazolyl moieties. Furthermore, interactions involving chlorine atoms and pyrazolyl moieties are also key in sustaining the supramolecular network (Figure 2 and S.I.: Figure S15). Relevant interactions for all compounds are summarized on Table 2.



**Table 2.** Selected intra- and intermolecular interactions for compounds **1-3**

	D-H...A (Å)	D-H (Å)	H-D...A (Å)	>D-H...A (°)
<b>1</b>				
<i>Intramolecular</i>				
C27-H27C...Cg1	3.180	0.980	3.885	130.21
<i>Intermolecular</i>				
C17-H17...N22	2.691	0.950	3.519	145.91
C18-H18A...Cg2	2.868	0.990	3.839	167.08
C20-H20B...Cg2	3.532	0.990	4.297	135.71
C5-H5...C12	2.961	0.950	3.861	158.72
C27-H27B...C12	3.048	0.980	4.011	167.61
<b>2</b>				
<i>Intramolecular</i>				
C22-H22A...Cg3	3.354	0.979	4.039	128.71
<i>Intermolecular</i>				
C3-H3...C11	2.809	0.950	3.716	159.91
C5-H5A...Cg3	2.797	0.979	3.662	147.56
C14-H14...N4	2.717	0.949	3.549	146.72
C15-H15B...Cg4	2.865	0.991	3.824	163.28
C16-H16A...Cg4	3.430	0.990	4.205	136.64
C22-H22B...C12	2.849	0.980	3.823	172.48
<b>3</b>				
<i>Intramolecular</i>				
C5-H5B...Cg5	3.338	0.979	4.004	126.92
<i>Intermolecular</i>				
C5-H5A...C11	2.841	0.980	3.818	179.63
C20-H20...C12	2.789	0.951	3.692	159.11
C8-H8A...Cg6	2.883	0.991	3.843	163.54
C7-H7B...Cg6	3.487	0.990	4.251	135.64

Cg1 = C12-C13-C14-C15-C16-C17; Cg2 = N1-N2-C3-C5-C6; Cg3 = C9-C10-C11-C12-C13-C14;  
Cg4 = N1-N2-C1-C3-C4; Cg5 = C9-C10-C11-C12-C13-C14; Cg6 = N3-N4-C18-C20-C21

**Figure 2.** Detail of the non-bonding interactions in **1**, showing only hydrogen atoms involved in the interactions. View along *c* axis.

Intermolecular interactions of compounds **1-3** have been also studied by Hirshfeld surface analysis, using CrystalExplorer 2.1 software [44-46]. Surfaces have been calculated using an isovalue of  $0.5 \text{ e au}^{-3}$ . The normalized contact distance ( $d_{\text{norm}}$ ) surface mapping shows red spots where relevant intramolecular interactions occur. For **1**, in the  $d_{\text{norm}}$  surface mapping red spots can be seen over hydrogen atoms of the ether chains and phenyl rings, as well as over both pyrazolyl moieties, confirming their role in its supramolecular structure (Figure 3a). However, the biggest red spots in **2** and **3** (and thus the strongest intermolecular interactions) correspond to the ones involving chlorine atoms. Interactions involving phenyl, methyl and pyrazolyl moieties are also identified (Figure 3b and 3c). Additional mapping surfaces have also been calculated (S.I.: Figure S16).

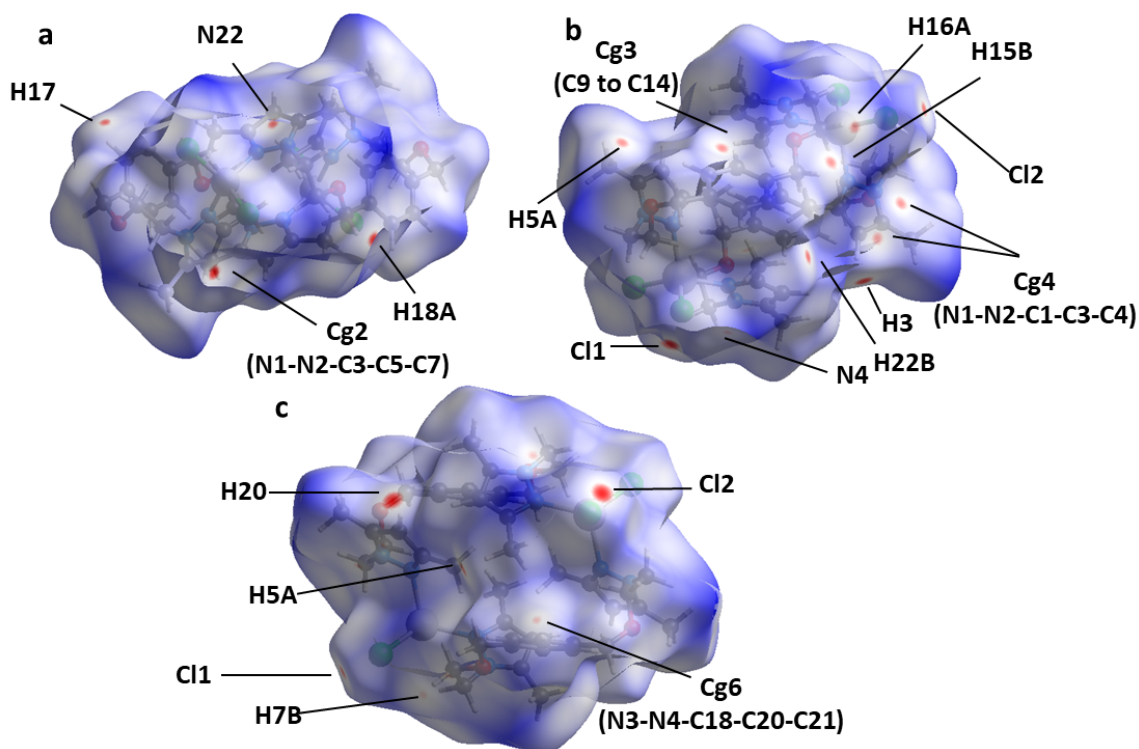


**Figure 3.** Hirshfeld surface mapped with  $d_{\text{norm}}$  of a. **1**, b. **2**, c. **3**. Surface transparency has been enabled and relevant atoms labelled.

The fingertip plots of compounds **1-3** (S.I.: Figures S17-19) show an overall rounded shape, lacking defined spikes, which suggest weak directional intramolecular interactions. Their decomposition show that the majority of the Hirshfeld surface (55.5-58.6%) is dominated by  $\text{H}\cdots\text{H}$  interactions, which can be attributed to dispersive London

forces [47]. Concerning C-H $\cdots$ C contacts (11.0-11.6%), they appear as “wings” instead of spikes, showing its C-H $\cdots$  $\pi$  character [48] while C-H $\cdots$ N contacts (3.6-3.9%) appear as more defined spikes. Lastly, it is remarkable the high percentage of interactions involving C-H $\cdots$ Cl contacts (22.7-24.5%). These last ones appear as sharp peaks, thus being the strongest directional supramolecular interactions.

### 2.3 Crystal and Extended Structure of 4.

Compound **4** has a  $[M(N_{Pz})_2Cl_2]$  core, comprising two chlorine atoms and two different pyrazolyl nitrogen atoms provided by **L2** (Figure 4a). The coordination structure of the Zn(II) is a slightly distorted tetrahedron ( $\tau_4 = 0.90$  [37]), with angles ranging from  $102.99(13)^\circ$  to  $117.18(9)^\circ$ . As stated before, this Zn(II) core is reported in sixty-one crystal structures [38]. Most of them are discrete molecules, and only eight of them have a polymeric structure. However, coordination compounds containing the bis(dipyrazolyl) analogue of **L2** and Ag(I) are also known to have polymeric structures [49]. Selected bond lengths and angles are shown on Table 3. All values agree with similar compounds reported in the literature [33,34,50,51].

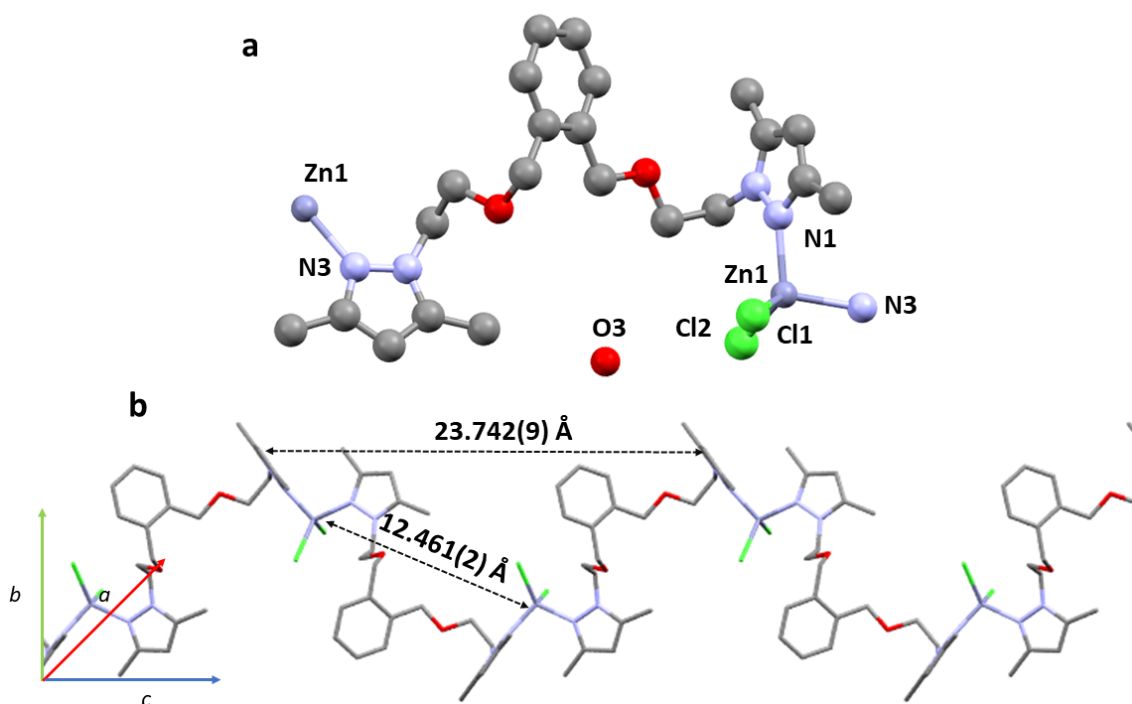


**Figure 4.** a. Compound **4**, showing all its non-hydrogen atoms and their corresponding numbering scheme. b. Representation of the infinite 1D polymeric chain, showing relevant intra-chain distances.

**Table 3.** Selected bond lengths and angles for compounds 4-6

4		5		6	
Bond lengths (Å)					
Zn(1)-Cl(1)	2.2313(11)	Cd(1)-Cl(1)	2.4286(11)	Hg(1)-Cl(1)	2.399(2)
Zn(1)-Cl(2)	2.2623(11)	Cd(1)-Cl(2)	2.4312(9)	Hg(1)-Cl(2)	2.391(2)
Zn(1)-N(1)	2.036(3)	Cd(1)-N(1)	2.248(3)	Hg(1)-N(1)	2.313(5)
Zn(1)-N(3)#1	2.050(3)	Cd(1)-N(3)#1	2.361(3)	Hg(1)-N(3)#1	2.498(5)
Zn(1)⋯Zn(1)	12.461(2)	Cd(1)-O(1)	2.743(3)	Hg(1)-O(1)	2.987(4)
		Cd(1)⋯Cd(1)	9.4935(4)	Hg(1)⋯Hg(1)	9.610(1)
Bond angles (°)					
Cl(1)-Zn(1)-Cl(2)	108.41(4)	Cl(1)-Cd(1)-Cl(2)	120.81(4)	Cl(1)-Hg(1)-Cl(2)	131.16(9)
N(3)#1-Zn(1)-Cl(2)	105.89(9)	N(1)-Cd(1)-Cl(1)	117.00(9)	N(1)-Hg(1)-Cl(1)	109.22(15)
N(3)#1-Zn(1)-Cl(1)	116.28(9)	N(1)-Cd(1)-Cl(2)	113.67(9)	N(1)-Hg(1)-Cl(2)	112.12(16)
N(1)-Zn(1)-Cl(2)	117.18(9)	N(1)-Cd(1)-N(3)#1	96.51(11)	N(1)-Hg(1)-N(3)#1	96.75(18)
N(1)-Zn(1)-Cl(1)	106.45(10)	N(3)#1-Cd(1)-Cl(1)	95.02(9)	N(3)#1-Hg(1)-Cl(1)	107.25(14)
N(1)-Zn(1)-N(3)#1	102.99(13)	N(3)#1-Cd(1)-Cl(2)	107.74(8)	N(3)#1-Hg(1)-Cl(2)	92.68(15)
		Cl(1)-Cd(1)-O(1)	84.63(7)	Cl(1)-Hg(1)-O(1)	84.35(9)
		Cl(2)-Cd(1)-O(1)	85.29(7)	Cl(2)-Hg(1)-O(1)	89.2(1)
		N(1)-Cd(1)-O(1)	70.3(1)	N(1)-Hg(1)-O(1)	66.4(2)
		N(3)#1-Cd(1)-O(1)	164.71(1)	N(3)#1-Hg(1)-O(1)	162.3(1)
#1: x, y+1, z+1/2		#1 -x+1/2, y-1/2, -z+3/2			

In this polymer, adjacent Zn(II) atoms are connected by **L2** via a *NN'*-bridged mode in an *anti* conformation, resulting in an infinite helical-chain along the *c* axis. The distance between repeating units is 23.742(9) Å, and between adjacent Zn(II) atoms is 12.461(2) Å (Figure 4b). This M⋯M distance is larger than the ones found in related compounds [Zn(bpdo)Cl<sub>2</sub>]<sub>n</sub> (bpdo = 1,8-bis(3,5-dimethyl-1*H*-pyrazol-1-yl)-3,6-dioxaoctane, 9.523 Å [33]) and [Zn(bpmx)Cl<sub>2</sub>]<sub>n</sub> (bpmx = α,α-bis(pyrazolyl)-*m*-xylene, 7.976 Å [52]). The dihedral angle between the mean planes of the pyrazolyl rings in the centrosymmetric **L2** ligands is 68.82°, which shows its twisting around the benzene rings.

The extended structure of compound **4** could be described as a dense three-dimensional thread of parallel chains. In this thread, the occluded H<sub>2</sub>O molecules play a key role, as they bind one left-handed and one right-handed helical-chain thanks to a double symmetrical O3-H3A⋯Cl2 interaction, forming a supramolecular chain parallel to the *c* axis. These double helical-chains are stacked together thanks to another set of distinct interactions. They involve the hydrogen of the pyrazolyl ring and chlorine moieties (C20-H20⋯Cl2) and the methyl and chlorine moieties (C2-H2B⋯Cl1). Lastly, a C-H⋯C interaction between the methyl groups and the phenyl rings also reinforces the 3D structure (C5-H5B⋯C12) (Figure 5). Relevant H-bond interactions are summarized on Table 4.

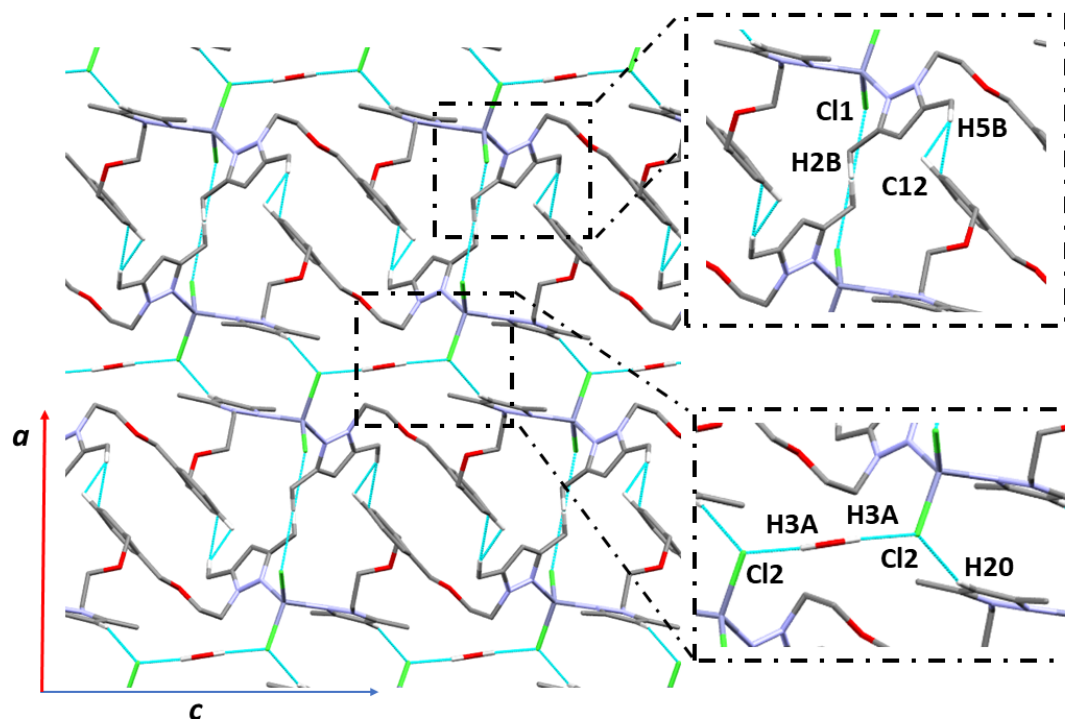


**Figure 5.** Detail of the H-bond interactions in **4**, showing only hydrogen atoms involved in the interactions. View along *b* axis.

**Table 4.** Selected intermolecular interactions for **4**

	D-H...A (Å)	D-H (Å)	H-D...A (Å)	>D-H...A (°)
<b>4</b>				
O3-H3A...Cl2	2.587	0.983	3.531	161.08
C5-H5B...Cl2	2.755	0.980	3.727	171.85
C2-H2B...Cl1	2.847	0.980	3.794	162.76
C20-H20...Cl2	2.849	0.950	3.755	159.77

The H<sub>2</sub>O molecules occupy cavities defined by these sets of double helical-chains. These non-connected cavities have a volume of 91.22 Å<sup>3</sup> (1.9 % of unit cell), calculated defining a probe radius of 1.2 Å (Figure 6).

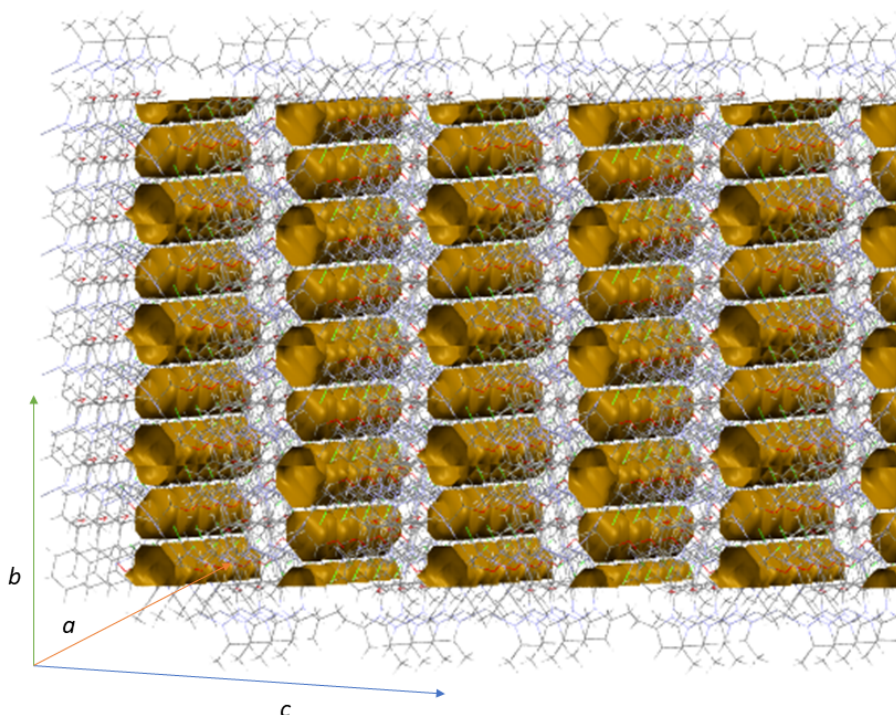


**Figure 6.** Voids ( $91.22\text{\AA}^3$ ) representation in **4**.

#### 2.4 Crystal and Extended Structure of **5** and **6**.

Isostructural compounds **5** and **6** have a  $[\text{M}(\text{N}_{\text{Pz}})_2\text{OCl}_2]$  core ( $\text{M} = \text{Cd}(\text{II})$  (**5**),  $\text{Hg}(\text{II})$  (**6**)) which results from the coordination of one ether group to the metal center (Figure 7 and S.I. Figure S20). Their coordination structure is a distorted trigonal bipyramid ( $\tau = 0.73$  (**5**),  $0.52$  (**6**) [53]). In them, the basal plane comprises two chlorine atoms and the nitrogen of the pyrazolyl closest to the coordinating oxygen, forming a six-membered ring. The apical positions are occupied by an oxygen atom and the nitrogen of the other pyrazolyl group. Remarkably, crystal structures with a  $[\text{M}(\text{N}_{\text{Pz}})_2\text{OCl}_2]$  core ( $\text{M} = \text{Cd}(\text{II}), \text{Hg}(\text{II})$ ) have been not reported [38]. Other reported structures including similar bispyrazolyl ligands show that  $\text{Cd}(\text{II})$  tends to form either dimers or polymers through double chlorine bridges [54-56]. Regarding  $\text{Hg}(\text{II})$ , reported crystal structures containing bispyrazolyl ligands show great morphological variability, as monomers [57,58], dimers [58], tetramers [43], polymers [59] or even more complicated architectures [60] have been reported. Selected bond lengths and bond angles are shown on Table 3. All values are in agreement with other reported  $\text{Cd}(\text{II})$  [32,33,54-56] and  $\text{Hg}(\text{II})$  compounds [57,58].

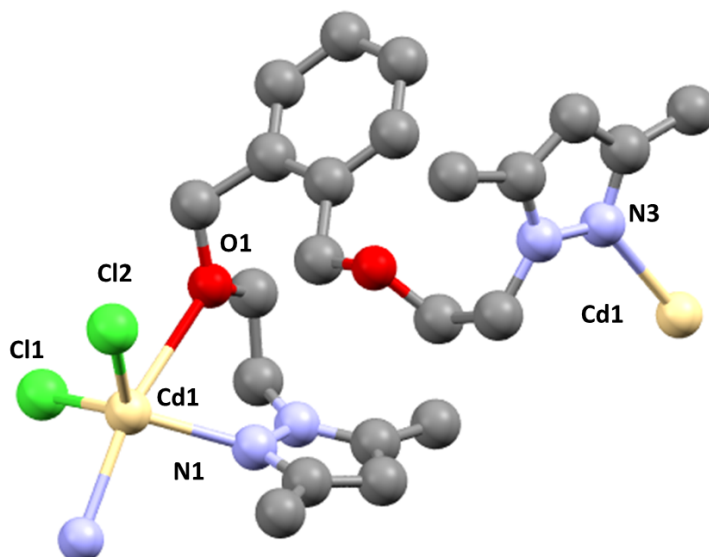


**Figure 7.** Polymer **5** showing all its non-hydrogen atoms and their corresponding numbering scheme.

In compounds **5** and **6**, **L2** acts as a *NON'*-chelated and bridged ligand in an *anti* configuration, resulting in an infinite helical-chain along the *b* axis. The distance between repeating units is 12.999(6) (**5**)/13.094(9) (**6**) Å, and between adjacent metal centers is 9.4935(4) (**5**)/9.610(1) (**6**) Å. These distances are shorter than in **4** (23.742(9) Å and 12.461(2) Å, respectively) due to the coordination of one ether group of **L2** (Figure 8). Pyrazole rings of different ligands coordinate to the same metal center are almost perpendicular in this conformation, being 83.49° (**5**)/83.76° (**6**) the dihedral angles between their mean planes. Phenyl rings of two consecutive bridging ligands are also perpendicular, as the dihedral angle between their mean planes is 84.78° (**5**)/84.15° (**6**). A similar coordination behavior has been observed for the related monomer [Cd(bpdo)Cl<sub>2</sub>] [33], as both oxygen atoms of the two ether groups are bonded to the metal center, resulting in a *NOON'*-chelated coordination mode. Probably, the steric hindrance of the phenyl group in **L2** prevents both the coordination of the second ether group and the chelation of the ligand, resulting in the formation of a polymer.

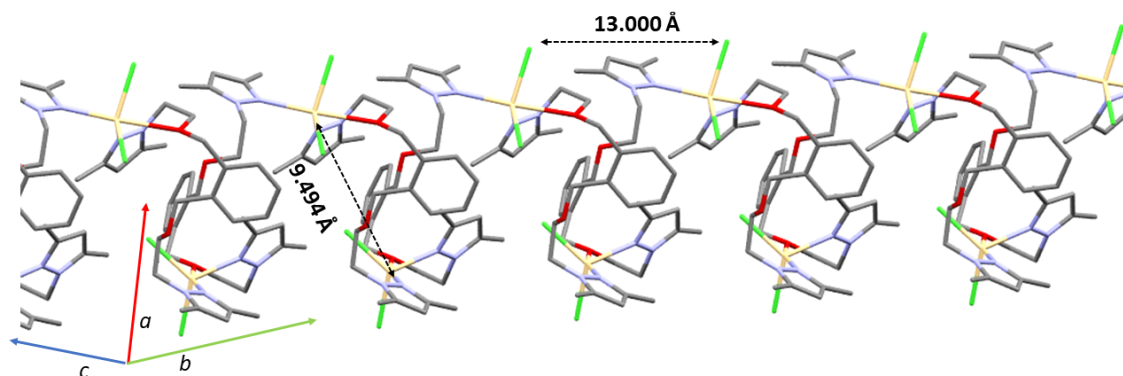


**Figure 8.** Representation of the infinite 1D polymeric chain for **5**, showing relevant intra-chain distances.

For both compounds, each chain is surrounded by six other parallel chains, resulting in a dense thread of alternating left-handed and right-handed polymeric chains (Figure 9 and S.I.: Figure S21). As in **4**, the main supramolecular interactions are related to the disordered solvent, which occupies non-connected cavities for a total volume of 227.28 / 229.75 Å<sup>3</sup> (8.6%/8.5% of unit cell for **5/6**), calculated defining a probe radius of 1.2 Å (S.I.: Figure S22). This volume is notably bigger than in **4** (91.22 Å<sup>3</sup>, 1.9% of the unit cell), as the occluded solvent is H<sub>2</sub>O in **4**, whereas in **5** and **6** the solvent is EtOH. Because of the disorder present in this occluded solvent, its structural role cannot be determined precisely. Secondary C-H⋯Cl and C-H⋯π interactions involving methyl, chlorine and phenyl moieties also appear in the supramolecular structure.



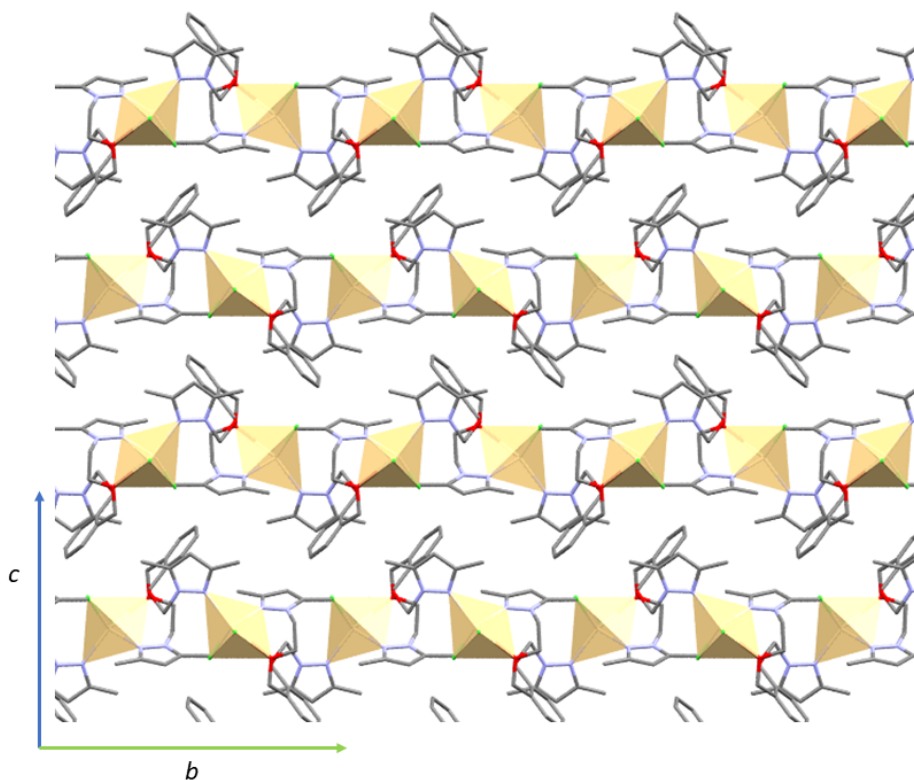


**Figure 9.** Supramolecular structure of **5** and **6**. View along *b* axis. Occluded solvent molecules have been removed for clarity.

### 2.5 Conformations and bonding modes of **L1** and **L2** in the complexes

In a previous work by our group, complexes obtained with **L2** and Pd(II) were either monomeric or dimeric [35], having a *syn* conformation. In this work, **L2** adopts a different *anti* conformation in all compounds (**4-6**), leading to the formation of polymeric helical-chains. On the other hand, **L1** proves much less flexible adopting *syn* conformations in all the reported compounds (**1-3**).

In Table 5 the behavior of **L1** and **L2** is summarized according to  $\theta$  (angular tilt between the coordinating *N* and the centroid of the phenyl ring),  $\square$  (dihedral angle between pyrazolyl rings of the same ligand), *d* (*M*⋯*M* distance), conformation and coordination mode.

For **1-3**,  $\theta$ ,  $\square$  and *d* have similar values, as **L1** has the same *NN'*-bridged coordination mode and *syn* conformation. In the case of **4-6**, the different coordination modes are reflected in several parameters. First, *NN'*-bridged and *NN'*-chelated coordination modes result in different  $\theta$  values, which are sensibly lower for *NN'*-chelated [Pd(**L2**)Cl<sub>2</sub>] [35] (31.16°) than for *NN'*-bridged compounds **4** and [Pd(**L2**)Cl<sub>2</sub>]<sub>2</sub> [35]

(105.10° and 110.66°). Second, the *NON'*-chelated and bridged coordination mode in **5** and **6** results in  $\theta$  values between *NN'*-bridged and *NN'*-chelated (82.50° and 82.94°). Last, in *NN'*-bridged compounds **4** and [Pd(**L2**)Cl<sub>2</sub>]<sub>2</sub> [35] the **d** values are higher (12.461(2) Å and 11.499(8) Å) than in the *NON'*-chelated and bridged compounds **5** and **6** (9.4935(6) Å and 9.610(1) Å).

The *syn* or *anti* disposition governs the formation of polymers or monomers/dimers for these flexible bispyrazolyl ligands. In the case of *syn* conformations, M<sub>2</sub>L<sub>2</sub> metallacycles and monomers are obtained, whereas for *anti* conformations, polymers are obtained. For **L2**, the compounds with *syn* conformations [Pd(**L2**)Cl<sub>2</sub>] [35] and [Pd(**L2**)Cl<sub>2</sub>]<sub>2</sub> [35] show low  $\square$  values (10.53° and 10.58°) when compared to  $\square$  values for *anti* conformation in compounds **4-6** (68.82°-83.49°). On the contrary, for **L1**,  $\square$  values in **1-3** (87.11°-89.13°), are comparable to those in **4-6**, but a *syn* conformation is observed.

When **1-6** compounds are compared, *syn* or *anti* conformation is reflected in  $\theta$  parameter: higher values (82.50°-105.10°) result in *anti* (**4-6**) while *syn* (**1-3**) is obtained with lower values (76.58°-77.03°). According to this data, the turning point is at  $\theta \approx 80^\circ$ . Nevertheless, the use of Pd(II) as metal center severely disrupts this pattern. This can be attributable to spatial constraints induced to **L2** by Pd(II) square planar coordination structure. Further details about the selected distances and angles are provided on Table 5.

**Table 5.** Coordination modes of **L1** and **L2**

Compounds	$\theta$ (°)	$\square$ (°)	<b>d</b> (Å)	Conformation	Coordination Mode
<b>1</b> (work)	76.58	89.13	9.3697(6)	<i>syn</i>	<i>NN'</i> -bridged
<b>2</b> (work)	76.67	87.78	9.5206(7)		
<b>3</b> (work)	77.03	87.11	9.6636(5)		
<b>4</b> (work)	105.10	68.82	12.461(2)	<i>anti</i>	<i>NON'</i> -chelated and bridged
<b>5</b> (work)	82.50	83.48	9.4935(4)	Distorted <i>anti</i>	
<b>6</b> (work)	82.94	83.49	9.610(1)		
[Pd( <b>L2</b> )Cl <sub>2</sub> ] [35]	31.16	10.63	-	<i>syn</i>	<i>NN'</i> -chelated
[Pd( <b>L2</b> )Cl <sub>2</sub> ] <sub>2</sub> [35]	110.66	10.58	11.499(8)	<i>syn</i>	<i>NN'</i> -bridged

$\theta$ : Angle between coordinating nitrogen atoms and the phenyl rings' centroid.

$\square$ : Dihedral angles between pyrazolyl planes.

**d**: Metal...Metal distance.

## 2.6 NMR Studies

NMR spectra of compounds **1-6** were recorded in CDCl<sub>3</sub> at r.t. The NMR signals were assigned by <sup>1</sup>H, <sup>13</sup>C{<sup>1</sup>H} and HSQC NMR experiments (S.I.: Figures S23-S41). For all of them, <sup>1</sup>H NMR spectra show the coordination of the ligands to the metal center as an upfield displacement on the 1-*H*-pyrazolyl proton signal (5.79-5.97 ppm (**1-6**) vs. 5.77 (**L1**) and 5.76 (**L2**) ppm). In the <sup>1</sup>H NMR spectra the phenyl protons appear mostly as a singlet (7.15-7.25 ppm) for **1-3**, whereas for **4-6** where they appear as a multiplet (7.24-7.26 ppm). The protons of the -OCH<sub>2</sub>Ph- fragment appear as singlets (4.40-4.53 ppm) and the protons of the -OCH<sub>2</sub>CH<sub>2</sub>Pz- appear as triplets (4.17-4.67 ppm and 3.71-3.84 ppm) with *J* = 5.2-5.7 Hz. For Zn(II) complexes (**1** and **4**) these protons appear as broad bands.

Regarding the <sup>13</sup>C{<sup>1</sup>H} NMR spectra, there is an upfield displacement in the 1-*H*-pyrazolyl carbon signal (106.1-107.0 ppm in **1-3**, 105.6-107.0 ppm in **4-6**) respect to the free ligand (104.9 ppm in free **L1** and 105.1 ppm in free **L2**) due to coordination of the metal center. The carbon signals of the -OCH<sub>2</sub>Ph- fragments also show an upfield displacement in **1-3** (73.1-73.8 ppm) respect to free **L1** (70.7 ppm). However, in compounds **4-6**, the same carbon signals show a downfield displacement (69.9-71.8 ppm) respect to non-coordinated **L2** ligand (73.2 ppm). Further NMR details are provided in the experimental section.

We were interested in establishing if compounds **4-6** remain as polymers in solution. In this sense, DOSY-NMR spectroscopy [61] could allow to elucidate if compounds **4-6** revert to different species or preserve their polymeric structure [62,63]. Thus, DOSY-NMR spectra of **4-6** (Figure 10 and S.I.: Figures S42 and S43) were carried out in CDCl<sub>3</sub> at 298 K. DOSY-NMR of **1** was carried out for comparison purposes (S.I.: Figure S44). The spectra of **1** shows a single diffusion peak at *D* = 6.83·10<sup>-10</sup> m<sup>2</sup>s<sup>-1</sup>. For both polymers **4** and **6**, also single diffusion peaks appear at *D* = 16.3·10<sup>-10</sup> m<sup>2</sup>s<sup>-1</sup> (**4**) and *D* = 8.95·10<sup>-10</sup> m<sup>2</sup>s<sup>-1</sup> (**6**). These higher diffusion coefficient values mean that the hydrodynamic radius of **4** and **6** in solution are smaller than **1**. If compound **1** maintains a dimeric structure in solution, those smaller species in **4** and **6** could be attributed to monomers. For **5**, a more sophisticated spectrum is obtained. Although there is severe line broadening, two main peaks are identified at *D* = 14.5·10<sup>-10</sup> m<sup>2</sup>s<sup>-1</sup> and *D* = 6.59·10<sup>-10</sup> m<sup>2</sup>s<sup>-1</sup> suggesting a dynamic equilibrium between monomeric and dimeric species. However, integration of the diffusion peaks show that the equilibrium is heavily tilted

towards the monomeric species, as it is fifty-two times more abundant than the dimeric one.

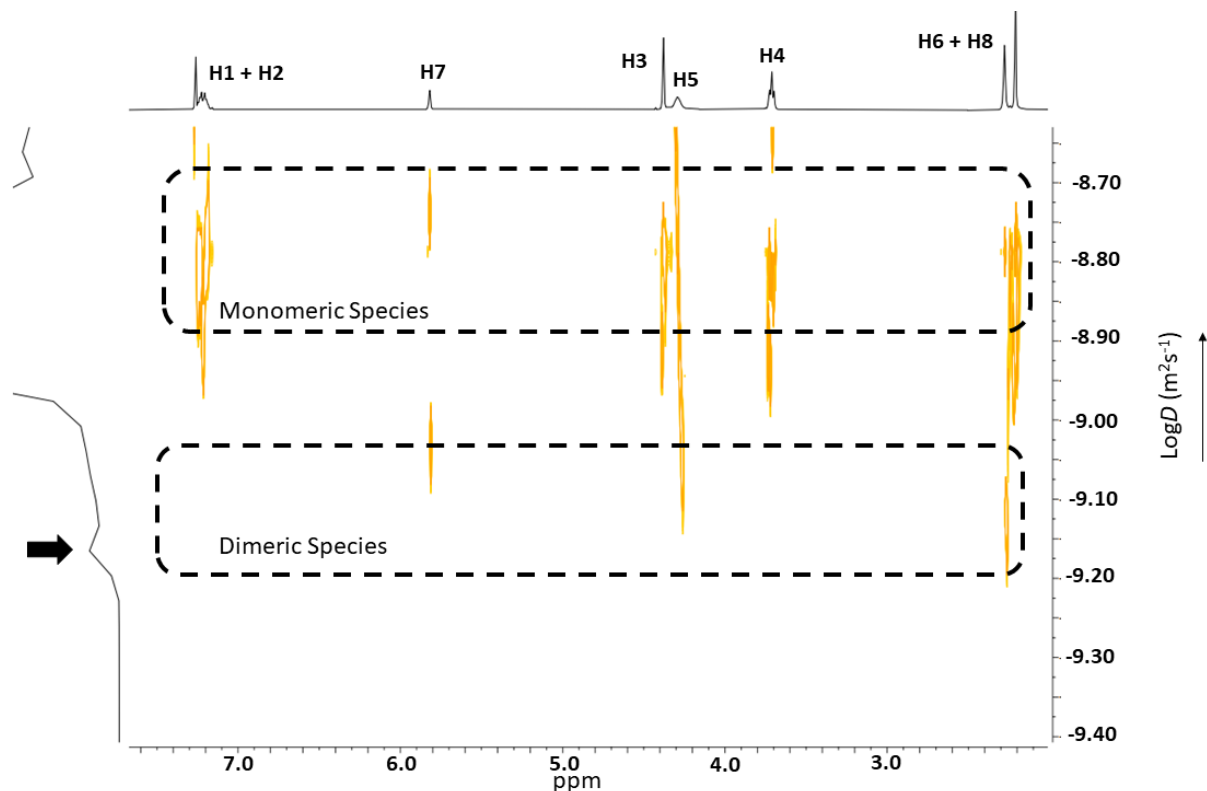


**Figure 10.** DOSY NMR spectrum of **5** (400 MHz, CDCl<sub>3</sub>). Note the minor diffusion peak at  $D = 6.59 \cdot 10^{-10} \text{ m}^2 \text{ s}^{-1}$ , highlighted with a black arrow.

We attempted to estimate the molecular weight (MW) of the species in solution using the model proposed by Evans et al. in Equation (1) [64]. In this equation, MW and MW<sub>S</sub> stand for the solute and solvent MW respectively,  $\eta$  for the viscosity parameter, K<sub>B</sub> for the Boltzmann constant and N<sub>A</sub> for the Avogadro number. The parameter  $\alpha$  is defined as the cubic root of the molecular weight of the solvent divided by the molecular weight of the solute. Lastly,  $\rho_{\text{eff}}$  is an empirical parameter whose value has been optimized for CDCl<sub>3</sub> at 647 Kg m<sup>-3</sup> [64]. Further optimization is required for calculations in CDCl<sub>3</sub>, establishing an effective MW<sub>S</sub> value of 83 g mol<sup>-1</sup> [64]. Deviations from the ideal behavior are expected when heavy atoms are present [64,65].

$$D = \frac{K_B T \left( \frac{3\alpha}{2} + \frac{1}{1+\alpha} \right)}{6\pi\eta^3 \sqrt{\frac{3MW}{4\pi\rho_{\text{eff}}N_A}}}, \quad \text{where } \alpha = \sqrt[3]{\frac{MW_S}{MW}} \quad (1)$$

For compound **1** an estimated MW of 917 g mol<sup>-1</sup> is obtained (1037.54 g mol<sup>-1</sup>), which suggests the conservation of its dimeric structure in solution. For **5**, the diffusion peak at  $D = 6.59 \cdot 10^{-10} \text{ m}^2\text{s}^{-1}$  results in an estimated MW of 995 g mol<sup>-1</sup> (1177.7 g mol<sup>-1</sup> for dimeric **5**), suggesting a dimeric species, whereas for **6** its only diffusion peak results in an estimated MW of 510 g mol<sup>-1</sup>, suggesting a monomeric species (677.02 g mol<sup>-1</sup> for monomeric **6**). This model, however, severely underestimated the MW of lighter, monomeric species of **4** and **5**. In any case, this data supports the reversion of polymeric compounds **4-6** to monomeric and dimeric species in solution.

### 2.7 Photoluminescence Properties

The fluorescence emission spectra were carried out with an excitation wavelength of 260 nm and recorded between 270-600 nm. The **L1** and **L2** and coordination compounds **1-6** show emission bands in the range of 282-286 nm (Figure 11). Regarding compounds **1-3**, hyperchromicity is detected for **3**, while in **1** and **2**, the intensity value is lower than for free **L1**. Neither of them does show a bathochromic shift. For compounds **4-6**, however, both bathochromic ( $\lambda_{\text{max}}$ : 286 nm for **4-6**, 282 nm for free **L2**) and hyperchromic shifts are detected in all cases (S.I.: Figures S45 and S46). There is a similar enhancement of the fluorescence intensity for **4** and **5**, whereas for **6** this enhancement is stronger. In both families, Hg(II) compounds (**3** and **6**) show the strongest fluorescence enhancement effect, especially in compound **6**.

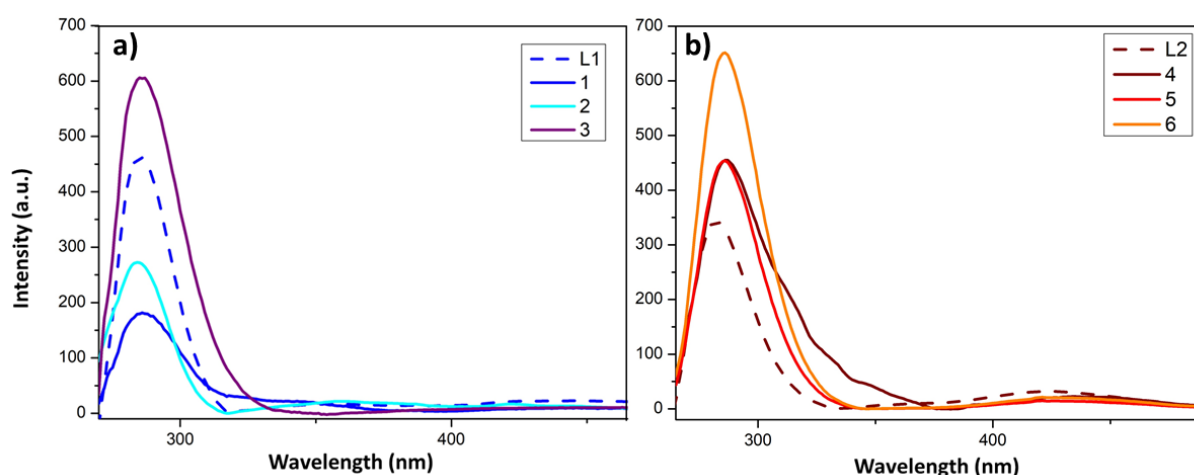


**Figure 11.** a. Fluorescence spectra of **L1** and **1-3** recorded in a CH<sub>3</sub>CN solution at r.t. b. Fluorescence spectra of **L2** and **4-6** recorded in a CH<sub>3</sub>CN solution at r.t.

### 3. Conclusions

The reactivity of **L1** and **L2** against Zn(II), Cd(II) and Hg(II) has been studied, obtaining six new coordination compounds. Compounds **1-3** are isostructural metallacyclic dimers where **L1** shows *NN'*-bridged coordination mode with a *syn* conformation. Compounds **4-6** are coordination polymers where **L2** shows two different coordination modes depending on the metal: *NN'*-bridged in compound **4** or *NON'*-chelated and bridged in isostructural **5** and **6** compounds. In all of them **L2** displays an *anti* conformation. The coordination of one ether group causes the *NON'*-chelated and bridged coordination mode. Thus, *para*- substitution (**L1**) results in a domination of the metallacyclic motif, while *ortho*- substitution (**L2**) results in a domination of the linear polymeric motif.

It has been demonstrated that the use of coordinatively flexible metal cations Zn(II) (**1** and **4**), Cd(II) (**2** and **5**) and Hg(II) (**3** and **6**), allows the adoption of new coordination modes (*NON'*-chelate and bridged) and conformations (*anti*) for this family of flexible bispyrazole ligands.

The behavior of compounds **1-6** in solution was studied *via* NMR and photoluminescence measurements. Moreover, DOSY NMR spectra of compounds **1** and **4-6** were also recorded, showing the presence of monomeric species for **4** and **6**, monomeric and dimeric (52:1 ratio) for **5** and dimeric for **1**. Finally, regarding the photoluminescent properties, all polymeric compounds (**4-6**) display a photoluminescence enhancement respect to free **L2**. However, for dimeric metallacycles (**1-3**) only compound **3** displays a photoluminescence enhancement respect to free **L1**. Furthermore, Hg(II) compounds (**3** and **6**) show the highest fluorescence enhancement. These results could be promoted by the lengthening of the conjugation and enhancement of the rigidity of the coordinated ligand in these complexes [66,67].

### 4. Experimental Section

#### 4.1 Materials and General Details

Metal(II) chloride (Metal = zinc(II), cadmium(II) and mercury(II)), absolute ethanol (EtOH) and diethyl ether (Et<sub>2</sub>O) were purchased from Sigma-Aldrich and used without further purification. Spectroscopic grade acetonitrile (CH<sub>3</sub>CN) was purchased from ROMIL-SpS and used without further purification. Deuterated chloroform (CDCl<sub>3</sub>)

was purchased from Eurisotop and used without further purification. All reactions and manipulations were carried out in air. Powder X-ray patterns (PXRD) were measured with a Siemens D5000 apparatus (with 40 kW and 45 mA using Cu  $k\alpha$  radiation with  $\lambda = 1.5406 \text{ \AA}$ ). Patterns were recorded from  $2\theta = 5^\circ$  to  $40^\circ$  with a step scan of  $0.02^\circ$  counting for 1s at each step.  $^1\text{H}$  NMR,  $^{13}\text{C}\{^1\text{H}\}$  NMR, HSQC and DOSY spectra were recorded on an NMR-FT Bruker 400 MHz NMR spectrometer in  $\text{CDCl}_3$  solutions at 298 K. All chemical shifts ( $\delta$ ) are given in ppm relative to TMS as internal standard. FTIR-ATR spectra were recorded on a high-resolution spectrometer FT-IR Perkin Elmer Spectrum One equipped with a universal attenuated total reflectance (ATR) accessory with a diamond window in the range  $4000\text{-}500 \text{ cm}^{-1}$ . The electronic spectra were run on a Varian Cary 500 spectrophotometer, using spectroscopic grade  $\text{CH}_3\text{CN}$ , in a normal quartz cell having a path length of 10 mm in the range of 200-800 nm, with concentrations between  $1.05 \cdot 10^{-4}$ - $1.34 \cdot 10^{-4} \text{ M}$  at room temperature (r.t.). The fluorescence emission and excitation spectra were recorded in a Varian Cary Eclipse Fluorescence Spectrometer at r.t., equipped with a quartz cell having a path length of 10 mm. The samples were excited at 260 nm and the emission was recorded in the range of 270-600 nm in spectroscopic grade  $\text{CH}_3\text{CN}$  ( $4.87 \cdot 10^{-4} \text{ M}$  for **L1**,  $5.02 \cdot 10^{-4} \text{ M}$  for **L2** and  $1.21 \cdot 10^{-4}$ - $1.38 \cdot 10^{-4} \text{ M}$  for **1-6**). The dilution effects of the obtained data were corrected using Origin Pro 8 software [68]. Ligands **L1** and **L2** were synthesized according to the procedure reported in the literature [32,35]. Elemental analyses (C, H, N) were carried out on a Thermo Scientific Flash 2000 CHNS Analyser.

#### 4.2. Synthesis of $[\text{Zn}(\text{L1})\text{Cl}_2]_2$ (**1**).

A solution of  $\text{ZnCl}_2$  (0.094 g, 0.690 mmol) in absolute EtOH (20 mL) was added dropwise to a solution of **L1** (0.264 g, 0.690 mmol) in absolute EtOH (20 mL). The resulting solution was stirred for 48 h at r.t. After that period, the solution was concentrated under vacuum until a white solid precipitated. The resulting solid was filtered off, washed with 5 mL of cold  $\text{Et}_2\text{O}$  and dried under vacuum. Suitable crystals for X-ray diffraction were obtained by recrystallization of the white powder in EtOH for 16 days in air.

Yield: 74.1% (0.265 g).  $^1\text{H}$  NMR ( $\text{CDCl}_3$ , 400 MHz, ppm):  $\delta = 7.26$  (overlapped with  $\text{CDCl}_3$ , br, 4H, *Ph*), 5.97 (s, 2H, *CH(Pz)*), 4.72 (br, 4H, *OCH}\_2\text{Ph}*), 4.53 (s, 4H,  $\text{N}_{\text{Pz}}\text{CH}_2\text{CH}_2\text{O}$ ), 3.84 (br, 4H,  $\text{N}_{\text{Pz}}\text{CH}_2\text{CH}_2\text{O}$ ), 2.34 (s, 6H,  $\text{CH}_3(\text{Pz})$ ), 2.29 (s, 6H,

$CH_3(Pz)$ ).  $^{13}C\{^1H\}$  NMR ( $CDCl_3$ , 100.6 MHz, ppm):  $\delta = 150.4$ , 143.5 (Pz-C), 136.3 (*Ph-CH<sub>2</sub>O*), 128.8 (*Ph-H*), 107.1 (*CH(Pz)*), 73.8 (*Ph-CH<sub>2</sub>O*), 69.2 ( $N_{Pz}CH_2CH_2O$ ), 47.8 ( $N_{Pz}CH_2CH_2O$ ), 13.4, 11.6 ( $CH_3(Pz)$ ). FTIR-ATR (wavenumber,  $cm^{-1}$ ): 2935-2859(m) [ $\nu(C-H)_{al}$ ], 1551(s) [ $\nu(C=C)_{ar}/\nu(C=N)_{ar}$ ], 1479(w), 1457(w), 1455(m), 1424(m) [ $\delta(C=C)_{ar}/\delta(C=N)_{ar}$ ], 1375(w), 1371(w), 1345(m), 1306(m), 1266(w), 1254(w), 1209(m), 1099(s) [ $\nu(C-O-C)$ ], 1067(m), 1033(s) [ $\delta(C-H)_{ip}$ ], 873(w), 843(m), 816(s) [ $\delta(C-H)_{oop}$ ], 772(s) [ $\delta(C-H)_{oop}$ ], 650(w), 631(s). UV-Vis: ( $CH_3CN$ ,  $1.07 \cdot 10^{-4}$  M)  $\lambda_{max}$  ( $\square$  ( $M^{-1}cm^{-1}$ )) = 221 nm ( $3.42 \cdot 10^4$ ). Fluorescence ( $CH_3CN$ ):  $\lambda_{ex} = 260$  nm,  $\lambda_{em} = 283$  nm. Elemental analysis calc. (%) for  $C_{44}H_{60}Zn_2Cl_4N_8O_4$  (1037.54): C 50.93; H 5.83; N 10.80. Found: C 50.74; H 5.85; N 10.71.

### 4.3 Synthesis of $[Cd(L1)Cl_2]_2$ (2).

A solution of  $CdCl_2$  (0.209 g, 1.14 mmol) in absolute EtOH (20 mL) was added to a solution of **L1** (0.436 g, 1.14 mmol) in absolute EtOH (20 mL). The resulting solution was stirred for 48 h at r.t. After that period, the solution was concentrated under vacuum until a white precipitate appeared. The white precipitate was filtered off, washed with 5 mL of cold Et<sub>2</sub>O and dried under vacuum. Suitable crystals for X-ray diffraction were obtained by recrystallization of the white precipitate in EtOH for 19 days in air.

Yield: 73.6% (0.475 g).  $^1H$  NMR ( $CDCl_3$ , 400 MHz, ppm):  $\delta = 7.16$  (s, 4H, *Ph*), 5.79 (s, 2H, *CH(Pz)*), 4.47 (s, 4H, *OCH<sub>2</sub>Ph*), 4.17 (t, 4H,  $^3J = 5.8$  Hz,  $N_{Pz}CH_2CH_2O$ ), 3.78 (t, 4H,  $^3J = 5.7$  Hz,  $N_{Pz}CH_2CH_2O$ ), 2.24 (s, 6H,  $CH_3(Pz)$ ), 2.22 (s, 6H,  $CH_3(Pz)$ ).  $^{13}C\{^1H\}$  NMR ( $CDCl_3$ , 100.6 MHz, ppm):  $\delta = 147.8$ , 140.3 (Pz-C), 137.6 (*Ph-CH<sub>2</sub>O*), 127.7 (*Ph-H*), 106.1 (*CH(Pz)*), 73.1 (*Ph-CH<sub>2</sub>O*), 69.4 ( $N_{Pz}CH_2CH_2O$ ), 48.7 ( $N_{Pz}CH_2CH_2O$ ), 13.7, 11.4 ( $CH_3(Pz)$ ). FTIR-ATR (wavenumber,  $cm^{-1}$ ): 3188(w) [ $\nu(C-H)_{ar}$ ], 2951-2850(s) [ $\nu(C-H)_{al}$ ], 1547(s) [ $\nu(C=C)_{ar}/\nu(C=N)_{ar}$ ], 1496(w), 1465(s), 1440(w), 1423(s) [ $\delta(C=C)_{ar}/\delta(C=N)_{ar}$ ], 1397(w), 1387(w), 1376(m), 1373(m), 1357(w), 1307(m), 1267(w), 1254(w), 1207(m), 1162(w), 1112(m), 1105(s) [ $\nu(C-O-C)$ ], 1065(m), 1043(m) [ $\delta(C-H)_{ip}$ ], 1013(m), 982(w), 870(m), 836(m), 816(s) [ $\delta(C-H)_{oop}$ ], 762(s) [ $\delta(C-H)_{oop}$ ], 649(w), 628(m). UV-Vis: ( $CH_3CN$ ,  $1.17 \cdot 10^{-4}$  M)  $\lambda_{max}$  ( $\square$  ( $M^{-1}cm^{-1}$ )) = 219 nm ( $1.40 \cdot 10^4$ ). Fluorescence ( $CH_3CN$ ):  $\lambda_{ex} = 260$  nm,  $\lambda_{em} = 282$  nm. Elemental analysis calc. (%) for  $C_{44}H_{60}Cd_2Cl_4N_8O_4$  (1131.60): C 46.70; H 5.34; N 9.90. Found: C 46.55; H 5.20; N 9.60.



#### 4.4 Synthesis of $[Hg(\mathbf{L1})Cl_2]_2$ (**3**).

A solution of  $HgCl_2$  (0.163 g, 0.600 mmol) in absolute EtOH (20 mL) was added to a solution of **L1** (0.230 g, 0.600 mmol) in absolute EtOH (20 mL). The resulting solution was stirred for 72 h at r.t. After that period, the solution was left to slowly evaporate in air. After two weeks, a crystalline precipitate appeared. The white precipitate was filtered off, washed with 5 mL of cold  $Et_2O$  and dried under vacuum. Suitable crystals for X-ray diffraction were obtained by recrystallization of the white solid in EtOH for 20 days in air.

Yield: 61.7% (0.242 g).  $^1H$  NMR ( $CDCl_3$ , 400 MHz, ppm):  $\delta$  = 7.15 (s, 4H, *Ph*), 5.90 (s, 2H, *CH*(Pz)), 4.47 (s, 4H,  $OCH_2Ph$ ), 4.33 (t, 4H,  $^3J = 5.26$  Hz,  $N_{Pz}CH_2CH_2O$ ), 3.79 (t, 4H,  $^3J = 5.33$  Hz,  $N_{Pz}CH_2CH_2O$ ), 2.31 (s, 6H,  $CH_3$ (Pz)), 2.27 (s, 6H,  $CH_3$ (Pz)).  $^{13}C\{^1H\}$  NMR ( $CDCl_3$ , 100.6 MHz, ppm):  $\delta$  = 147.7, 141.2 (Pz-C), 137.3 (*Ph-CH*<sub>2</sub>O), 128.1 (*Ph-H*), 107.0 (*CH*(Pz)), 73.1 (*Ph-CH*<sub>2</sub>O), 68.8 ( $N_{Pz}CH_2CH_2O$ ), 48.7 ( $N_{Pz}CH_2CH_2O$ ), 13.3, 11.4 ( $CH_3$ (Pz)). FTIR-ATR (wavenumber,  $cm^{-1}$ ): 3117(w) [ $\nu$ (C-H)<sub>ar</sub>], 2961-2860(s) [ $\nu$ (C-H)<sub>al</sub>], 1547(s) [ $\nu$ (C=C)<sub>ar</sub>/ $\nu$ (C=N)<sub>ar</sub>], 1494(w), 1463(m), 1423(m) [ $\delta$ (C=C)<sub>ar</sub>/ $\delta$ (C=N)<sub>ar</sub>], 1387(w), 1376(m), 1347(w), 1307(m), 1266(m), 1207(m), 1122(s), 1105(s) [ $\nu$ (C-O-C)], 1065(m), 1040(m) [ $\delta$ (C-H)<sub>ip</sub>], 1014(m), 870(w), 821(m), 816(s) [ $\delta$ (C-H)<sub>oop</sub>], 763(w), 630(m), 533(m). UV-Vis: ( $CH_3CN$ ,  $1.05 \cdot 10^{-4}$  M)  $\lambda_{max}$  ( $\square$  ( $M^{-1}cm^{-1}$ )) = 219 nm ( $2.45 \cdot 10^4$ ). Fluorescence ( $CH_3CN$ ):  $\lambda_{ex}$  = 260 nm,  $\lambda_{em}$  = 286 nm. Elemental analysis calc. (%) for  $C_{44}H_{60}Hg_2Cl_4N_8O_4$  (1307.98): C 40.40; H 4.62; N 8.57. Found: C 40.27; H 4.54; N 8.30.

#### 4.5 Synthesis of $\{[Zn(\mathbf{L2})Cl_2] \cdot 1/2H_2O\}_n$ (**4**).

A solution of  $ZnCl_2$  (0.127 g, 0.934 mmol) in absolute EtOH (20 mL) was added to a solution of **L2** (0.357 g, 0.934 mmol) in absolute EtOH (20 mL). The resulting solution was stirred for 48 h. at r.t. After that period, a white precipitate appears, which was filtered off, cleaned with 5 mL of cold  $Et_2O$  and dried under vacuum. Suitable crystals for X-ray diffraction were obtained by recrystallization of the white precipitate in EtOH for 12 days in air.

Yield: 92.9% (0.458 g).  $^1H$  NMR ( $CDCl_3$ , 400 MHz, ppm):  $\delta$  = 7.25 (s, 4H, *Ph*), 5.95 (s, 2H, *CH*(Pz)), 4.67 (t, 4H,  $^3J = 5.6$  Hz,  $N_{Pz}CH_2CH_2O$ ), 4.40 (s, 4H,  $OCH_2Ph$ ), 3.84

(br, 4H,  $N_{Pz}CH_2CH_2O$ ), 2.32 (s, 6H,  $CH_3(Pz)$ ), 2.25 (s, 6H,  $CH_3(Pz)$ ).  $^{13}C\{^1H\}$  NMR ( $CDCl_3$ , 100.6 MHz, ppm):  $\delta$  = 150.1, 144.0 (Pz-C), 136.1 (*Ph*- $CH_2O$ ), 128.2, 128.1 (*Ph*-H), 107.4 (*CH*(Pz)), 69.9 (*Ph-CH\_2O*), 68.7 ( $N_{Pz}CH_2CH_2O$ ), 48.5 ( $N_{Pz}CH_2CH_2O$ ), 13.7, 11.7 ( $CH_3(Pz)$ ). FTIR-ATR (wavenumber,  $cm^{-1}$ ): 3600-3200(br) [ $\nu(O-H)$ ], 3125(w) [ $\nu(C-H)_{ar}$ ], 2954-2855(s) [ $\nu(C-H)_{al}$ ], 1554(m) [ $\nu(C=C)_{ar}/\nu(C=N)_{ar}$ ], 1470(w), 1440(m), 1420(m) [ $\delta(C=C)_{ar}/\delta(C=N)_{ar}$ ], 1385(w), 1374(m), 1353(m), 1314(w), 1286(w), 1261(w), 1220(w), 1218(w), 1189(w), 1168(w), 1148(w), 1124(s), 1105(s) [ $\nu(C-O-C)$ ], 1065(m), 1050(s) [ $\delta(C-H)_{ip}$ ], 1014(w), 876(w), 816(m), 786(s) [ $\delta(C-H)_{oop}$ ], 758(s) [ $\delta(C-H)_{oop}$ ], 656(m), 634(m). UV-Vis: ( $CH_3CN$ ,  $1.26 \cdot 10^{-4} M$ )  $\lambda_{max}$  ( $\square (M^{-1}cm^{-1})$ ) = 218 nm ( $1.84 \cdot 10^4$ ). Fluorescence ( $CH_3CN$ ):  $\lambda_{ex}$  = 260 nm,  $\lambda_{em}$  = 286 nm. Elemental analysis calc. (%) for  $C_{44}H_{62}Zn_2Cl_4N_8O_5$  (1055.55): C 50.06; H 5.92; N 10.62. Found: C 49.96; H 5.64; N 10.33.

#### 4.6 Synthesis of $\{[Cd(L2)Cl_2] \cdot 1/2EtOH\}_n$ (5).

A solution of  $CdCl_2$  (0.086 g, 0.47 mmol) in absolute EtOH (20 mL) was added to a solution of **L2** (0.180 g, 0.471 mmol) in absolute EtOH (20 mL). The resulting solution was stirred for 48 h at r.t. After that period, the solution was concentrated under vacuum until a white precipitate appeared. The white precipitate was filtered off, washed with 5 mL of cold  $Et_2O$  and dried under vacuum. Suitable crystals for X-ray diffraction were obtained by recrystallization of the white powder in EtOH for 25 days in air.

Yield: 88.3% (0.242 g).  $^1H$  NMR ( $CDCl_3$ , 400 MHz, ppm):  $\delta$  = 7.22 (m, 4H, *Ph*), 5.85 (s, 2H, *CH*(Pz)), 4.40 (s, 4H,  $OCH_2Ph$ ), 4.32 (br, 4H,  $N_{Pz}CH_2CH_2O$ ), 3.75 (t, 4H,  $^3J = 5.6$  Hz,  $N_{Pz}CH_2CH_2O$ ), 2.32 (s, 6H,  $CH_3(Pz)$ ), 2.23 (s, 6H,  $CH_3(Pz)$ ).  $^{13}C\{^1H\}$  NMR ( $CDCl_3$ , 100.6 MHz, ppm):  $\delta$  = 148.6, 148.2 (Pz-C), 136.2 (*Ph-CH\_2O*), 128.8, 128.0 (*Ph-H*), 105.6 (*CH*(Pz)), 71.8 (*Ph-CH\_2O*), 69.3 ( $N_{Pz}CH_2CH_2O$ ), 48.6 ( $N_{Pz}CH_2CH_2O$ ), 13.6, 11.4 ( $CH_3(Pz)$ ). FTIR-ATR (wavenumber,  $cm^{-1}$ ): 3496(br) [ $\nu(O-H)$ ], 2965-2866(m) [ $\nu(C-H)_{al}$ ], 1550(s) [ $\nu(C=C)_{ar}/\nu(C=N)_{ar}$ ], 1468(w), 1444(m), 1422(m) [ $\delta(C=C)_{ar}/\delta(C=N)_{ar}$ ], 1374(s), 1356(w), 1315(w), 1300(w), 1281(w), 1256(w), 1209(w), 1184(w), 1123(s), 1101(s) [ $\nu(C-O-C)$ ], 1069(m), 1036(s) [ $\delta(C-H)_{ip}$ ], 1019(m), 993(w), 838(w), 811(w), 791(m) [ $\delta(C-H)_{oop}$ ], 751(s) [ $\delta(C-H)_{oop}$ ], 631(m). UV-Vis: ( $CH_3CN$ ,  $1.05 \cdot 10^{-4} M$ )  $\lambda_{max}$  ( $\square (M^{-1}cm^{-1})$ ) = 219 nm ( $1.52 \cdot 10^4$ ). Fluorescence ( $CH_3CN$ ):  $\lambda_{ex}$  = 260 nm,  $\lambda_{em}$  = 286 nm. Elemental analysis calc. (%) for  $C_{23}H_{33}CdCl_2N_4O_{2.5}$  (588.83): C 46.91; H 5.65; N 9.52. Found: C 46.87; H 5.61; N 9.22.

#### 4.7 Synthesis of $\{[Hg(\mathbf{L2})Cl_2] \cdot 1/2EtOH\}_n$ (**6**).

A solution of  $HgCl_2$  (0.121 g, 0.446 mmol) in absolute EtOH (20 mL) was added to a solution of **L2** (0.171 g, 0.447 mmol) in absolute EtOH (20 mL). The resulting solution was stirred for 98 h at r.t. After that period, the solution was concentrated under vacuum to one-third of the original volume. The resulting solution was kept in the fridge. After two days, a white precipitate appeared, which was filtered off, washed with 5 mL of cold  $Et_2O$  and dried in vacuum. Suitable crystals for X-ray diffraction were obtained by recrystallization of the obtained solid in EtOH for 11 days in the fridge.

Yield: 24.5% (0.074 g).  $^1H$  NMR ( $CDCl_3$ , 400 MHz, ppm):  $\delta$  = 7.24 (m, 4H, *Ph*), 5.86 (s, 2H, *CH*(Pz)), 4.46 (s, 4H, *OCH\_2Ph*), 4.33 (t, 4H,  $^3J = 5.3$  Hz,  $N_{Pz}CH_2CH_2O$ ), 3.71 (t, 4H,  $^3J = 5.4$  Hz,  $N_{Pz}CH_2CH_2O$ ), 2.29 (s, 6H, *CH\_3*(Pz)), 2.20 (s, 6H, *CH\_3*(Pz)).  $^{13}C\{^1H\}$  NMR ( $CDCl_3$ , 100.6 MHz, ppm):  $\delta$  = 142.4, 141.5 (Pz-C), 136.0 (*Ph-CH\_2O*), 129.3, 128.3 (*Ph-H*), 106.2 (*CH*(Pz)), 71.3 (*Ph-CH\_2O*), 69.3 ( $N_{Pz}CH_2CH_2O$ ), 48.4 ( $N_{Pz}CH_2CH_2O$ ), 13.6, 11.5 (*CH\_3*(Pz)). FTIR-ATR (wavenumber,  $cm^{-1}$ ): 3515(br) [ $\nu(O-H)$ ], 2925-2863(m) [ $\nu(C-H)_{al}$ ], 1550(s) [ $\nu(C=C)_{ar}/\nu(C=N)_{ar}$ ], 1489(w), 1469(w), 1442(s), 1420(m) [ $\delta(C=C)_{ar}/\delta(C=N)_{ar}$ ], 1375(s), 1356(m), 1281(m), 1255(w), 1216(w), 1209(w), 1184(w), 1123(s), 1101(s) [ $\nu(C-O-C)$ ], 1068(m), 1027(s) [ $\delta(C-H)_{ip}$ ], 1022(m), 984(w), 874(w), 843(w), 805(m) [ $\delta(C-H)_{oop}$ ], 752(s) [ $\delta(C-H)_{oop}$ ], 658(w), 631(m). UV-Vis: ( $CH_3CN$ ,  $1.34 \cdot 10^{-4}$  M)  $\lambda_{max}$  ( $\square$  ( $M^{-1}cm^{-1}$ )) = 219 nm ( $1.66 \cdot 10^4$ ). Fluorescence ( $CH_3CN$ ):  $\lambda_{ex} = 260$  nm,  $\lambda_{em} = 286$  nm. Elemental analysis calc. (%) for  $C_{23}H_{33}HgCl_2N_4O_{2.5}$  (677.02): C 40.80; H 4.98; N 8.27. Found: C 40.70; H 4.76; N 8.05.

#### 4.8 Crystallographic Data

The crystallographic data of complexes **1-3** and **4-6** are gathered in Tables 6 and 7, respectively. Suitable crystals for X-ray elucidation were obtained by recrystallization of the compounds in EtOH. Measured crystals were prepared under inert conditions, immersed in perfluoropolyether as protecting oil for manipulation. Suitable crystals were mounted on MiTeGen Micromounts and used for data collection. Crystallographic data for **1-3** was collected at 100 K at XALOC beamline at ALBA synchrotron ( $\lambda = 0.72931$  Å). Crystallographic data for compounds **4-6** was collected with a Bruker D8 Venture

diffractometer ( $\lambda = 1.54178$  (**4**);  $\lambda = 0.71073$  (**5**, **6**). Data was processed with APEX2 program [69] and corrected for absorption using SADABS [70]. The structures were solved by direct methods and subsequently refined by correction of  $F^2$  against all reflections [71] and Olex2 as the graphical interface [72]. All non-hydrogen atoms were refined with anisotropic thermal parameters by full-matrix least-squares calculations on  $F^2$ . All hydrogen atoms were located in difference Fourier maps and included as fixed contributions riding on attached atoms with isotropic thermal displacement parameter 1.2 or 1.5 (O–H) times those of the respective atom. The contribution of the disordered solvent molecules to the diffraction pattern could not be rigorously included in the model and were consequently removed with the SQUEEZE routine of PLATON [73] (0.5 molecules of EtOH for **5** and **6**). This contribution has been included in the empirical formula to give the correct calculated density, absorption coefficient and molecular weight. Details of the structure determination and refinement of compounds are summarized in Tables 6 and 7. **5** was treated as a two-component non-merohedral twin; the exact twin matrix identified by the integration program was found to be  $\begin{pmatrix} -1 & 0 & -0.5 & 0 \\ -1 & 0 & 0 & 0 \\ 0 & 0 & 0 & 1 \end{pmatrix}$ . The structure of **5** was solved using direct methods with only the non-overlapping reflections of component 1. The structure was refined using the HKLF 5 routine with all reflections of component 1 (including the overlapping ones), resulting in a BASF value of 0.317. Complete information about crystal structure and molecular geometry is available in CIF format as Supporting Information. CCDC 1954385-1954390 (**1-6**) contain the supplementary data for this paper. Molecular graphics were generated using MERCURY software [74,75] with POV-Ray package [76]. Colour codes for all molecular graphics are: grey (C), red (O), light-blue (N), white (H), green (Cl), blue-grey (Zn), bone (Cd) and light-grey (Hg).

Formula	C <sub>44</sub> H <sub>60</sub> Zn <sub>2</sub> Cl <sub>4</sub> N <sub>8</sub> O <sub>4</sub> ( <b>1</b> )	C <sub>44</sub> H <sub>60</sub> Cd <sub>2</sub> Cl <sub>4</sub> N <sub>8</sub> O <sub>4</sub> ( <b>2</b> )	C <sub>44</sub> H <sub>60</sub> Hg <sub>2</sub> Cl <sub>4</sub> N <sub>8</sub> O <sub>4</sub> ( <b>3</b> )
Formula Weight	1037.54	1131.60	1307.98
Temperature (K)	100(2)	100(2)	100(2)
Wavelength (Å)	0.72932	0.72929	0.72931
System, space group	Monoclinic, P2 <sub>1</sub> /n	Monoclinic, P2 <sub>1</sub> /n	Monoclinic P2 <sub>1</sub> /n
a (Å)	9.5030(4)	9.5328(8)	9.5573(4)
b (Å)	19.1113(9)	19.3000(16)	19.2939(7)
c (Å)	13.3218(6)	13.5436(11)	13.5592(5)
α (°)	90	90	90
β (°)	96.203(2)	97.179(2)	97.3560(10)
γ (°)	90	90	90
U (Å <sup>3</sup> ) / Z	2405.27(19) / 2	2472.3(4) / 2	2479.71(17) / 2
D <sub>calc</sub> (g cm <sup>-3</sup> ) / μ (mm <sup>-1</sup> )	1.433 / 1.353	1.520 / 1.196	1.752 / 6.872
F(000)	1080	1152	1280
Crystal size (mm <sup>3</sup> )	0.12x0.1x0.1	0.11x0.1x0.1	0.1x0.1x0.08
hkl ranges	-11≤h≤11, -22≤k≤22, -15≤l≤15	-11≤h≤11, -23≤k≤23, -16≤l≤16	-11≤h≤11, -22≤k≤22, -16≤l≤16
θ Range (°)	1.920 to 25.773	2.461 to 25.812	1.894 to 25.728
Reflections collected/unique/ [R <sub>int</sub> ]	17476 / 4097 / 0.0516	19112 / 4111 / 0.0646	42758/ 4370 / 0.0719
Completeness to θ (%)	95.9	93.2	99.6
Absorption correction	Semi-empirical from equivalents	Semi-empirical from equivalents	Semi-empirical from equivalents
Max. and min. trans.	0.0189 and 0.0048	0.0922 and 0.0385	0.0961 to 0.0280
Data/restraints/ parameters	4097 / 0 / 284	4111 / 0 / 284	4370 / 0 / 285
Goodness-of-fit on F <sup>2</sup>	1.064	1.074	1.174
Final R indices [I>2σ (I)]	R1= 0.0457 wR2= 0.1320	R1= 0.0672 wR2= 0.1866	R1= 0.0695 wR2= 0.1714
R indices (all data)	R1= 0.0466 wR2= 0.1344	R1= 0.0688 wR2= 0.1906	R1= 0.0707 wR2= 0.1738
Largest diff. peak and hole (e Å <sup>-3</sup> )	1.134 and -0.723	1.108 and -0.889	2.049 and -4.641

**Table 6.** Crystallographic data for compounds **1-3**

Formula	$C_{44}H_{62}Zn_2Cl_4N_8O_5$ (4)	$C_{23}H_{33}CdCl_2N_4O_{2.5}$ (5)	$C_{23}H_{33}HgCl_2N_4O_{2.5}$ (6)
Formula Weight	1055.55	588.83	677.02
Temperature (K)	100.0	100(2)K	298(2)K
Wavelength (Å)	1.54178	0.71073	0.71073
System, space group	Monoclinic, C2/c	Monoclinic, P2 <sub>1</sub> /n	Monoclinic, P2 <sub>1</sub> /n
a (Å)	29.965(4)	11.1004(3)	11.1617(19)
b (Å)	8.0447(12)	12.9995(3)	13.094(2)
c (Å)	23.742(4)	18.6202(5)	18.698(4)
$\alpha$ (°)	90	90	90
$\beta$ (°)	122.071(7)	101.2850(10)	99.661(7)
$\gamma$ (°)	90	90	90
U (Å <sup>3</sup> ) / Z	4849.9(12) / 4	2634.94(12) / 4	2693.8(8) / 4
D <sub>calc</sub> (g cm <sup>-3</sup> ) / $\mu$ (mm <sup>-1</sup> )	1.446 / 3.665	1.484 / 1.060	1.669 / 5.940
F(000)	2200	1204	1332
Crystal size (mm <sup>3</sup> )	0.1 x 0.08 x 0.08	0.12 x 0.1 x 0.08	0.1 x 0.1 x 0.08
hkl ranges	-35 ≤ h ≤ 35, -7 ≤ k ≤ 9, -28 ≤ l ≤ 27	-14 ≤ h ≤ 14, 0 ≤ k ≤ 16, 0 ≤ l ≤ 24	-13 ≤ h ≤ 13, -15 ≤ k ≤ 15, -20 ≤ l ≤ 22
$\theta$ Range (°)	3.481 to 66.860	1.923 to 27.494	2.418 to 25.026
Reflections collected/unique/ [R <sub>int</sub> ]	15452 / 4279 / 0.0653	5995 / 5995 / 0.0945	37205 / 4760 / 0.1006
Completeness to $\theta$ (%)	99.3	99.1	99.8
Absorption correction	Semi-empirical from equivalents	Semi-empirical From equivalents	Semi-empirical From equivalents
Max. and min. trans.	0.7528 and 0.6573	0.745684 and 0.349755	0.7454 and 0.4502
Data/restraints/ parameters	4279 / 0 / 289	5995 / 0 / 285	4760 / 0 / 284
Goodness-of-fit on F <sup>2</sup>	1.058	1.057	1.011
Final R indices [I > 2 $\sigma$ (I)]	R1= 0.0452 wR2= 0.0909	R1= 0.0547 wR2= 0.1695	R1= 0.0409 wR2= 0.0719
R indices (all data)	R1= 0.0766 wR2= 0.1033	R1= 0.0589 wR2= 0.1799	R1= 0.0800 wR2= 0.0844
Largest diff. peak and hole (e Å <sup>-3</sup> )	0.356 and -0.527	1.961 and -1.256	0.851 and -0.977

**Table 7.** Crystallographic data for compounds 4-6

## Declaration of Competing Interest

The authors declare that they have no known competing financial interest or personal relationships that could have appeared to influence the work reported on this paper.

## Acknowledgements

J.P. thanks CB615921 project, the CB616406 project from “Fundació La Caixa”, and the Generalitat de Catalunya (2017/SGR/1687). J.G.P. thanks MEC grant CTQ2016-75150-R and the Generalitat de Catalunya (2017/SGR/1720). D.C.L thanks MEC grant PGC2018-102047-B for financial support. J.S. also acknowledges the PIF pre-doctoral Fellowship from the Universitat Autònoma de Barcelona for his pre-doctoral grant. Some of the experiments were performed at the XALOC beamline of the ALBA synchrotron with the support of ALBA staff.

## Appendix A. Supplementary Data

Complete Powder X-ray diffractograms, FTIR-ATR spectra, additional figures,  $^1\text{H}$ ,  $^{13}\text{C}\{^1\text{H}\}$ , HSQC and DOSY NMR spectra and UV-Vis spectra are available as Supporting Information. CCDC 1954385-1954390 (1-6) contain the supplementary crystallographic data for this paper. These data can be obtained free of charge via <http://www.ccdc.cam.ac.uk/conts/retrieving.html> or from the Cambridge Crystallographic Center, 12 Union Road, Cambridge CB2 1 Ez, UK; fax: (+44)1223-336-033; or e-mail: [deposit@ccdc.cam.ac.uk](mailto:deposit@ccdc.cam.ac.uk).

Supplementary data for this article can be found online at <https://doi.org/10.XXX/XXXXX>

## References

- [1] F.A. Almeida Paz, J. Klinowski, S.M.F. Vilela, J.P.C. Tomé, J.A.S. Cavaleiro, J. Rocha, *Chem. Soc. Rev.* 41 (2012) 1088-1110.
- [2] T.R. Cook, Y.R. Zheng, P.J. Stang, *Chem. Rev.* 113 (2013) 734-777.
- [3] M. Eddaoudi, D.B. Moler, H. Li, B. Chen, T.M. Reineke, M. O’Keeffe, O.M. Yaghi, *Acc. Chem. Res.* 34 (2001) 319-330.

- [4] M.E. Davis, *Nature* 417 (2002) 813-821.
- [5] R.J. Kuppler, D.J. Timmons, Q.R. Fang, J.R. Li, T.A. Makal, M.D. Young, D. Yuan, D. Zhao, W. Zhuang, H.C. Zhou, *Coord. Chem. Rev.* 253 (2009) 3042-3066.
- [6] P. Silva, S.M.F. Vilela, J.P.C. Tomé, F.A. Almeida Paz, *Chem. Soc. Rev.* 44 (2015) 6774-6803.
- [7] G. Maurin, C. Serre, A. Coper, G. Férey, *Chem. Soc. Rev.* 46 (2017) 3104-3107.
- [8] J.P. Zhang, Y.B. Zang, J.B. Lin, X.M. Chen, *Chem. Rev.* 112 (2012) 1001-1033.
- [9] F. Marchetti, C. Pettinari, C. Di Nicola, A. Tombesi, R. Pettinari, *Coord. Chem. Rev.* 401 (2019) 210369.
- [10] A. Otero, J. Fernández-Baeta, A. Lara-Sánchez, L.F. Sánchez-Barba, *Coord. Chem. Rev.* 257 (2013) 1806-1868.
- [11] Y.K. Kang, J.H. Jeong, N.Y. Lee, H. Lee, *Polyhedron* 12 (2010) 2404-2408.
- [12] S. Shin, S.H. Ahn, M.H. Jung, S. Nayab, H. Lee, *J. Coord. Chem.* 69 (2016) 2391-2402.
- [13] M. Strianese, S. Milione, V. Bertolasi, C. Pellechia, A. Grassi, *Inorg. Chem.* 3 (2011) 900-910.
- [14] S.S. Masoud, F.R. Louka, G.T. Ducharme, R.C. Fischer, F.A. Mautner, J. Vanco, R. Herchel, Z. Dvorak, Z. Travnicek, *J. Inorg. Biochem.* 180 (2018) 39-46.
- [15] F.L. Yang, G.Z. Zhu, B.B. Liang, Y.H. Shi, X.L. Li *Polyhedron* 128 (2017) 104-111.
- [16] G.N. Liu, W.J. Zhu, Y.N. Chu, C. Li, *Inorg. Chim. Acta* 425 (2015) 28-35.
- [17] R. Mukherjee, *Coord. Chem. Rev.* 203 (2000) 151-218.
- [18] C. Pettinari, A. Tabacaru, S. Galli, *Coord. Chem. Rev.* (2016) 1-31.
- [19] I. Alkorta, R.M. Claramunt, E. Díaz-Barra, J. Elguero, A. de La Hoz, *Coord. Chem. Rev.* 339 (2017) 153-182.



- [20] R. Mondal, T. Basu, D. Sadhukhan, T. Chattopadhyay, M.K. Bhunia, *Cryst. Growth Des.* 9 (2009) 1095-1105.
- [21] A. Tabacaru, C. Pettinari, N. Masciocci, S. Galli, F. Marchetti, M. Angjellari, *Inorg. Chem.* 50 (2011) 11506-11513.
- [22] A. Tabacaru, C. Pettinari, F. Marchietti, S. Galli, N. Masciocchi, *Cryst. Growth Des.* 14 (2014) 3142-3152.
- [23] V. Nobakht, A. Beheshti, D.M. Prosperio, L. Carlucci, C.T. Abrahams, *Inorg. Chim. Acta* 414 (2014) 217-225.
- [24] S.S. Masoud, M. Dubin, A.E. Guilbeau, M. Spell, R. Vicente, P. Wilfling, R.C. Fishcer, F.A. Mautner, *Polyhedron* 78 (2014) 135-140.
- [25] J. Cubanski, S. Cameron, J. Crowley, A. Blackman, *Dalton Trans.* 42 (2013) 2174-2185.
- [26] A. Adach, *J. Coord. Chem.* 5 (2017) 757-779.
- [27] A. Pañella, J. Pons, J. García-Antón, X. Solans, M. Font-Bardia, J. Ros, *Eur. J. Inorg. Chem.* 8 (2006) 1678-1685.
- [28] M.C. Castellano, J. Pons, J. García-Antón, X. Solans, M. Font-Bardia, J. Ros, *Inorg. Chim. Acta* 361 (2008) 2923-2928.
- [29] J. García-Antón, J. Pons, X. Solans, M. Font-Bardia, J. Ros, *Eur. J. Inorg. Chem.* 12 (2002) 3319-3327.
- [30] A. León, J. Pons, J. García-Antón, X. Solans, M. Font-Bardia, J. Ros, *Inorg. Chim. Acta* 360 (2007) 2071-2082.
- [31] A. León, M. Guerrero, J. García-Antón, J. Ros, M. Font-Bardia, J. Pons, *CrystEngComm* 15 (2013) 1762-1771.
- [32] M. Guerrero, J. García-Antón, M. Tristany, J. Pons, J. Ros, K. Philippot, P. Lecante, B. Chaudret, *Langmuir* 26 (2010) 15532-15540.
- [33] M. Guerrero, J. Pons, T. Parella, M. Font-Bardia, T. Calvet, J. Ros, *Inorg. Chem.* 48 (2009) 8736-8750.

- [34] M. Guerrero, J. Pons, J. Ros, M. Font-Bardia, V. Branchadell, *Cryst. Growth Des.* 12 (2012) 3700-3708.
- [35] M. Guerrero, J. Pons, V. Branchadell, T. Parella, X. Solans, M. Font-Bardia, J. Ros, *Inorg. Chem.* 47 (2008) 11084-11094.
- [36] K. Nakamoto, *Infrared and Raman spectra of inorganic and coordination compounds. Part B: Applications in Coordination, Organometallic and Bioinorganic Chemistry*, 6<sup>th</sup> ed.; Wiley-VCH: Weinheim, 2009.
- [37] L. Yang, D.R. Powell, R.P. Houser, *Dalton Trans.* 9 (2007) 955-964.
- [38] F. Allen, *Acta Cryst.* B58 (2002) 380-388.
- [39] L. Phil, L. Wang, J.W. Gilje, L. Hilfert, F.T. Edelman, *Polyhedron* 164 (2019) 228-235.
- [40] D.L. Reger, A.E. Pascui, P.J. Pellechia, M.D. Smith, *Inorg. Chem.* 52 (2013) 11638-11649.
- [41] D.L. Reger, A.E. Pascui, E.A. Foley, M.D. Smith, *Inorg. Chem.* 56 (2017) 2884-2901.
- [42] D.L. Reger, E.A. Foley, M.D. Smith, *Inorg. Chem.* 48 (2009) 936-945.
- [43] A. Beheshti, A. Lalegani, F. Behvandi, F. Safaeiyan, A. Sarkarzadeh, G. Bruno, H.A. Rudbari, *J. Mol. Struct.* 1082 (2015) 143-150.
- [44] M.A. Spackman, J.J. McKinnon, *CrystEngComm* 4 (2002) 378-382.
- [45] S.K. Wolff, D.J. Grimwood, J.J. McKinnon, D. Jayatilaka, M.A. Spackman, *Crystal Explorer (version 2.1)*, University of Western Australia: Crawley (Australia) 2007.
- [46] M. A. Spackman, D. Jayatilaka, *CrystEngComm* 11 (2009) 19-32.
- [47] O. Coughlin, N. De Bruyn, D.P.A. Kilgour, S.L. Benjamin, *J. Chem. Cryst.* (2019), DOI: 10.1007/s10870-019-00789-2.
- [48] S.K. Seth, G.C. Maity, T. Kar, *J. Mol. Struct.* 1000 (2011) 120-126.
- [49] D.L. Reger, E.A. Foley, R.F. Semeniuc, M.D. Smith, *Inorg. Chem.* 46 (2007) 11345-11355.

- [50] S. Shin, S. H. Ahn, S. Choi, S.I. Choi, S. Nayab, H. Lee, *Polyhedron* 110 (2016) 149-156.
- [51] S. Milione, C. Capacchione, C. Cuomo, M. Strianese, V. Bertolasi, A. Grassi, *Inorg. Chem.* 48 (2009) 9510-9518.
- [52] V. Balamurgan, R. Mukherjee, *CrystEngComm* 7 (2005) 337-341.
- [53] A. W. Addison, T.N. Rao, *J. Chem. Soc., Dalton Trans.* 1 (1984) 1349-1356.
- [54] A. Santra, P. Mondal, M. Acharjya, P. Bera, A. Panja, T.K. Mandal, P. Mitra, P. Bera, *Polyhedron* 113 (2016) 5-15.
- [55] B. Hollo, Z.D. Tomic, P. Pogany, A. Kovacs, V.M. Leovac, K.M. Szecsenyi, *Polyhedron* 28 (2009) 3881-3889.
- [56] J.H. Liu, X.Y. Wu, Q.Z. Zhang, X. He, W.B. Yang, C.Z. Lu, *J. Coord. Chem.* 60 (2007) 1373-1379.
- [57] I. Del Hierro, I. Sierra, F. Carrillo-Hermosilla, I. López-Solera, M. Fajardo, *Inorg. Chim. Acta* 355 (2003) 347-353.
- [58] A. Lalegani, M.K. Sardashti, H. Salavati, A. Asadi, R. Gajda, K. Wozniak, *J. Mol. Struct.* 1108 (2016) 288-293.
- [59] S. Javed, V. Balamurugan, W. Jacob, A.K. Shama, R. Mukherjee, *Indian J. Chem. Sect. A: Inorg., Bio-inorg., Phys., Theor. Anal. Chem.* 50 (2011) 1248-1258.
- [60] S.P. Argent, H. Adams, T. Riis-Johannessen, T.C. Jeffery, L.P. Harding, W. Clegg, R.W. Harrington, M.D. Ward, *Dalton Trans.* 46 (2006) 4996-5013.
- [61] K.F. Morris, C.S. Johnson, *J. Am. Chem. Soc.* 114 (1992) 3139-3141.
- [62] A. Gasnier, J.M. Barbe, C. Bucher, F. Denat, J.C. Moutet, E. Saint-Aman, P. Terech, G. Royal, *Inorg. Chem.* 47 (2008) 1862-1864.
- [63] J.M.J. Paulusse, R.P. Sijbesma, *Chem. Commun.* 9 (2003) 1494-1495.
- [64] R. Evans, Z. Deng, A.K. Rogerson, A.S. McLachlan, J.J. Richards, M. Nilsson, G.A. Morris, *Angew. Chem. Int. Ed.* 52 (2013) 3199-3202.

- [65] A.W.J. Poh, J.A. Aguilar, A.M. Kenwright, K. Mason, D. Parker, *Chem. Eur. J.* 24 (2018) 16170-16175.
- [66] E.L. Que, D.W. Domaille, C J. Chang, *Chem. Rev.* 108 (2008) 1517-1549.
- [67] A. Visscher, S. Bachmann, C. Schnegelsberg, T. Teuteberg, R.A. Mata, D. Stalke, *Dalton Trans.* 45 (2016) 5689-5699.
- [68] Origin(Pro) (Version 8.69), OriginLab Corporation, Northampton, Massachusetts (USA), 2011.
- [69] Bruker APEX2 Software, (V2014.0-1), Bruker AXS Inc., Madison, Wisconsin (USA), 2014.
- [70] L. Krause, R. Herbst-Irmer, G.M. Sheldrick, D. Stalke, *J. Appl. Cryst.* 48 (2015) 3-10.
- [71] G.M. Sheldrick, *Acta Cryst. A* 64 (2008) 112-122.
- [72] O.V. Dolomanov, L.J. Bourhis, R.J. Gildea, J.A.K. Howard, H. Puschmann, *J. Appl. Cryst.* 42 (2009) 339-341.
- [73] A.L. Spek, *J. Appl. Cryst.* 36 (2003) 7-13.
- [74] C.F. Macrae, P.R. Edgington, P. McCabe, E. Pidcock, G.P. Shields, R. Taylor, M. Towler, J. Van De Streek, *J. Appl. Cryst.* 39 (2006) 453-457.
- [75] C.F. Macrae, I.J. Bruno, J.A. Chisholm, P.R. Edgington, P. McCabe, E. Pidcock, L. Rodriguez-Mongue, R. Taylor, J. Van De Streek, P.A. Wood, *J. Appl. Cryst.* 41 (2008) 466-470.
- [76] Persistence of Vision Pty. Ltd., Persistence of Vision (TM) Raytracer, Persistence of Vision Pty. Ltd., Williamstown, Victoria (Australia), 2004.

## Declaration of interests

The authors declare that they have no known competing financial interests or personal relationships that could have appeared to influence the work reported in this paper.

The authors declare the following financial interests/personal relationships which may be considered as potential competing interests:

## checkCIF/PLATON report

You have not supplied any structure factors. As a result the full set of tests cannot be run.

THIS REPORT IS FOR GUIDANCE ONLY. IF USED AS PART OF A REVIEW PROCEDURE FOR PUBLICATION, IT SHOULD NOT REPLACE THE EXPERTISE OF AN EXPERIENCED CRYSTALLOGRAPHIC REFEREE.

No syntax errors found.      CIF dictionary      Interpreting this report

### Datablock: js98\_a

---

Bond precision:    C-C = 0.0041 A                      Wavelength=0.72932

Cell:                      a=9.5030(4)              b=19.1113(9)              c=13.3218(6)  
                                    alpha=90              beta=96.203(2)              gamma=90

Temperature:              100 K

	Calculated	Reported
Volume	2405.27(19)	2405.27(19)
Space group	P 21/n	P 1 21/n 1
Hall group	-P 2yn	-P 2yn
Moiety formula	C44 H60 Cl4 N8 O4 Zn2	C44 H60 Cl4 N8 O4 Zn2
Sum formula	C44 H60 Cl4 N8 O4 Zn2	C44 H60 Cl4 N8 O4 Zn2
Mr	1037.58	1037.54
Dx,g cm-3	1.433	1.433
Z	2	2
Mu (mm-1)	1.357	1.353
F000	1080.0	1080.0
F000'	1082.65	
h,k,lmax	11,22,15	11,22,15
Nref	4269	4097
Tmin,Tmax		0.005,0.019
Tmin'		

Correction method= # Reported T Limits: Tmin=0.005 Tmax=0.019  
AbsCorr = MULTI-SCAN

Data completeness= 0.960                      Theta(max)= 25.773

R(reflections)= 0.0457( 3906)              wR2(reflections)= 0.1344( 4097)

S = 1.064                      Npar= 284

---

The following ALERTS were generated. Each ALERT has the format

**test-name\_ALERT\_alert-type\_alert-level.**

Click on the hyperlinks for more details of the test.

---

**Alert level B**

PLAT029\_ALERT\_3\_B \_diffrn\_measured\_fraction\_theta\_full value Low . 0.959 Why?

**Author Response: A full set of data was collected, however the very high angle data was dominated by noise and was omitted.**

---

**Alert level C**

PLAT053\_ALERT\_1\_C Minimum Crystal Dimension Missing (or Error) ... Please Check  
PLAT054\_ALERT\_1\_C Medium Crystal Dimension Missing (or Error) ... Please Check  
PLAT055\_ALERT\_1\_C Maximum Crystal Dimension Missing (or Error) ... Please Check

---

**Alert level G**

PLAT072\_ALERT\_2\_G SHELXL First Parameter in WGHT Unusually Large 0.10 Report  
PLAT092\_ALERT\_4\_G Check: Wavelength Given is not Cu,Ga,Mo,Ag,In Ka 0.72932 Ang.  
PLAT933\_ALERT\_2\_G Number of OMIT Records in Embedded .res File ... 3 Note  
PLAT984\_ALERT\_1\_G The Zn-f'=' 0.297 Deviates from the B&C-Value 0.276 Ch  
PLAT985\_ALERT\_1\_G The Zn-f"=' 1.535 Deviates from the B&C-Value 1.505 Ch

- 
- 0 **ALERT level A** = Most likely a serious problem - resolve or explain  
1 **ALERT level B** = A potentially serious problem, consider carefully  
3 **ALERT level C** = Check. Ensure it is not caused by an omission or oversight  
5 **ALERT level G** = General information/check it is not something unexpected
- 5 ALERT type 1 CIF construction/syntax error, inconsistent or missing data  
2 ALERT type 2 Indicator that the structure model may be wrong or deficient  
1 ALERT type 3 Indicator that the structure quality may be low  
1 ALERT type 4 Improvement, methodology, query or suggestion  
0 ALERT type 5 Informative message, check
-

It is advisable to attempt to resolve as many as possible of the alerts in all categories. Often the minor alerts point to easily fixed oversights, errors and omissions in your CIF or refinement strategy, so attention to these fine details can be worthwhile. In order to resolve some of the more serious problems it may be necessary to carry out additional measurements or structure refinements. However, the purpose of your study may justify the reported deviations and the more serious of these should normally be commented upon in the discussion or experimental section of a paper or in the "special\_details" fields of the CIF. checkCIF was carefully designed to identify outliers and unusual parameters, but every test has its limitations and alerts that are not important in a particular case may appear. Conversely, the absence of alerts does not guarantee there are no aspects of the results needing attention. It is up to the individual to critically assess their own results and, if necessary, seek expert advice.

### **Publication of your CIF in IUCr journals**

A basic structural check has been run on your CIF. These basic checks will be run on all CIFs submitted for publication in IUCr journals (*Acta Crystallographica*, *Journal of Applied Crystallography*, *Journal of Synchrotron Radiation*); however, if you intend to submit to *Acta Crystallographica Section C* or *E* or *IUCrData*, you should make sure that full publication checks are run on the final version of your CIF prior to submission.

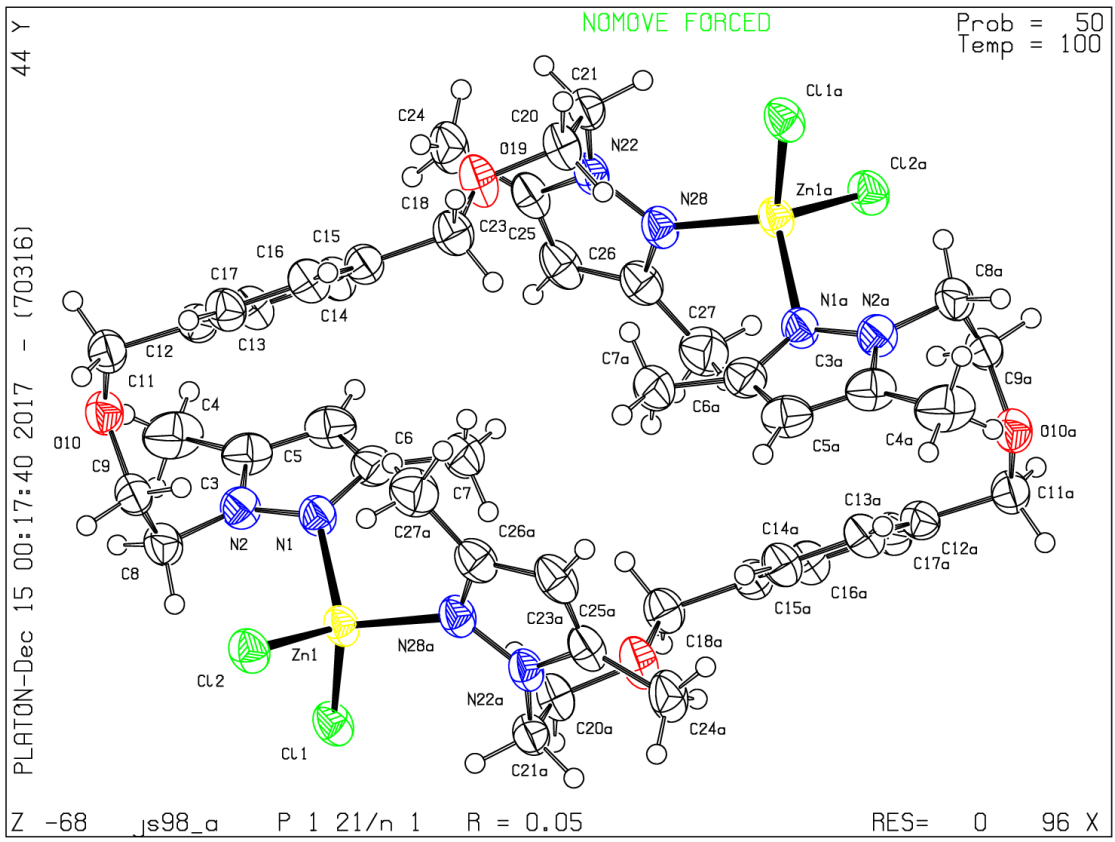
### **Publication of your CIF in other journals**

Please refer to the *Notes for Authors* of the relevant journal for any special instructions relating to CIF submission.

---

**PLATON version of 13/12/2017; check.def file version of 12/12/2017**





# checkCIF/PLATON report

You have not supplied any structure factors. As a result the full set of tests cannot be run.

THIS REPORT IS FOR GUIDANCE ONLY. IF USED AS PART OF A REVIEW PROCEDURE FOR PUBLICATION, IT SHOULD NOT REPLACE THE EXPERTISE OF AN EXPERIENCED CRYSTALLOGRAPHIC REFEREE.

No syntax errors found.      CIF dictionary      Interpreting this report

## Datablock: js173

---

Bond precision:    C-C = 0.0081 A                      Wavelength=0.72929

Cell:                      a=9.5328(8)              b=19.3000(16)              c=13.5436(11)  
                                    alpha=90                      beta=97.179(2)              gamma=90

Temperature:              100 K

	Calculated	Reported
Volume	2472.3(4)	2472.3(4)
Space group	P 21/n	P2(1)/n
Hall group	-P 2yn	-P 2yn
Moiety formula	C44 H60 Cd2 Cl4 N8 O4	C44 H60 Cd2 Cl4 N8 O4
Sum formula	C44 H60 Cd2 Cl4 N8 O4	C44 H60 Cd2 Cl4 N8 O4
Mr	1131.62	1131.60
Dx,g cm-3	1.520	1.520
Z	2	2
Mu (mm-1)	1.190	1.196
F000	1152.0	1152.0
F000'	1150.66	
h,k,lmax	11,23,16	11,23,16
Nref	4411	4111
Tmin,Tmax		0.038,0.092
Tmin'		

Correction method= # Reported T Limits: Tmin=0.038 Tmax=0.092  
AbsCorr = MULTI-SCAN

Data completeness= 0.932                      Theta(max)= 25.812

R(reflections)= 0.0672( 3963)              wR2(reflections)= 0.1906( 4111)

S = 1.074                      Npar= 284

---

The following ALERTS were generated. Each ALERT has the format

**test-name\_ALERT\_alert-type\_alert-level.**

Click on the hyperlinks for more details of the test.


---

 **Alert level A**

PLAT029\_ALERT\_3\_A \_diffrn\_measured\_fraction\_theta\_full value Low . 0.932 Why?


**Author Response: Crystal diffracted quite weakly at high angle due to their rather low quality and data were cut off according to intensity statistics**

---

 **Alert level C**

PLAT342\_ALERT\_3\_C Low Bond Precision on C-C Bonds ..... 0.00806 Ang.

---

 **Alert level G**

ABSMU01\_ALERT\_1\_G Calculation of \_exptl\_absorpt\_correction\_mu  
not performed for this radiation type.

PLAT012_ALERT_1_G No _shelx_res_checksum Found in CIF .....	Please Check
PLAT072_ALERT_2_G SHELXL First Parameter in WGHT Unusually Large	0.14 Report
PLAT092_ALERT_4_G Check: Wavelength Given is not Cu,Ga,Mo,Ag,In Ka	0.72929 Ang.
PLAT794_ALERT_5_G Tentative Bond Valency for Cd1 (II) .	2.05 Info
PLAT883_ALERT_1_G No Info/Value for _atom_sites_solution_primary .	Please Do !
PLAT933_ALERT_2_G Number of OMIT Records in Embedded .res File ...	62 Note
PLAT984_ALERT_1_G The Cd-f' = -0.7547 Deviates from the B&C-Value	-0.7317 Check
PLAT985_ALERT_1_G The Cd-f" = 1.2858 Deviates from the B&C-Value	1.2647 Check

- 
- 1 **ALERT level A** = Most likely a serious problem - resolve or explain
  - 0 **ALERT level B** = A potentially serious problem, consider carefully
  - 1 **ALERT level C** = Check. Ensure it is not caused by an omission or oversight
  - 9 **ALERT level G** = General information/check it is not something unexpected

- 5 ALERT type 1 CIF construction/syntax error, inconsistent or missing data
  - 2 ALERT type 2 Indicator that the structure model may be wrong or deficient
  - 2 ALERT type 3 Indicator that the structure quality may be low
  - 1 ALERT type 4 Improvement, methodology, query or suggestion
  - 1 ALERT type 5 Informative message, check
- 
-

It is advisable to attempt to resolve as many as possible of the alerts in all categories. Often the minor alerts point to easily fixed oversights, errors and omissions in your CIF or refinement strategy, so attention to these fine details can be worthwhile. In order to resolve some of the more serious problems it may be necessary to carry out additional measurements or structure refinements. However, the purpose of your study may justify the reported deviations and the more serious of these should normally be commented upon in the discussion or experimental section of a paper or in the "special\_details" fields of the CIF. checkCIF was carefully designed to identify outliers and unusual parameters, but every test has its limitations and alerts that are not important in a particular case may appear. Conversely, the absence of alerts does not guarantee there are no aspects of the results needing attention. It is up to the individual to critically assess their own results and, if necessary, seek expert advice.

### **Publication of your CIF in IUCr journals**

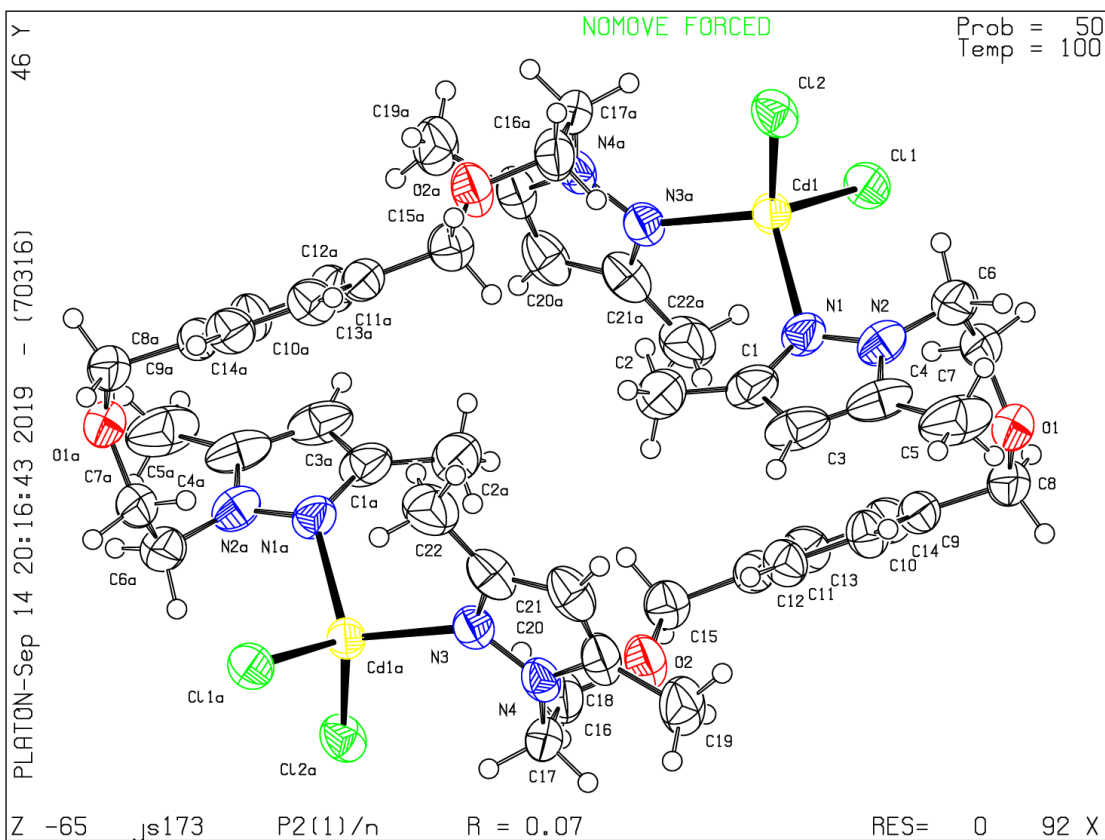
A basic structural check has been run on your CIF. These basic checks will be run on all CIFs submitted for publication in IUCr journals (*Acta Crystallographica*, *Journal of Applied Crystallography*, *Journal of Synchrotron Radiation*); however, if you intend to submit to *Acta Crystallographica Section C* or *E* or *IUCrData*, you should make sure that full publication checks are run on the final version of your CIF prior to submission.

### **Publication of your CIF in other journals**

Please refer to the *Notes for Authors* of the relevant journal for any special instructions relating to CIF submission.

---

**PLATON version of 07/08/2019; check.def file version of 30/07/2019**



# checkCIF/PLATON report

You have not supplied any structure factors. As a result the full set of tests cannot be run.

THIS REPORT IS FOR GUIDANCE ONLY. IF USED AS PART OF A REVIEW PROCEDURE FOR PUBLICATION, IT SHOULD NOT REPLACE THE EXPERTISE OF AN EXPERIENCED CRYSTALLOGRAPHIC REFEREE.

No syntax errors found.      CIF dictionary      Interpreting this report

## Datablock: js272

---

Bond precision:    C-C = 0.0108 A                      Wavelength=0.72931

Cell:                      a=9.5573(4)              b=19.2939(7)              c=13.5592(5)  
                            alpha=90              beta=97.356(1)              gamma=90

Temperature:              100 K

	Calculated	Reported
Volume	2479.71(17)	2479.71(17)
Space group	P 21/n	P2(1)/n
Hall group	-P 2yn	-P 2yn
Moiety formula	C44 H60 Cl4 Hg2 N8 O4	C44 H60 Cl4 Hg2 N8 O4
Sum formula	C44 H60 Cl4 Hg2 N8 O4	C44 H60 Cl4 Hg2 N8 O4
Mr	1307.98	1307.98
Dx,g cm-3	1.752	1.752
Z	2	2
Mu (mm-1)	6.850	6.872
F000	1280.0	1280.0
F000'	1271.47	
h,k,lmax	11,22,16	11,22,16
Nref	4387	4370
Tmin,Tmax		0.028,0.096
Tmin'		

Correction method= # Reported T Limits: Tmin=0.028 Tmax=0.096  
AbsCorr = MULTI-SCAN

Data completeness= 0.996                      Theta(max)= 25.728

R(reflections)= 0.0695( 4329)              wR2(reflections)= 0.1738( 4370)

S = 1.174                      Npar= 285

---

The following ALERTS were generated. Each ALERT has the format  
**test-name\_ALERT\_alert-type\_alert-level.**  
Click on the hyperlinks for more details of the test.

---

### ● Alert level C

PLAT342\_ALERT\_3\_C Low Bond Precision on C-C Bonds ..... 0.01083 Ang.

---

### ● Alert level G

ABSMU01\_ALERT\_1\_G Calculation of \_exptl\_absorpt\_correction\_mu  
not performed for this radiation type.

PLAT012\_ALERT\_1\_G No \_shelx\_res\_checksum Found in CIF ..... Please Check  
PLAT072\_ALERT\_2\_G SHELXL First Parameter in WGHT Unusually Large 0.13 Report  
PLAT092\_ALERT\_4\_G Check: Wavelength Given is not Cu,Ga,Mo,Ag,In Ka 0.72931 Ang.  
PLAT883\_ALERT\_1\_G No Info/Value for \_atom\_sites\_solution\_primary . Please Do !  
PLAT984\_ALERT\_1\_G The Hg-f' = -2.6293 Deviates from the B&C-Value -2.6410 Check  
PLAT985\_ALERT\_1\_G The Hg-f" = 9.6981 Deviates from the B&C-Value 9.6442 Check

---

- 0 **ALERT level A** = Most likely a serious problem - resolve or explain  
0 **ALERT level B** = A potentially serious problem, consider carefully  
1 **ALERT level C** = Check. Ensure it is not caused by an omission or oversight  
7 **ALERT level G** = General information/check it is not something unexpected
- 5 ALERT type 1 CIF construction/syntax error, inconsistent or missing data  
1 ALERT type 2 Indicator that the structure model may be wrong or deficient  
1 ALERT type 3 Indicator that the structure quality may be low  
1 ALERT type 4 Improvement, methodology, query or suggestion  
0 ALERT type 5 Informative message, check
- 

It is advisable to attempt to resolve as many as possible of the alerts in all categories. Often the minor alerts point to easily fixed oversights, errors and omissions in your CIF or refinement strategy, so attention to these fine details can be worthwhile. In order to resolve some of the more serious problems it may be necessary to carry out additional measurements or structure refinements. However, the purpose of your study may justify the reported deviations and the more serious of these should normally be commented upon in the discussion or experimental section of a paper or in the "special\_details" fields of the CIF. checkCIF was carefully designed to identify outliers and unusual parameters, but every test has its limitations and alerts that are not important in a particular case may appear. Conversely, the absence of alerts does not guarantee there are no aspects of the results needing attention. It is up to the individual to critically assess their own results and, if necessary, seek expert advice.

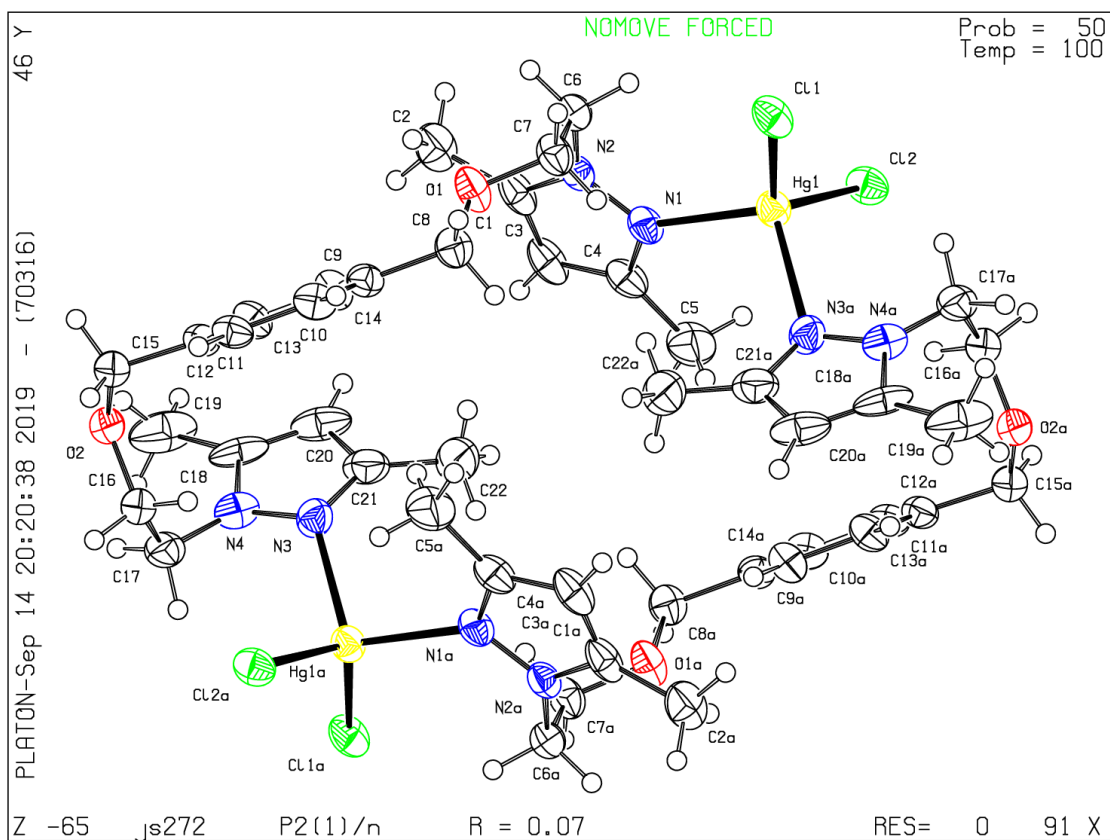
### Publication of your CIF in IUCr journals

A basic structural check has been run on your CIF. These basic checks will be run on all CIFs submitted for publication in IUCr journals (*Acta Crystallographica*, *Journal of Applied Crystallography*, *Journal of Synchrotron Radiation*); however, if you intend to submit to *Acta Crystallographica Section C* or *E* or *IUCrData*, you should make sure that full publication checks are run on the final version of your CIF prior to submission.

### Publication of your CIF in other journals

Please refer to the *Notes for Authors* of the relevant journal for any special instructions relating to CIF submission.

Datablock js272 - ellipsoid plot





## checkCIF/PLATON report

You have not supplied any structure factors. As a result the full set of tests cannot be run.

THIS REPORT IS FOR GUIDANCE ONLY. IF USED AS PART OF A REVIEW PROCEDURE FOR PUBLICATION, IT SHOULD NOT REPLACE THE EXPERTISE OF AN EXPERIENCED CRYSTALLOGRAPHIC REFEREE.

No syntax errors found.      CIF dictionary      Interpreting this report

### Datablock: js109\_7

---

Bond precision:	C-C = 0.0063 A	Wavelength=1.54178	
Cell:	a=29.965(4)	b=8.0447(12)	c=23.742(4)
	alpha=90	beta=122.071(7)	gamma=90
Temperature:	100 K		
	Calculated	Reported	
Volume	4849.8(13)	4849.9(12)	
Space group	C 2/c	C 1 2/c 1	
Hall group	-C 2yc	-C 2yc	
Moiety formula	2(C22 H30 Cl2 N4 O2 Zn), H2 O	2(C22 H30 Cl2 N4 O2 Zn), H2 O	
Sum formula	C44 H62 Cl4 N8 O5 Zn2	C44 H62 Cl4 N8 O5 Zn2	
Mr	1055.60	1055.55	
Dx, g cm-3	1.446	1.446	
Z	4	4	
Mu (mm-1)	3.665	3.665	
F000	2200.0	2200.0	
F000'	2198.23		
h,k,lmax	35,9,28	35,9,28	
Nref	4310	4279	
Tmin,Tmax	0.739,0.746	0.657,0.753	
Tmin'	0.660		

Correction method= # Reported T Limits: Tmin=0.657 Tmax=0.753  
AbsCorr = MULTI-SCAN

Data completeness= 0.993      Theta(max)= 66.860

R(reflections)= 0.0452( 3077)      wR2(reflections)= 0.1033( 4279)

S = 1.058      Npar= 289

---

The following ALERTS were generated. Each ALERT has the format

**test-name\_ALERT\_alert-type\_alert-level.**

Click on the hyperlinks for more details of the test.



### Alert level C

PLAT341\_ALERT\_3\_C Low Bond Precision on C-C Bonds ..... 0.00628 Ang.

---



### Alert level G

PLAT004\_ALERT\_5\_G Polymeric Structure Found with Maximum Dimension 1 Info  
PLAT007\_ALERT\_5\_G Number of Unrefined Donor-H Atoms ..... 1 Report  
PLAT066\_ALERT\_1\_G Predicted and Reported Tmin&Tmax Range Identical ? Check  
PLAT083\_ALERT\_2\_G SHELXL Second Parameter in WGHT Unusually Large 16.17 Why ?  
PLAT128\_ALERT\_4\_G Alternate Setting for Input Space Group C2/c I2/a Note

---

0 **ALERT level A** = Most likely a serious problem - resolve or explain  
0 **ALERT level B** = A potentially serious problem, consider carefully  
1 **ALERT level C** = Check. Ensure it is not caused by an omission or oversight  
5 **ALERT level G** = General information/check it is not something unexpected

1 ALERT type 1 CIF construction/syntax error, inconsistent or missing data  
1 ALERT type 2 Indicator that the structure model may be wrong or deficient  
1 ALERT type 3 Indicator that the structure quality may be low  
1 ALERT type 4 Improvement, methodology, query or suggestion  
2 ALERT type 5 Informative message, check

---

It is advisable to attempt to resolve as many as possible of the alerts in all categories. Often the minor alerts point to easily fixed oversights, errors and omissions in your CIF or refinement strategy, so attention to these fine details can be worthwhile. In order to resolve some of the more serious problems it may be necessary to carry out additional measurements or structure refinements. However, the purpose of your study may justify the reported deviations and the more serious of these should normally be commented upon in the discussion or experimental section of a paper or in the "special\_details" fields of the CIF. checkCIF was carefully designed to identify outliers and unusual parameters, but every test has its limitations and alerts that are not important in a particular case may appear. Conversely, the absence of alerts does not guarantee there are no aspects of the results needing attention. It is up to the individual to critically assess their own results and, if necessary, seek expert advice.

### Publication of your CIF in IUCr journals

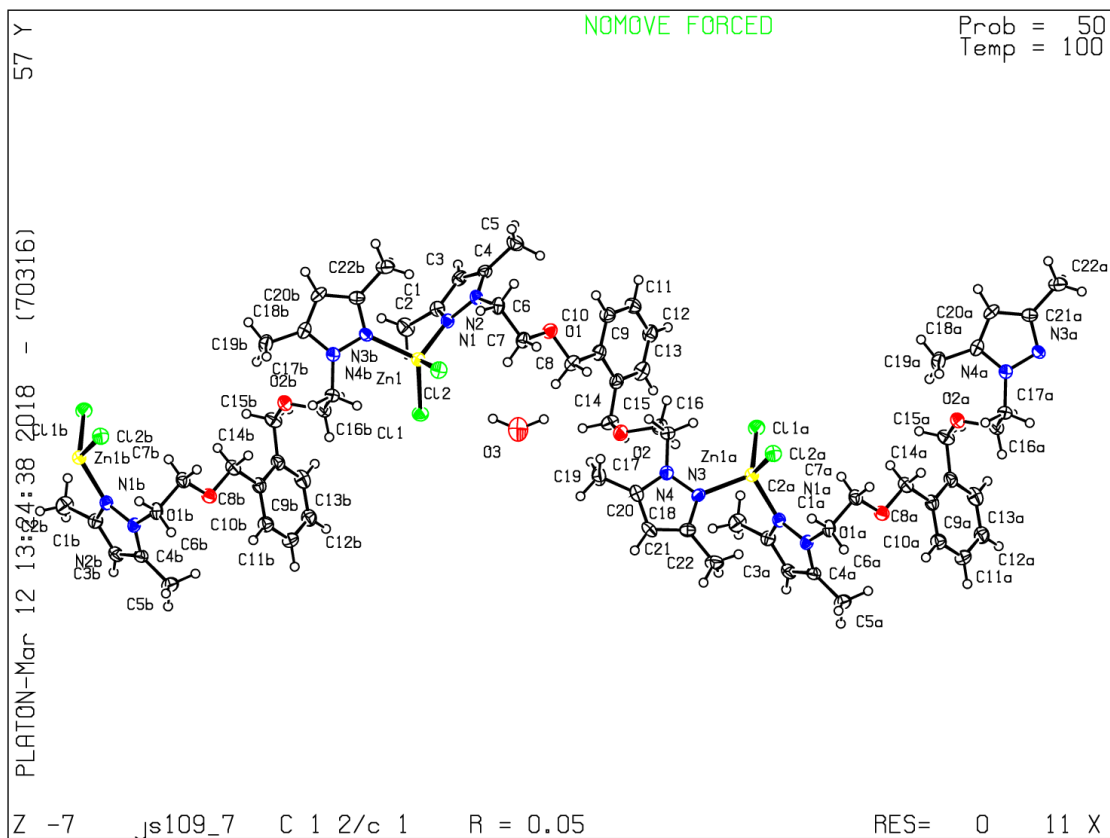
A basic structural check has been run on your CIF. These basic checks will be run on all CIFs submitted for publication in IUCr journals (*Acta Crystallographica*, *Journal of Applied Crystallography*, *Journal of Synchrotron Radiation*); however, if you intend to submit to *Acta Crystallographica Section C* or *E* or *IUCrData*, you should make sure that full publication checks are run on the final version of your CIF prior to submission.

### Publication of your CIF in other journals

Please refer to the *Notes for Authors* of the relevant journal for any special instructions relating to CIF submission.

PLATON version of 30/01/2018; check.def file version of 30/01/2018

Datablock js109\_7 - ellipsoid plot



## checkCIF/PLATON report

You have not supplied any structure factors. As a result the full set of tests cannot be run.

THIS REPORT IS FOR GUIDANCE ONLY. IF USED AS PART OF A REVIEW PROCEDURE FOR PUBLICATION, IT SHOULD NOT REPLACE THE EXPERTISE OF AN EXPERIENCED CRYSTALLOGRAPHIC REFEREE.

No syntax errors found.      CIF dictionary      Interpreting this report

### Datablock: js108r1\_a\_sq

---

Bond precision:	C-C = 0.0061 A	Wavelength=0.71073
Cell:	a=11.1004(3)      b=12.9995(3)      c=18.6202(5)	alpha=90      beta=101.285(1)      gamma=90
Temperature:	100 K	
	Calculated	Reported
Volume	2634.94(12)	2634.94(12)
Space group	P 21/n	P2(1)/n
Hall group	-P 2yn	-P 2yn
Moiety formula	C22 H30 Cd Cl2 N4 O2 [+ solvent]	C22 H30 Cd Cl2 N4 O2, 0.5[C2H6O]
Sum formula	C22 H30 Cd Cl2 N4 O2 [+ solvent]	C23 H33 Cd Cl2 N4 O2.50
Mr	565.81	588.83
Dx, g cm <sup>-3</sup>	1.426	1.484
Z	4	4
Mu (mm <sup>-1</sup> )	1.055	1.060
F000	1152.0	1204.0
F000'	1150.28	
h,k,lmax	14,16,24	14,16,24
Nref	6061	5995
Tmin,Tmax	0.881,0.919	0.350,0.746
Tmin'	0.881	

Correction method= # Reported T Limits: Tmin=0.350 Tmax=0.746  
AbsCorr = MULTI-SCAN

Data completeness= 0.989

Theta(max)= 27.494

R(reflections)= 0.0547( 5443)

wR2(reflections)= 0.1799( 5995)

S = 1.057

Npar= 285

---

The following ALERTS were generated. Each ALERT has the format

**test-name\_ALERT\_alert-type\_alert-level.**

Click on the hyperlinks for more details of the test.

---

### ● Alert level G

FORMU01\_ALERT\_2\_G There is a discrepancy between the atom counts in the  
\_chemical\_formula\_sum and the formula from the \_atom\_site\* data.

Atom count from \_chemical\_formula\_sum: C23 H33 Cd1 Cl2 N4 O2.5

Atom count from the \_atom\_site data: C22 H30 Cd1 Cl2 N4 O2

CELLZ01\_ALERT\_1\_G Difference between formula and atom\_site contents detected.

CELLZ01\_ALERT\_1\_G ALERT: Large difference may be due to a

symmetry error - see SYMMG tests

From the CIF: \_cell\_formula\_units\_Z 4

From the CIF: \_chemical\_formula\_sum C23 H33 Cd Cl2 N4 O2.50

TEST: Compare cell contents of formula and atom\_site data

atom	Z*formula	cif sites	diff
C	92.00	88.00	4.00
H	132.00	120.00	12.00
Cd	4.00	4.00	0.00
Cl	8.00	8.00	0.00
N	16.00	16.00	0.00
O	10.00	8.00	2.00

PLAT004_ALERT_5_G	Polymeric Structure Found with Maximum Dimension	1	Info
PLAT012_ALERT_1_G	No _shelx_res_checksum Found in CIF .....		Please Check
PLAT014_ALERT_1_G	No _shelx_fab_checksum Found in CIF .....		Please Check
PLAT041_ALERT_1_G	Calc. and Reported SumFormula Strings Differ		Please Check
PLAT068_ALERT_1_G	Reported F000 Differs from Calcd (or Missing)...		Please Check
PLAT072_ALERT_2_G	SHELXL First Parameter in WGHT Unusually Large	0.13	Report
PLAT605_ALERT_4_G	Largest Solvent Accessible VOID in the Structure	132	A**3
PLAT794_ALERT_5_G	Tentative Bond Valency for Cd1 (II) .	2.01	Info
PLAT869_ALERT_4_G	ALERTS Related to the Use of SQUEEZE Suppressed		! Info
PLAT883_ALERT_1_G	No Info/Value for _atom_sites_solution_primary .		Please Do !

---

0 **ALERT level A** = Most likely a serious problem - resolve or explain

0 **ALERT level B** = A potentially serious problem, consider carefully

0 **ALERT level C** = Check. Ensure it is not caused by an omission or oversight

13 **ALERT level G** = General information/check it is not something unexpected

7 **ALERT type 1** CIF construction/syntax error, inconsistent or missing data

2 **ALERT type 2** Indicator that the structure model may be wrong or deficient

0 **ALERT type 3** Indicator that the structure quality may be low

2 **ALERT type 4** Improvement, methodology, query or suggestion

2 **ALERT type 5** Informative message, check

---

---

It is advisable to attempt to resolve as many as possible of the alerts in all categories. Often the minor alerts point to easily fixed oversights, errors and omissions in your CIF or refinement strategy, so attention to these fine details can be worthwhile. In order to resolve some of the more serious problems it may be necessary to carry out additional measurements or structure refinements. However, the purpose of your study may justify the reported deviations and the more serious of these should normally be commented upon in the discussion or experimental section of a paper or in the "special\_details" fields of the CIF. checkCIF was carefully designed to identify outliers and unusual parameters, but every test has its limitations and alerts that are not important in a particular case may appear. Conversely, the absence of alerts does not guarantee there are no aspects of the results needing attention. It is up to the individual to critically assess their own results and, if necessary, seek expert advice.

### **Publication of your CIF in IUCr journals**

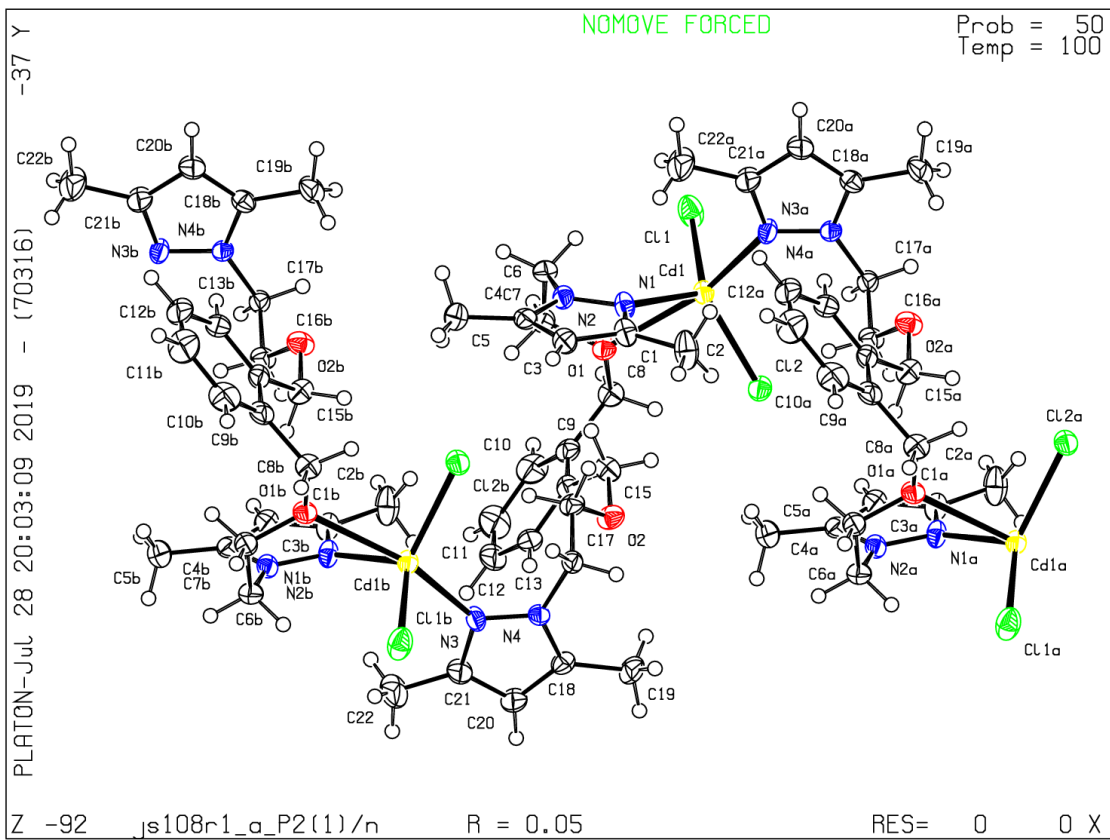
A basic structural check has been run on your CIF. These basic checks will be run on all CIFs submitted for publication in IUCr journals (*Acta Crystallographica*, *Journal of Applied Crystallography*, *Journal of Synchrotron Radiation*); however, if you intend to submit to *Acta Crystallographica Section C* or *E* or *IUCrData*, you should make sure that full publication checks are run on the final version of your CIF prior to submission.

### **Publication of your CIF in other journals**

Please refer to the *Notes for Authors* of the relevant journal for any special instructions relating to CIF submission.

---

**PLATON version of 03/05/2019; check.def file version of 29/04/2019**



# checkCIF/PLATON report

You have not supplied any structure factors. As a result the full set of tests cannot be run.

THIS REPORT IS FOR GUIDANCE ONLY. IF USED AS PART OF A REVIEW PROCEDURE FOR PUBLICATION, IT SHOULD NOT REPLACE THE EXPERTISE OF AN EXPERIENCED CRYSTALLOGRAPHIC REFEREE.

No syntax errors found.      CIF dictionary      Interpreting this report

## Datablock: js250

---

Bond precision:	C-C = 0.0111 A	Wavelength=0.71073	
Cell:	a=11.1617(19)	b=13.094(2)	c=18.698(4)
	alpha=90	beta=99.661(7)	gamma=90
Temperature:	298 K		
	Calculated	Reported	
Volume	2694.0(8)	2693.8(8)	
Space group	P 21/n	P 1 21/n 1	
Hall group	-P 2yn	-P 2yn	
Moiety formula	C22 H30 Cl2 Hg N4 O2 [+ solvent]	C22 H30 Cl2 Hg N4 O2, 0.5[C2H6O]	
Sum formula	C22 H30 Cl2 Hg N4 O2 [+ solvent]	C23 H33 Cl2 Hg N4 O2.50	
Mr	653.99	677.02	
Dx, g cm <sup>-3</sup>	1.612	1.669	
Z	4	4	
Mu (mm <sup>-1</sup> )	5.935	5.940	
F000	1280.0	1332.0	
F000'	1272.35		
h,k,lmax	13,15,22	13,15,22	
Nref	4769	4760	
Tmin,Tmax	0.558,0.622	0.450,0.745	
Tmin'	0.547		

Correction method= # Reported T Limits: Tmin=0.450 Tmax=0.745  
AbsCorr = MULTI-SCAN

Data completeness= 0.998      Theta(max)= 25.026

R(reflections)= 0.0409( 3161)      wR2(reflections)= 0.0844( 4760)

S = 1.011      Npar= 284

---



The following ALERTS were generated. Each ALERT has the format

**test-name\_ALERT\_alert-type\_alert-level.**

Click on the hyperlinks for more details of the test.

---

**Alert level C**

PLAT342\_ALERT\_3\_C Low Bond Precision on C-C Bonds ..... 0.01111 Ang.

---

**Alert level G**

FORMU01\_ALERT\_2\_G There is a discrepancy between the atom counts in the  
\_chemical\_formula\_sum and the formula from the \_atom\_site\* data.

Atom count from \_chemical\_formula\_sum: C23 H33 Cl2 Hg1 N4 O2.5

Atom count from the \_atom\_site data: C22 H30 Cl2 Hg1 N4 O2

CELLZ01\_ALERT\_1\_G Difference between formula and atom\_site contents detected.

CELLZ01\_ALERT\_1\_G ALERT: Large difference may be due to a

symmetry error - see SYMMG tests

From the CIF: \_cell\_formula\_units\_Z 4

From the CIF: \_chemical\_formula\_sum C23 H33 Cl2 Hg N4 O2.50

TEST: Compare cell contents of formula and atom\_site data

atom	Z*formula	cif sites	diff
C	92.00	88.00	4.00
H	132.00	120.00	12.00
Cl	8.00	8.00	0.00
Hg	4.00	4.00	0.00
N	16.00	16.00	0.00
O	10.00	8.00	2.00

PLAT004_ALERT_5_G Polymeric Structure Found with Maximum Dimension	1 Info
PLAT041_ALERT_1_G Calc. and Reported SumFormula Strings Differ	Please Check
PLAT068_ALERT_1_G Reported F000 Differs from Calcd (or Missing)...	Please Check
PLAT083_ALERT_2_G SHELXL Second Parameter in WGHT Unusually Large	7.50 Why ?
PLAT605_ALERT_4_G Largest Solvent Accessible VOID in the Structure	139 A**3
PLAT868_ALERT_4_G ALERTS Due to the Use of _smtbx_masks Suppressed	! Info
PLAT883_ALERT_1_G No Info/Value for _atom_sites_solution_primary .	Please Do !
PLAT933_ALERT_2_G Number of OMIT Records in Embedded .res File ...	6 Note

---

0 **ALERT level A** = Most likely a serious problem - resolve or explain  
0 **ALERT level B** = A potentially serious problem, consider carefully  
1 **ALERT level C** = Check. Ensure it is not caused by an omission or oversight  
11 **ALERT level G** = General information/check it is not something unexpected

5 ALERT type 1 CIF construction/syntax error, inconsistent or missing data  
3 ALERT type 2 Indicator that the structure model may be wrong or deficient  
1 ALERT type 3 Indicator that the structure quality may be low  
2 ALERT type 4 Improvement, methodology, query or suggestion  
1 ALERT type 5 Informative message, check

---

---

It is advisable to attempt to resolve as many as possible of the alerts in all categories. Often the minor alerts point to easily fixed oversights, errors and omissions in your CIF or refinement strategy, so attention to these fine details can be worthwhile. In order to resolve some of the more serious problems it may be necessary to carry out additional measurements or structure refinements. However, the purpose of your study may justify the reported deviations and the more serious of these should normally be commented upon in the discussion or experimental section of a paper or in the "special\_details" fields of the CIF. checkCIF was carefully designed to identify outliers and unusual parameters, but every test has its limitations and alerts that are not important in a particular case may appear. Conversely, the absence of alerts does not guarantee there are no aspects of the results needing attention. It is up to the individual to critically assess their own results and, if necessary, seek expert advice.

### **Publication of your CIF in IUCr journals**

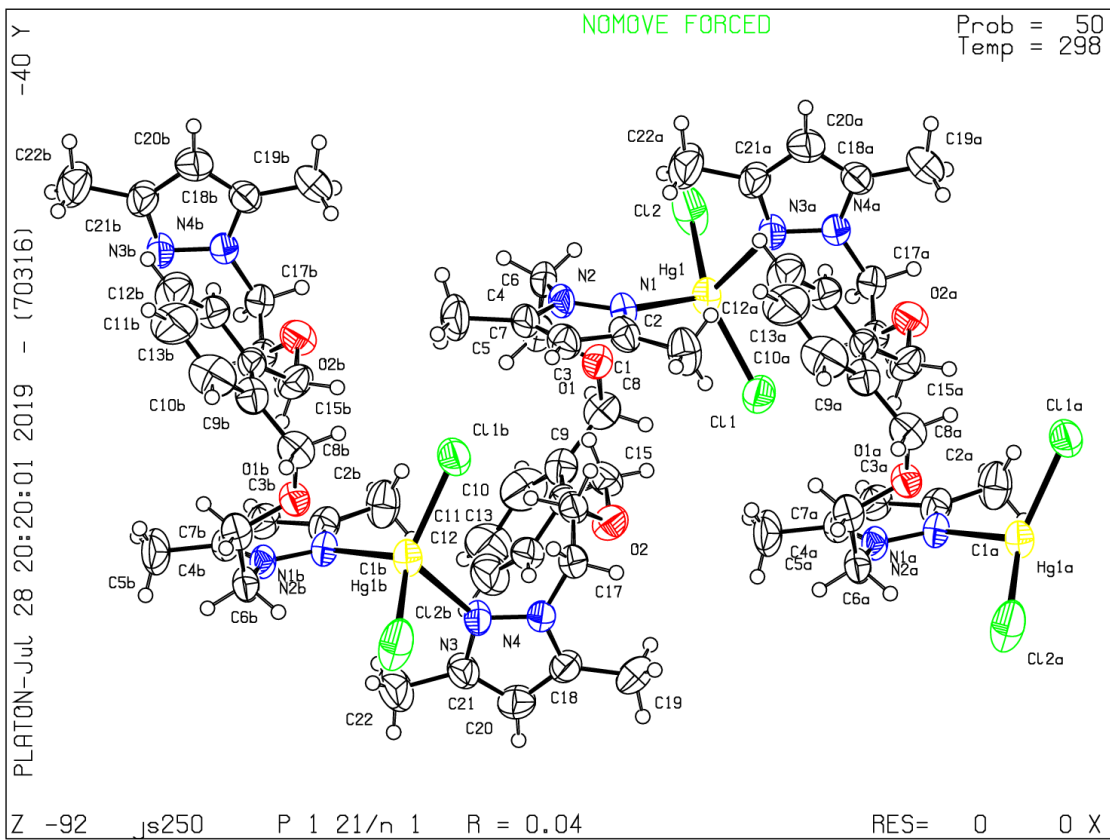
A basic structural check has been run on your CIF. These basic checks will be run on all CIFs submitted for publication in IUCr journals (*Acta Crystallographica*, *Journal of Applied Crystallography*, *Journal of Synchrotron Radiation*); however, if you intend to submit to *Acta Crystallographica Section C* or *E* or *IUCrData*, you should make sure that full publication checks are run on the final version of your CIF prior to submission.

### **Publication of your CIF in other journals**

Please refer to the *Notes for Authors* of the relevant journal for any special instructions relating to CIF submission.

---

**PLATON version of 03/05/2019; check.def file version of 29/04/2019**



## Supporting Information

### **Dimeric metallacycles and coordination polymers: Zn(II), Cd(II) and Hg(II) complexes of two positional isomers of a flexible *N,O*-hybrid bispyrazole derived ligand.**

Joan Soldevila-Sanmartín<sup>a</sup>, Miguel Guerrero<sup>a</sup>, Duane Choquesillo-Lazarte<sup>b</sup>, José Giner Planas<sup>c</sup> and Josefina Pons<sup>a,\*</sup>.

<sup>a</sup> *Departament de Química, Universitat Autònoma de Barcelona, 08913-Bellaterra, Barcelona, Spain.*

<sup>b</sup> *Laboratorio de Estudios Cristalógraficos, IACT (CSIC-Universidad de Granada), Avda. de las Palmeras 4, Armilla, 18100 Granada, Spain.*

<sup>c</sup> *Institut de Ciència de Materials de Barcelona (ICMAB-CSIC), Campus UAB, 08913-Bellaterra, Barcelona, Spain.*

## Table of contents

### Powder X-ray diffraction data

**Figure S1.** X-ray diffractogram of  $[\text{Zn}(\text{L1})\text{Cl}_2]_2$  (**1**, bottom) measured at r.t. Calculated pattern from resolved crystal structure is also included (top) as a reference, from monocrystal XRD measured at 100(2) K

**Figure S2.** X-ray diffractogram of  $[\text{Cd}(\text{L1})\text{Cl}_2]_2$  (**2**, bottom) measured at r.t. Calculated pattern from resolved crystal structure is also included (top) as a reference, from monocrystal XRD measured at 100(2) K

**Figure S3.** X-ray diffractogram of  $[\text{Hg}(\text{L1})\text{Cl}_2]_2$  (**3**, bottom) measured at r.t. Calculated pattern from resolved crystal structure is also included (top) as a reference, from monocrystal XRD measured at 100(2) K

**Figure S4.** X-ray diffractogram of  $\{[\text{Zn}(\text{L2})\text{Cl}_2] \cdot 1/2\text{H}_2\text{O}\}_n$  (**4**, bottom) measured at r.t. Calculated pattern from resolved crystal structure is also included (top) as a reference, from monocrystal XRD measured at 100.0 K

**Figure S5.** X-ray diffractogram of  $\{[\text{Cd}(\text{L2})\text{Cl}_2] \cdot 1/2\text{EtOH}\}_n$  (**5**, bottom) measured at r.t. Calculated pattern from resolved crystal structure is also included (top) as a reference, from monocrystal XRD measured at 100(2) K

**Figure S6.** X-ray diffractogram of  $\{[\text{Hg}(\text{L2})\text{Cl}_2] \cdot 1/2\text{EtOH}\}_n$  (**6**, bottom) measured at r.t. Calculated pattern from resolved crystal structure is also included (top) as a reference, from monocrystal XRD measured at 298(2) K

### FTIR-ATR Spectra

**Figure S7.** FTIR-ATR spectrum of  $[\text{Zn}(\text{L1})\text{Cl}_2]_2$  (**1**)

**Figure S8.** FTIR-ATR spectrum of  $[\text{Cd}(\text{L1})\text{Cl}_2]_2$  (**2**)

**Figure S9.** FTIR-ATR spectrum of  $[\text{Hg}(\text{L1})\text{Cl}_2]_2$  (**3**)

**Figure S10.** FTIR-ATR spectrum of  $\{[\text{Zn}(\text{L2})\text{Cl}_2] \cdot 1/2\text{H}_2\text{O}\}_n$  (**4**)

**Figure S11.** FTIR-ATR spectrum of  $\{[\text{Cd}(\text{L2})\text{Cl}_2] \cdot 1/2\text{EtOH}\}_n$  (**5**)

**Figure S12.** FTIR-ATR spectrum of  $\{[\text{Hg}(\text{L2})\text{Cl}_2] \cdot 1/2\text{EtOH}\}_n$  (**6**)

### Crystal and Extended Structures. Hirshfeld Surface Analyses.

**Figure S13.** Compound a. **2** b. **3** showing all its non-hydrogen atoms and their corresponding numbering scheme

**Figure S14.** Schematic representation of intramolecular distances in compounds **1** (top-left), **2** (top-right) and **3** (bottom)

**Figure S15.** a. Supramolecular structure of **2**, view along *c* axis (right). Detail of the non-bonding interactions in **2**, view along *c* axis (left). b. Supramolecular structure of **3**, view along *c* axis (right). Detail of the non-bonding interactions in **3**, view along *c* axis (left).

**Figure S16.** Curvedness (left) and shape index (right) mapping surface for: a. **1**. b. **2**. c. **3**

**Figure S17.** Fingertip plot of **1**

**Figure S18.** Fingertip plot of **2**

**Figure S19.** Fingertip plot of **3**

**Figure S20.** Polymer **6** showing all its non-hydrogen atoms and their corresponding numbering scheme

**Figure S21.** Supramolecular structure of **6**. View along *b* axis (left), and along *a* axis (right). Solvent occluded molecules have been removed for clarity

**Figure S22.** Cavities ( $227.28 \text{ \AA}^3$ ) in **5** (left) and ( $229.75 \text{ \AA}^3$ ) **6** (right)

## NMR Spectra

**Figure S23.**  $^1\text{H}$  NMR spectra of **L1** (top) and **L2** (bottom)

**Figure S24.**  $^1\text{H}$  NMR spectrum of **1** (400 MHz,  $\text{CDCl}_3$ )

**Figure S25.**  $^{13}\text{C}\{^1\text{H}\}$  NMR spectrum of **1** (100.6 MHz,  $\text{CDCl}_3$ )

**Figure S26.** HSQC NMR spectrum of **1** (400 MHz,  $\text{CDCl}_3$ )

**Figure S27.**  $^1\text{H}$  NMR spectrum of **2** (400 MHz,  $\text{CDCl}_3$ )

**Figure S28.**  $^{13}\text{C}\{^1\text{H}\}$  NMR spectrum of **2** (100.6 MHz,  $\text{CDCl}_3$ )

**Figure S29.** HSQC NMR spectrum of **2** (400 MHz,  $\text{CDCl}_3$ )

**Figure S30.**  $^1\text{H}$  NMR spectrum of **3** (400 MHz,  $\text{CDCl}_3$ )

**Figure S31.**  $^{13}\text{C}\{^1\text{H}\}$  NMR spectrum of **3** (100.6 MHz,  $\text{CDCl}_3$ )

**Figure S32.** HSQC NMR spectrum of **3** (400 MHz,  $\text{CDCl}_3$ )

**Figure S33.**  $^1\text{H}$  NMR spectrum of **4** (400 MHz,  $\text{CDCl}_3$ )

**Figure S34.**  $^{13}\text{C}\{^1\text{H}\}$  NMR spectrum of **4** (100.6 MHz,  $\text{CDCl}_3$ )

**Figure S35.** HSQC NMR spectrum of **4** (400 MHz,  $\text{CDCl}_3$ )

**Figure S36.**  $^1\text{H}$  NMR spectrum of **5** (400 MHz,  $\text{CDCl}_3$ )

**Figure S37.**  $^{13}\text{C}\{^1\text{H}\}$  NMR spectrum of **5** (100.6 MHz,  $\text{CDCl}_3$ )

**Figure S38.** HSQC NMR spectrum of **5** (400 MHz,  $\text{CDCl}_3$ )

**Figure S39.**  $^1\text{H}$  NMR spectrum of **6** (400 MHz,  $\text{CDCl}_3$ )

**Figure S40.**  $^{13}\text{C}\{^1\text{H}\}$  NMR spectrum of **6** (100.6 MHz,  $\text{CDCl}_3$ )

**Figure S41.** HSQC NMR spectrum of **6** (400 MHz,  $\text{CDCl}_3$ )

**Figure S42.** DOSY NMR spectrum of **4** (400 MHz,  $\text{CDCl}_3$ )

**Figure S43.** DOSY NMR spectrum of **6** (400 MHz,  $\text{CDCl}_3$ )

**Figure S44.** DOSY-NMR spectra of **1** (400 MHz,  $\text{CDCl}_3$ )

### UV-Vis Spectra

**Figure S45.** UV-Vis spectrum of **L1** and **1-3** recorded in  $\text{CH}_3\text{CN}$  at r.t.

**Figure S46.** UV-Vis spectrum of **L2** and **4-6** recorded in  $\text{CH}_3\text{CN}$  at r.t.

## Powder X-ray diffraction data

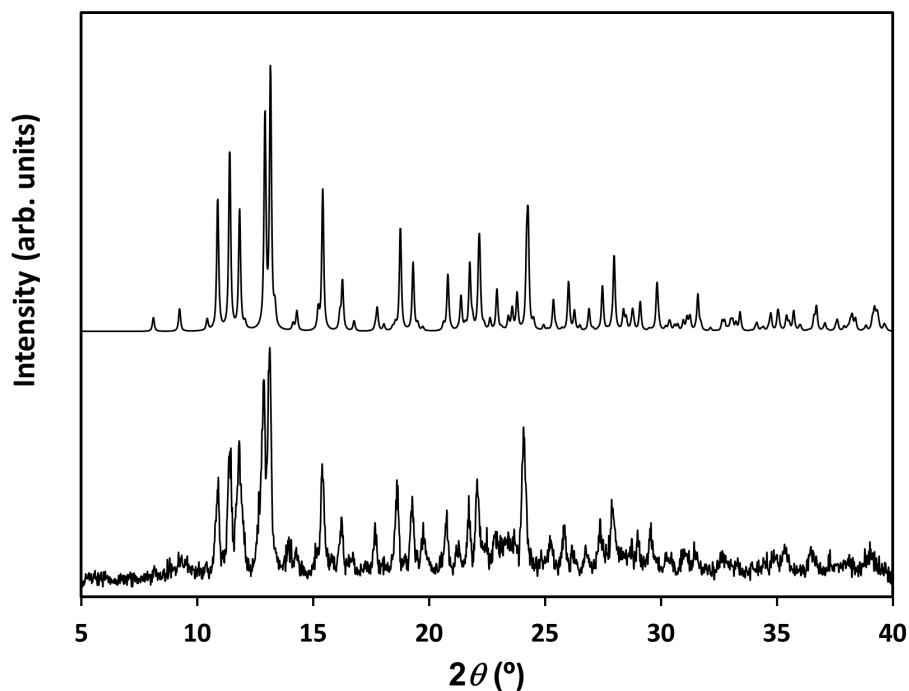


**Figure S1.** X-ray diffractogram of  $[\text{Zn}(\text{L1})\text{Cl}_2]_2$  (**1**, bottom) measured at r.t. Calculated pattern from resolved crystal structure is also included (top) as a reference, from monocrystal XRD measured at 100(2) K

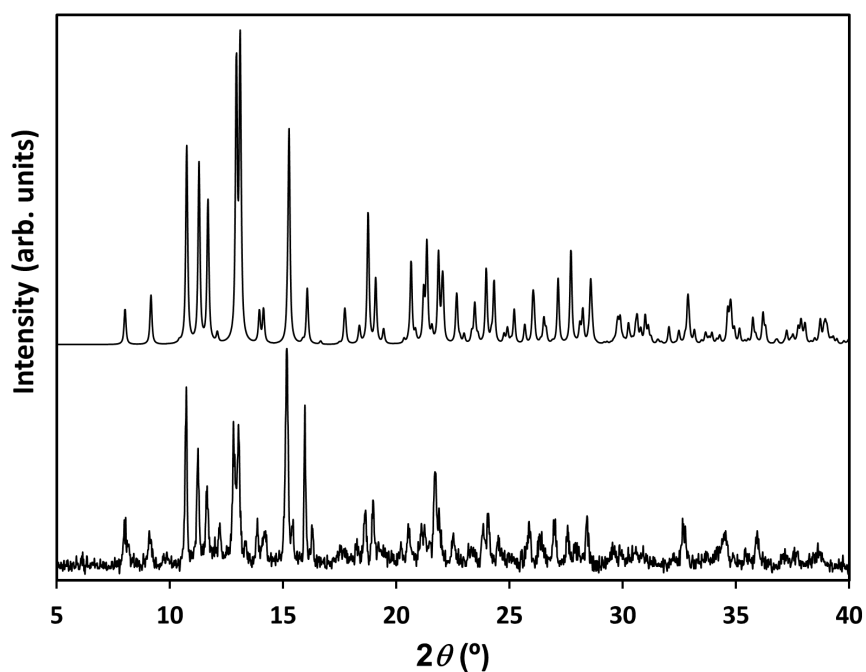


**Figure S2.** X-ray diffractogram of  $[\text{Cd}(\text{L1})\text{Cl}_2]_2$  (**2**, bottom) measured at r.t. Calculated pattern from resolved crystal structure is also included (top) as a reference, from monocrystal XRD measured at 100(2) K



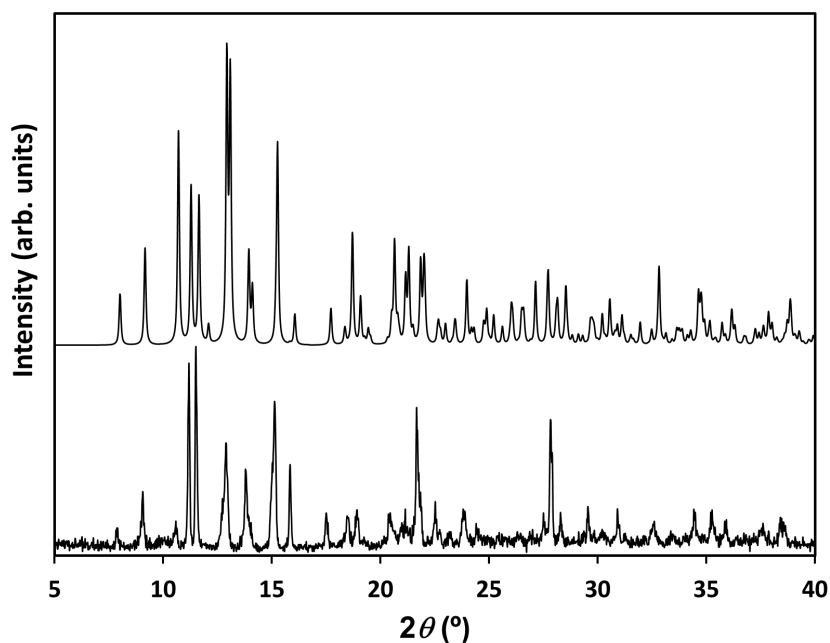


**Figure S3.** X-ray diffractogram of  $[\text{Hg}(\text{L1})\text{Cl}_2]_2$  (**3**, bottom) measured at r.t. Calculated pattern from resolved crystal structure is also included (top) as a reference, from monocrystal XRD measured at 100(2) K

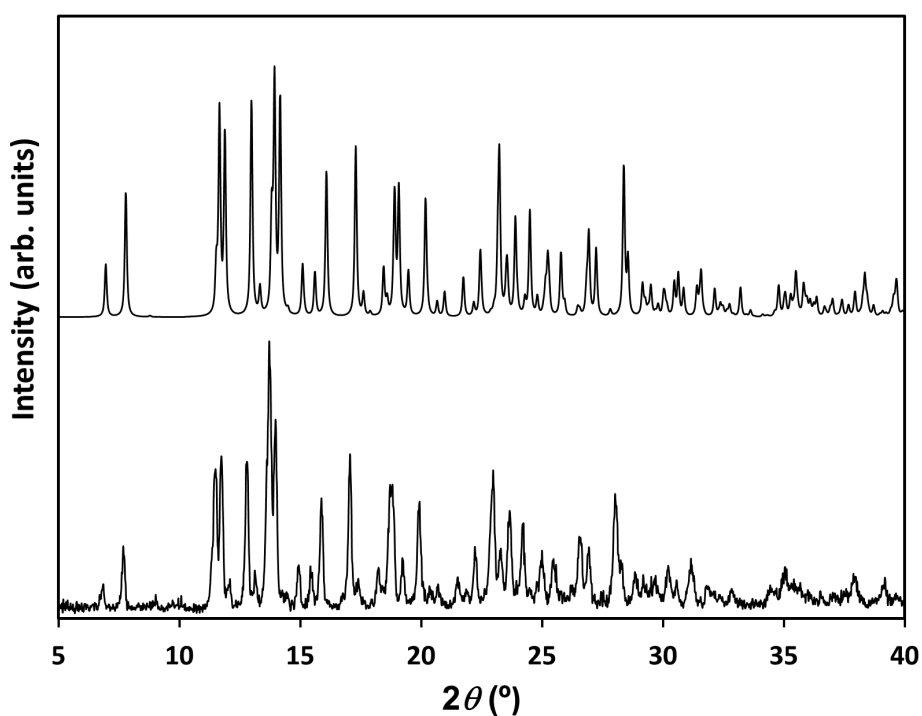


**Figure S4.** X-ray diffractogram of  $\{[\text{Zn}(\text{L2})\text{Cl}_2] \cdot 1/2\text{H}_2\text{O}\}_n$  (**4**, bottom) measured at r.t. Calculated pattern from resolved crystal structure is also included (top) as a reference, from monocrystal XRD measured at 100.0 K

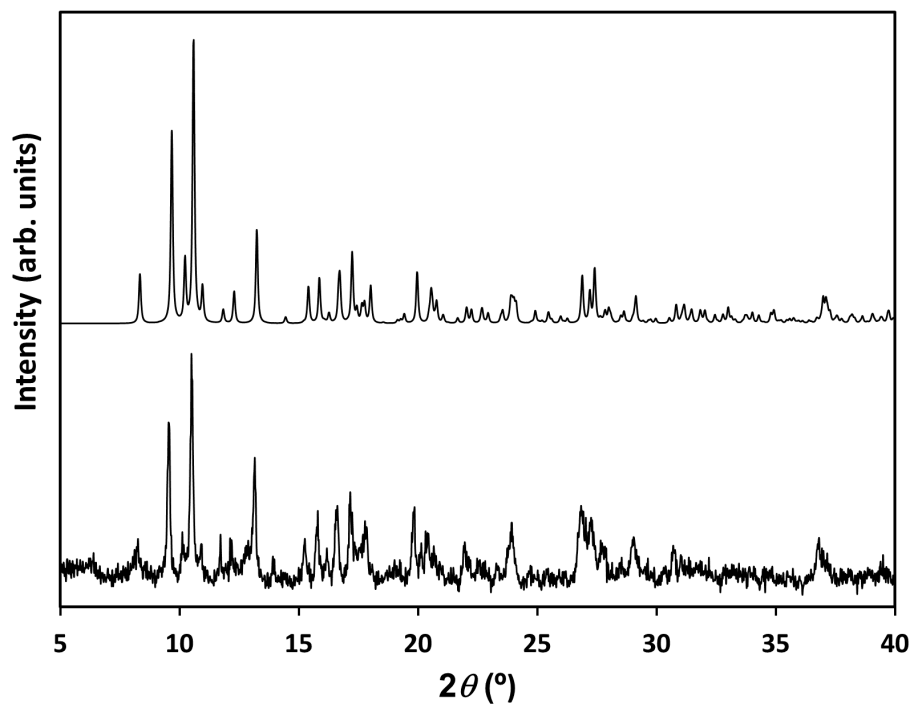


**Figure S5.** X-ray diffractogram of  $\{[\text{Cd}(\text{L2})\text{Cl}_2]\cdot 1/2\text{EtOH}\}_n$  (**5**, bottom) measured at r.t. Calculated pattern from resolved crystal structure is also included (top) as a reference, from monocrystal XRD measured at 100(2) K

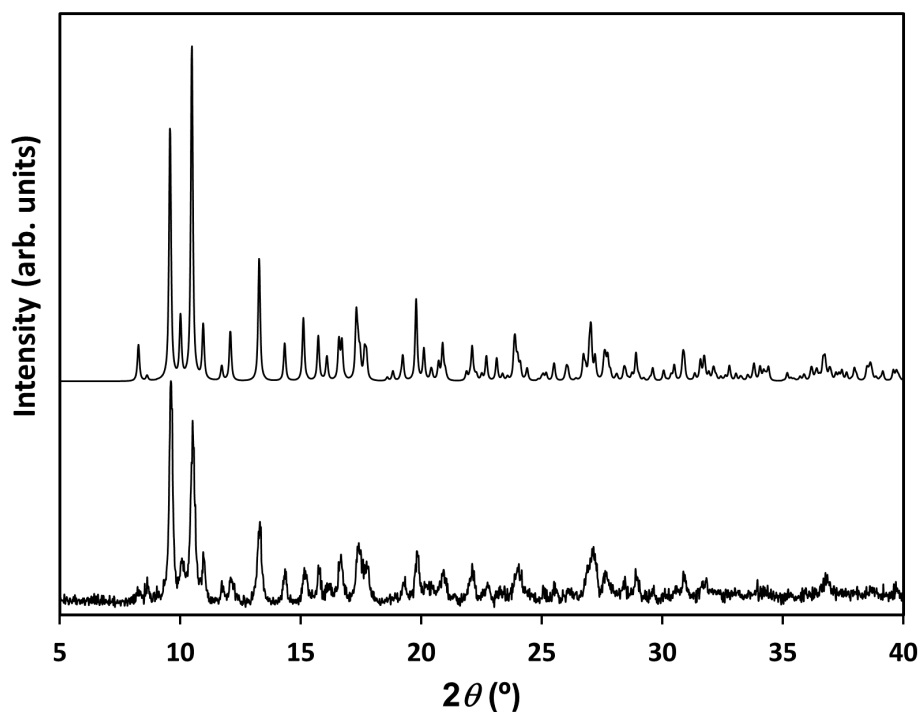


**Figure S6.** X-ray diffractogram of  $\{[\text{Hg}(\text{L2})\text{Cl}_2]\cdot 1/2\text{EtOH}\}_n$  (**6**, bottom) measured at r.t. Calculated pattern from resolved crystal structure is also included (top) as a reference, from monocrystal XRD measured at 298(2) K

### FTIR-ATR spectrum

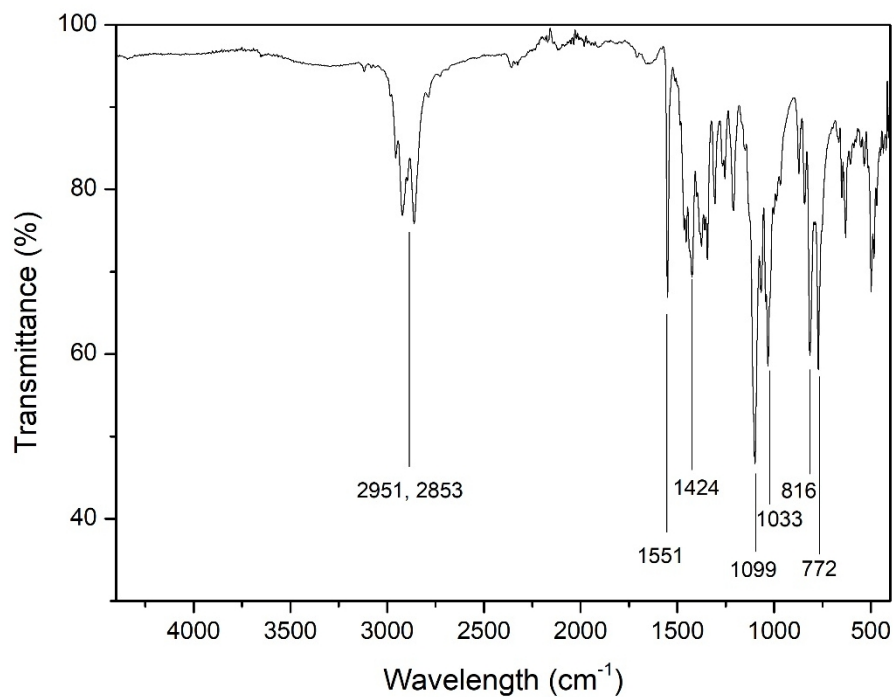


**Figure S7.** FTIR-ATR spectrum of [Zn(L1)Cl<sub>2</sub>]<sub>2</sub> (1)

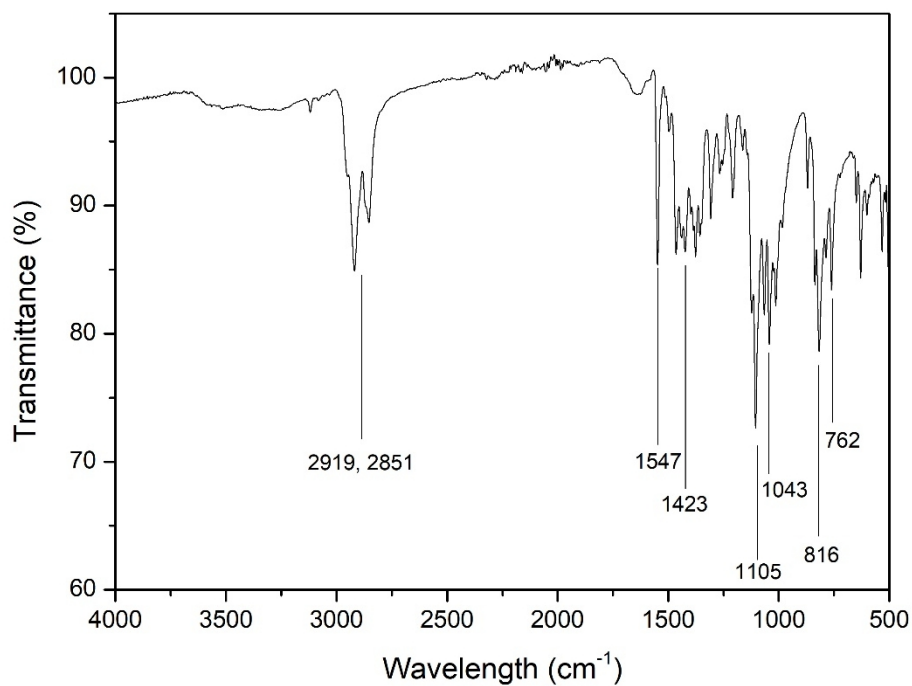


**Figure S8.** FTIR-ATR spectrum of [Cd(L1)Cl<sub>2</sub>]<sub>2</sub> (2)

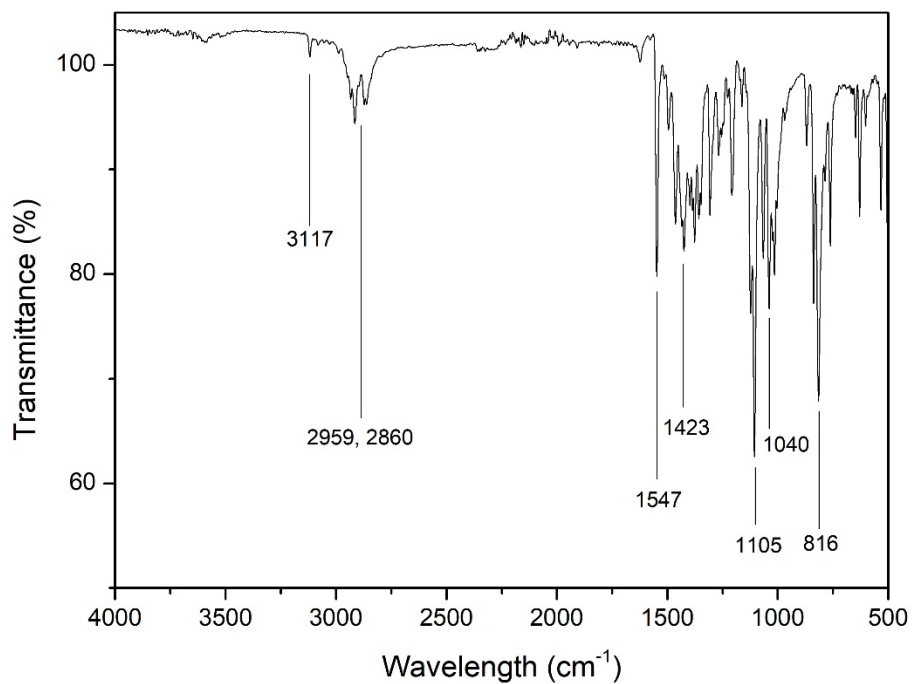


**Figure S9.** FTIR-ATR spectrum of  $[\text{Hg}(\text{L1})\text{Cl}_2]_2$  (**3**)

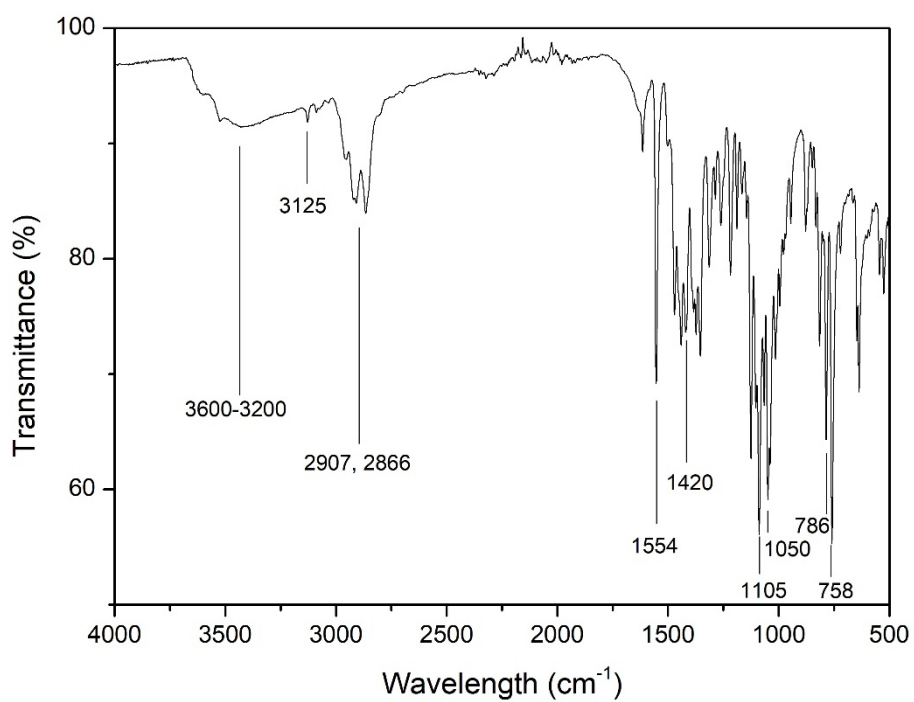


**Figure S10.** FTIR-ATR spectrum of  $\{[\text{Zn}(\text{L2})\text{Cl}_2] \cdot 1/2\text{H}_2\text{O}\}_n$  (**4**)

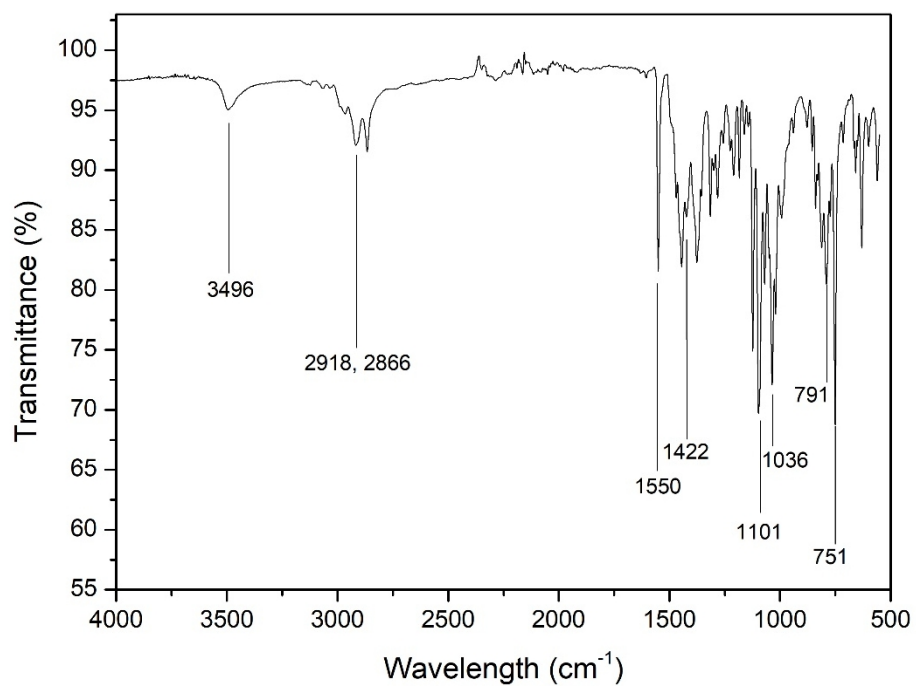


**Figure S11.** FTIR-ATR spectrum of  $\{[Cd(L2)Cl_2] \cdot 1/2EtOH\}_n$  (5)

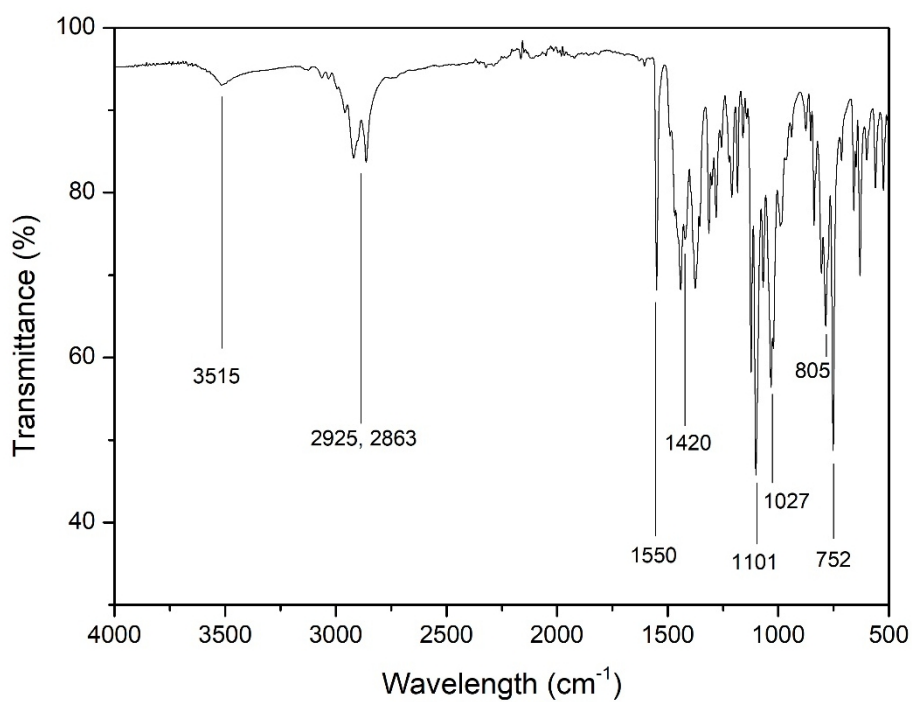


**Figure S12.** FTIR-ATR spectrum of  $\{[Hg(L2)Cl_2] \cdot 1/2EtOH\}_n$  (6)

## Crystal and Extended Structures. Hirshfeld Surface Analyses.

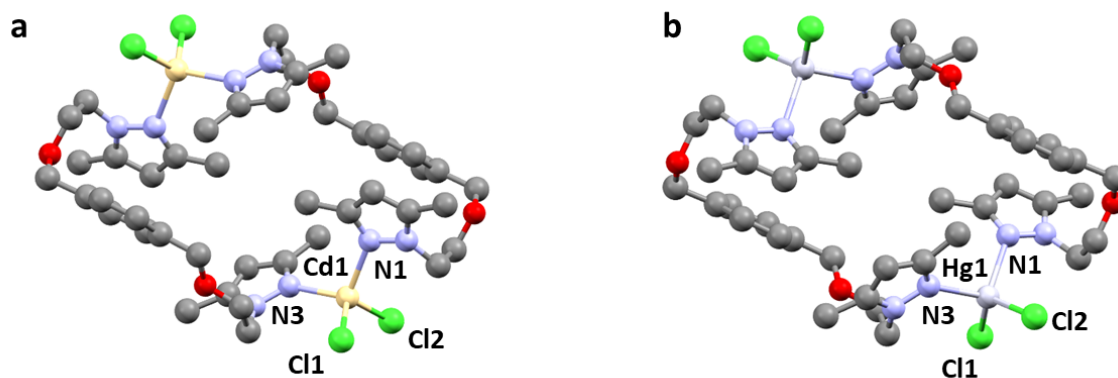


**Figure S13.** Compound a. 2 b. 3 showing all its non-hydrogen atoms and their corresponding numbering scheme

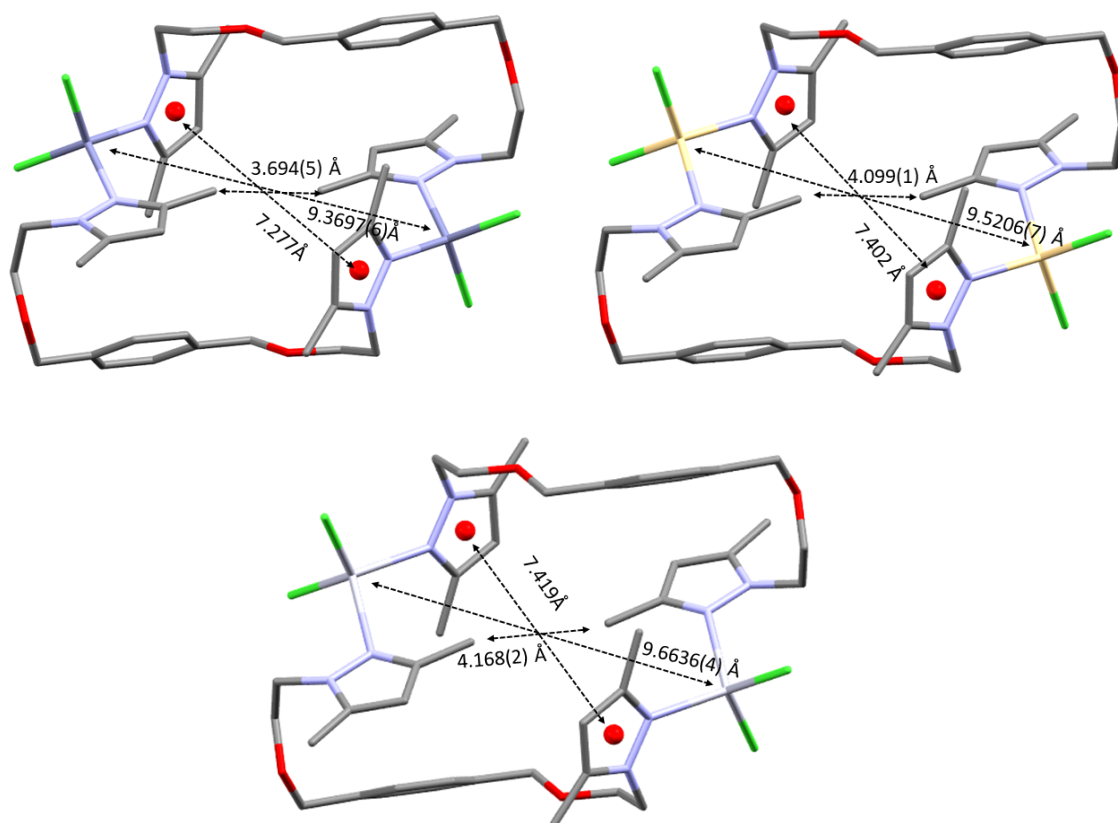


**Figure S14.** Schematic representation of intramolecular distances in compounds 1 (top-left), 2 (top-right) and 3 (bottom)

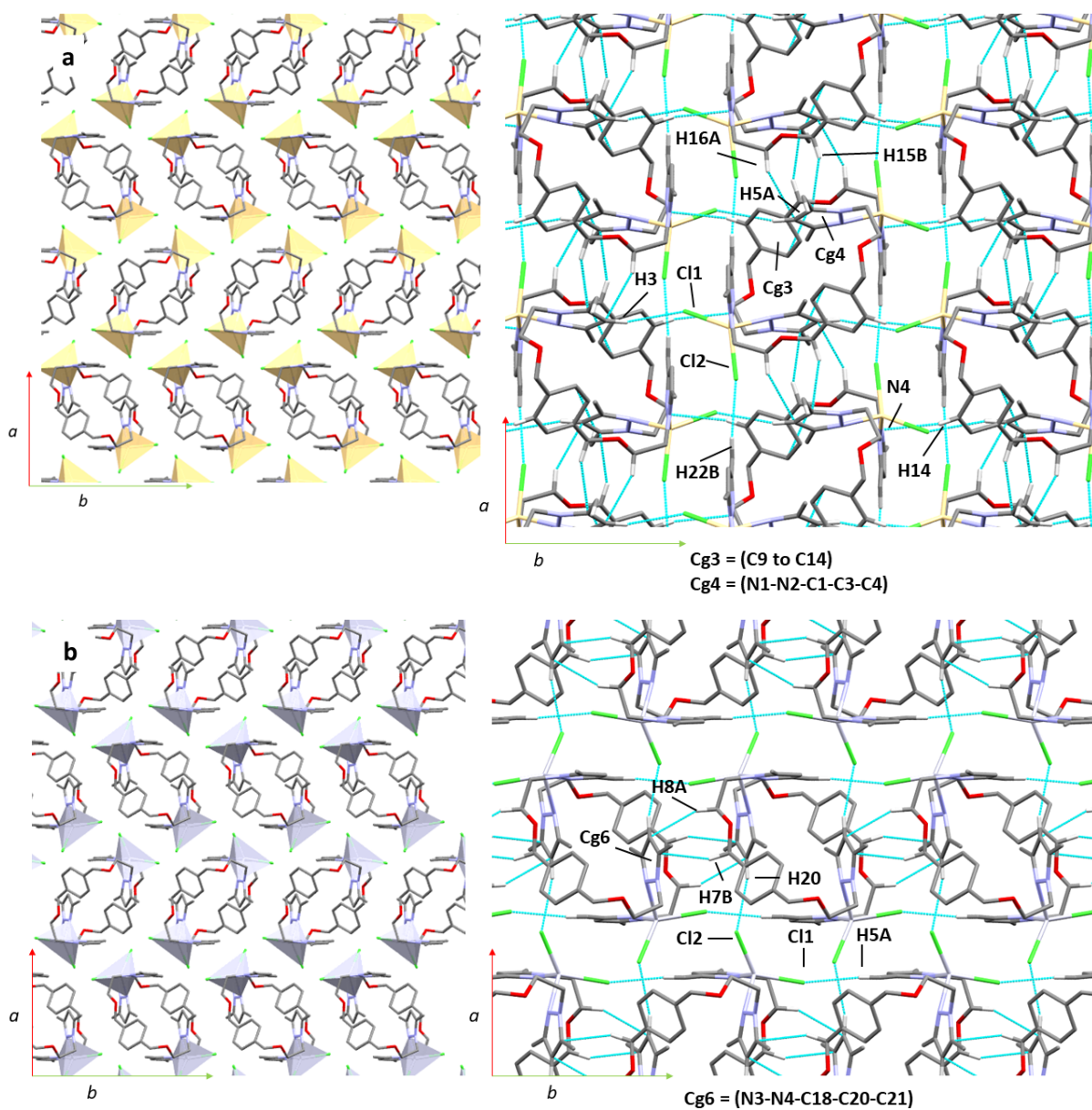
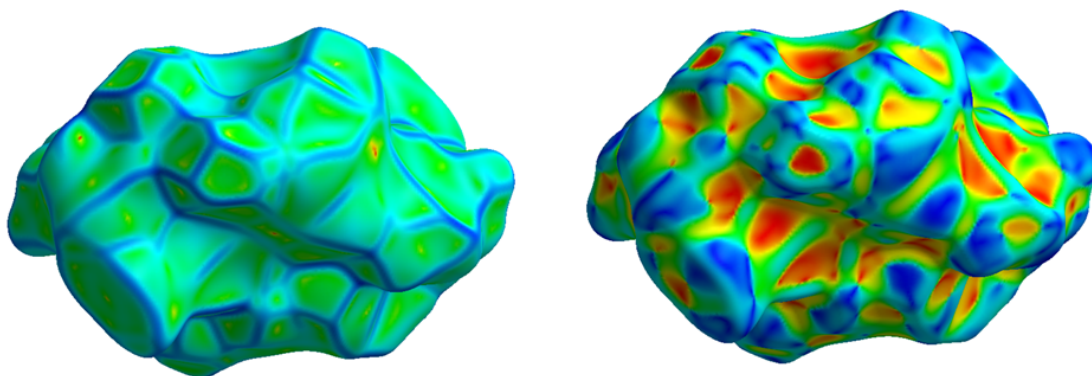
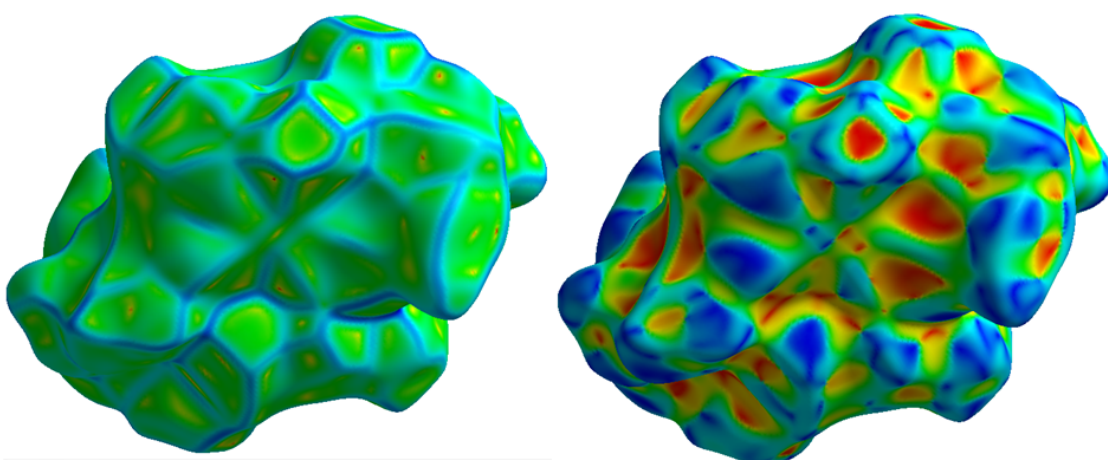


**Figure S15.** a. Supramolecular structure of **2**, view along *c* axis (right). Detail of the non-bonding interactions in **2**, view along *c* axis (left). b. Supramolecular structure of **3**, view along *c* axis (right). Detail of the non-bonding interactions in **3**, view along *c* axis (left)

a



b



c

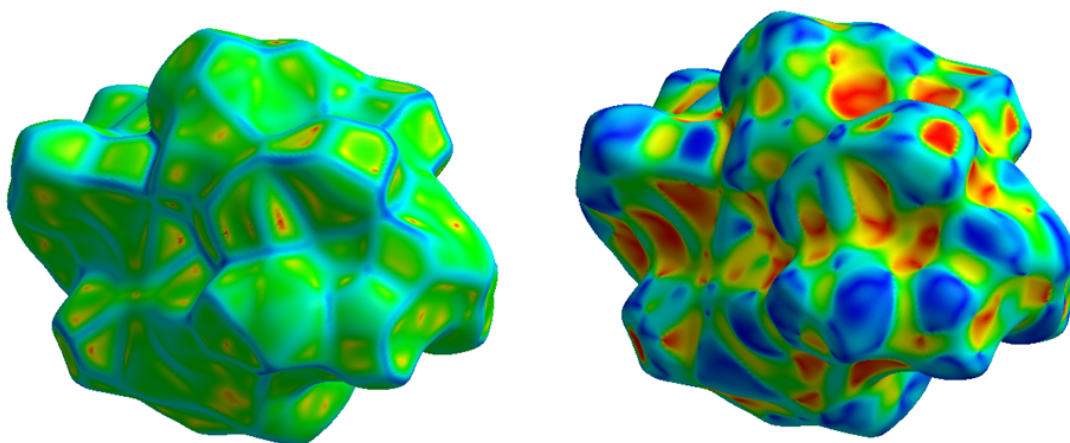


**Figure S16.** Curvedness (left) and shape index (right) mapping surface for: a. 1. b. 2. c. 3



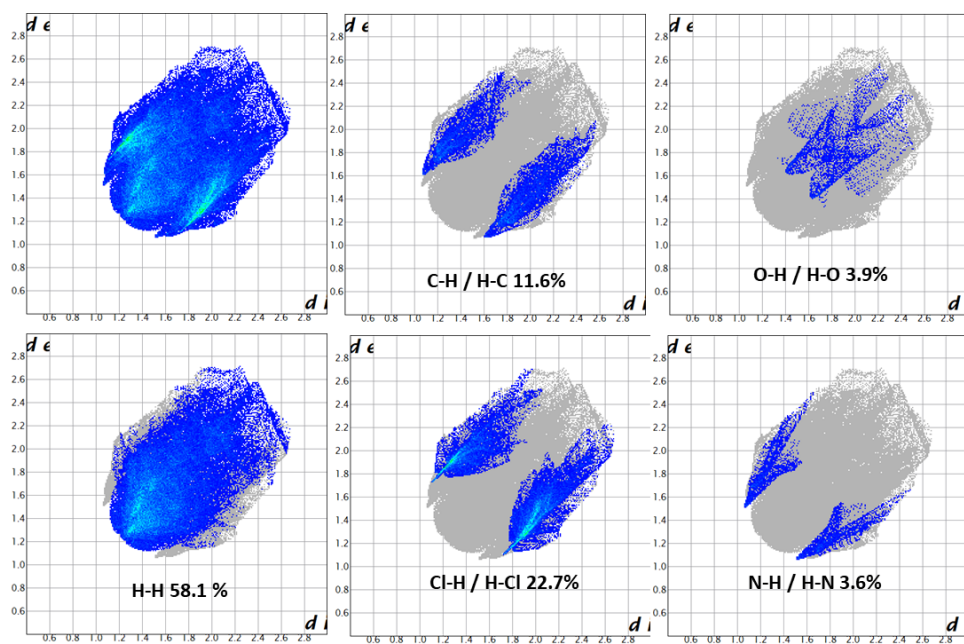


Figure S17. Fingertip plot of 1

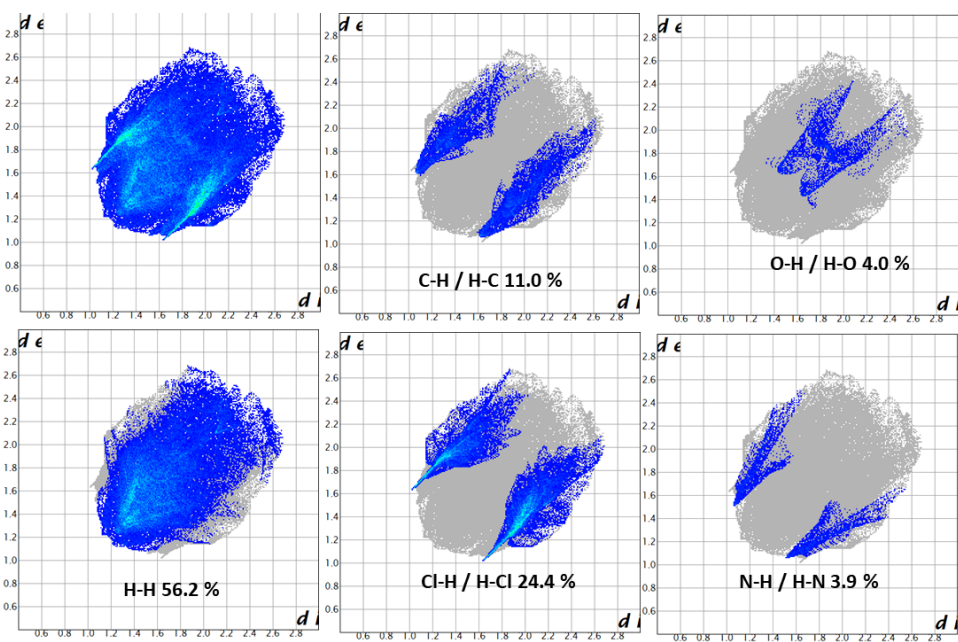
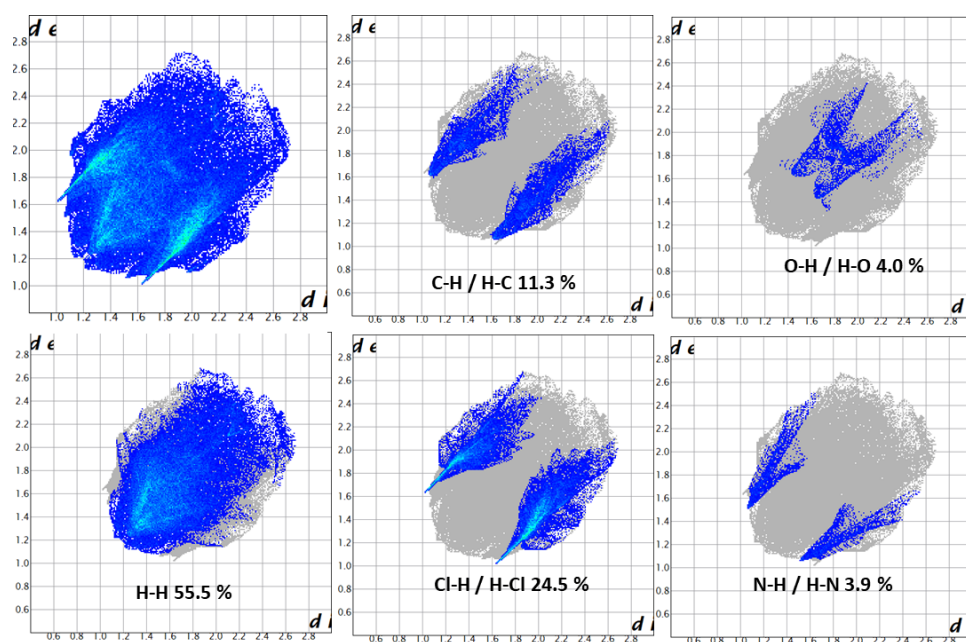
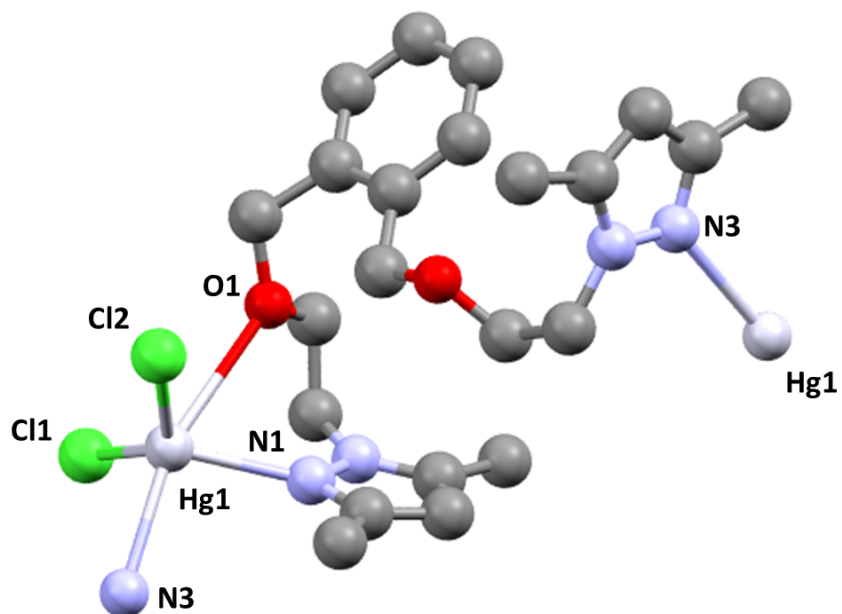


Figure S18. Fingertip plot of 2



**Figure S19.** Fingertip plot of 3



**Figure S20.** Polymer 6 showing all its non-hydrogen atoms and their corresponding numbering scheme

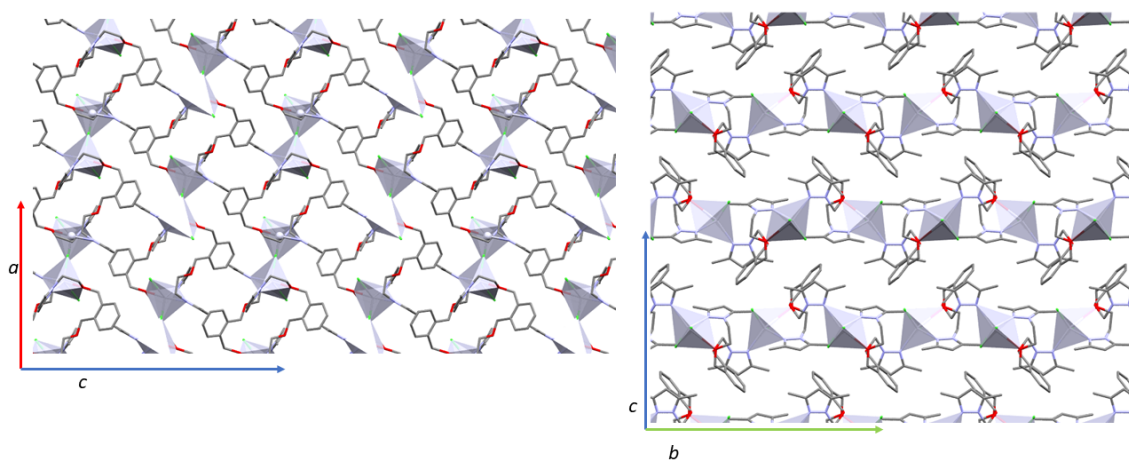


**Figure S21.** Supramolecular structure of **6**. View along *b* axis (left), and along *a* axis (right). Solvent occluded molecules have been removed for clarity

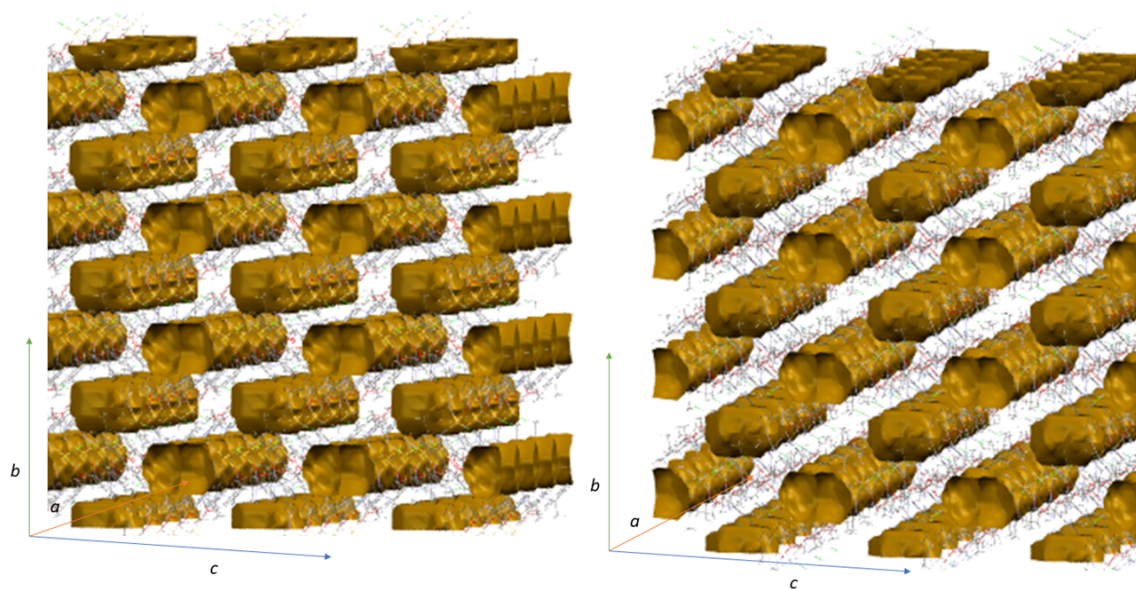


**Figure S22.** Cavities ( $227.28 \text{ \AA}^3$ ) in **5** (left) and ( $229.75 \text{ \AA}^3$ ) **6** (right)

## NMR spectra

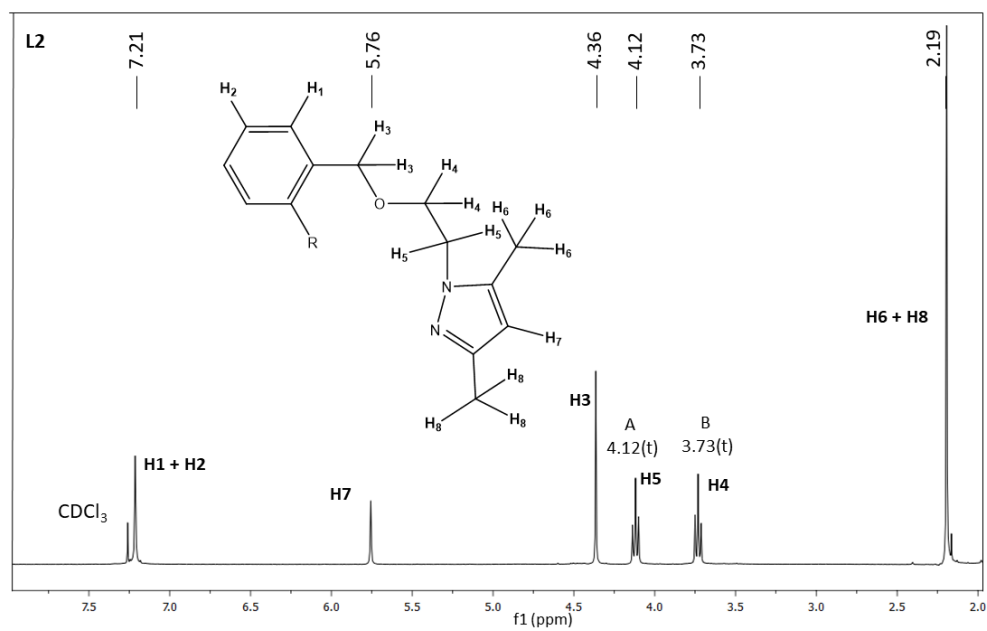
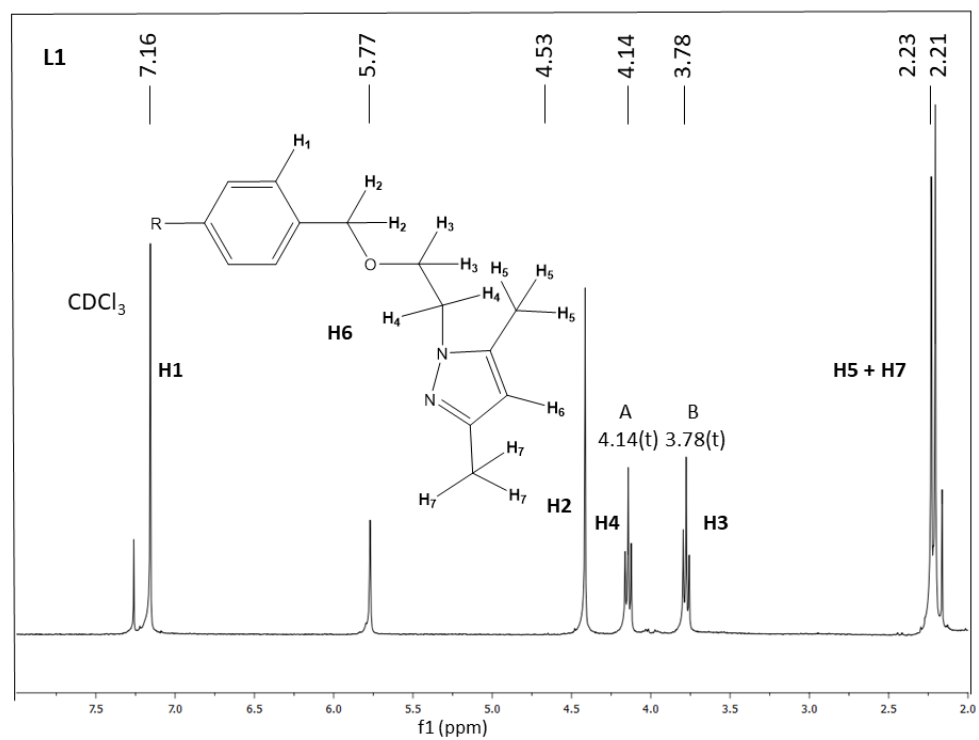


**Figure S23.** <sup>1</sup>H NMR spectra of **L1** (top) and **L2** (bottom)

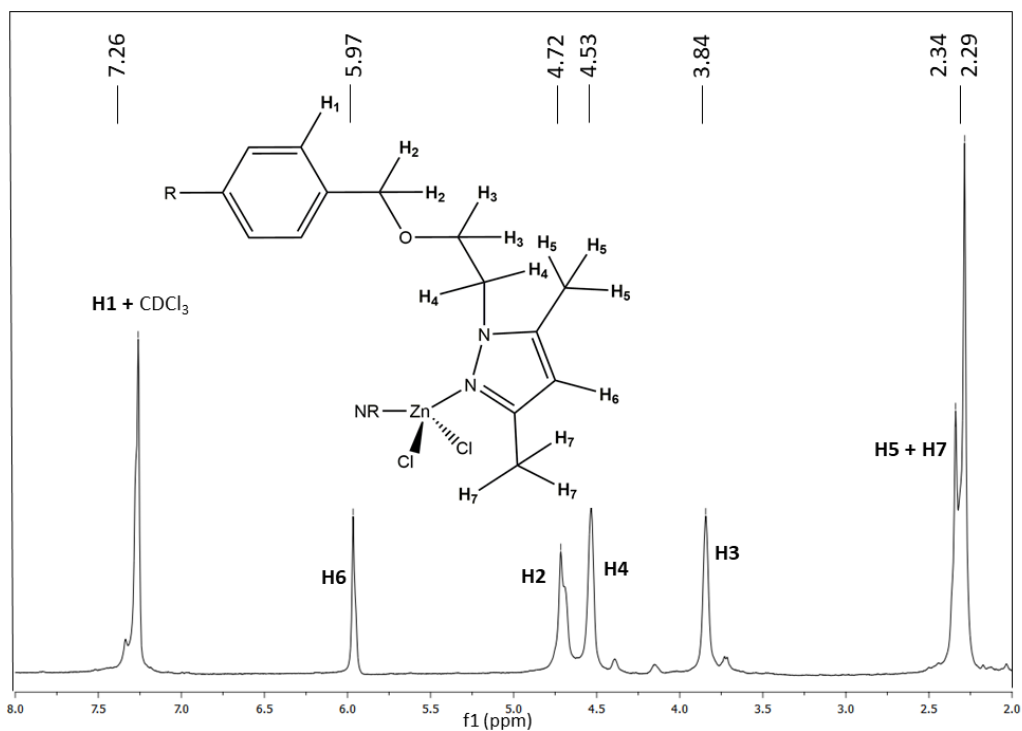


**Figure S24.**  $^1\text{H}$  NMR spectrum of **1** (400 MHz,  $\text{CDCl}_3$ )

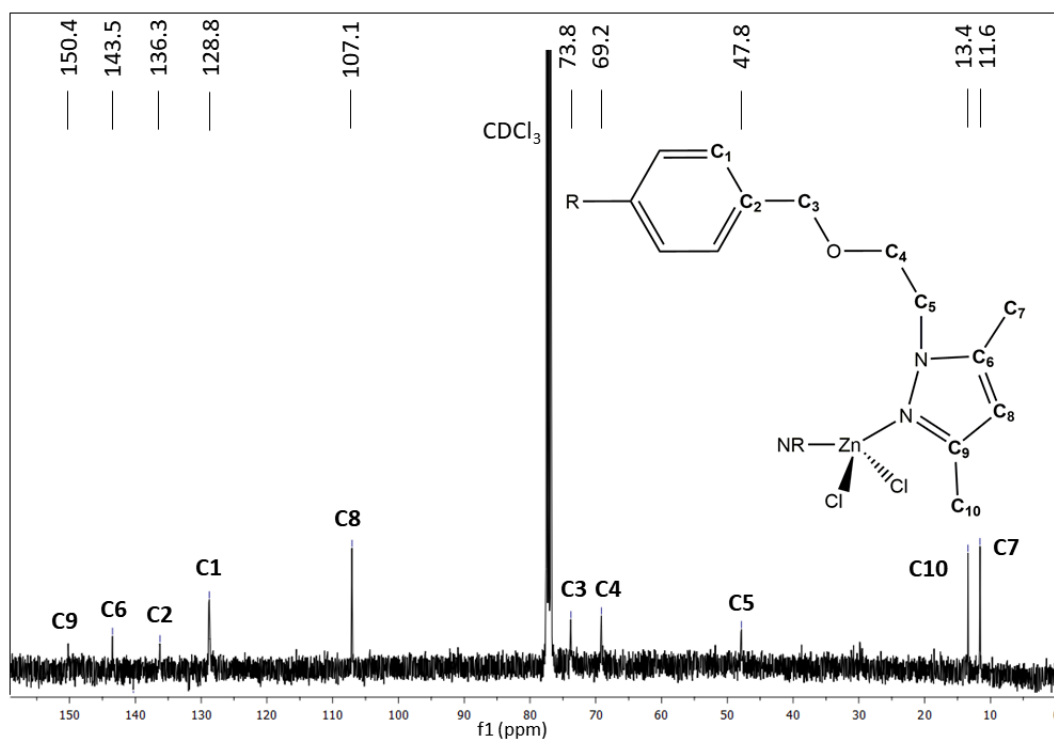


**Figure S25.**  $^{13}\text{C}\{^1\text{H}\}$  NMR spectrum of **1** (100.6 MHz,  $\text{CDCl}_3$ )

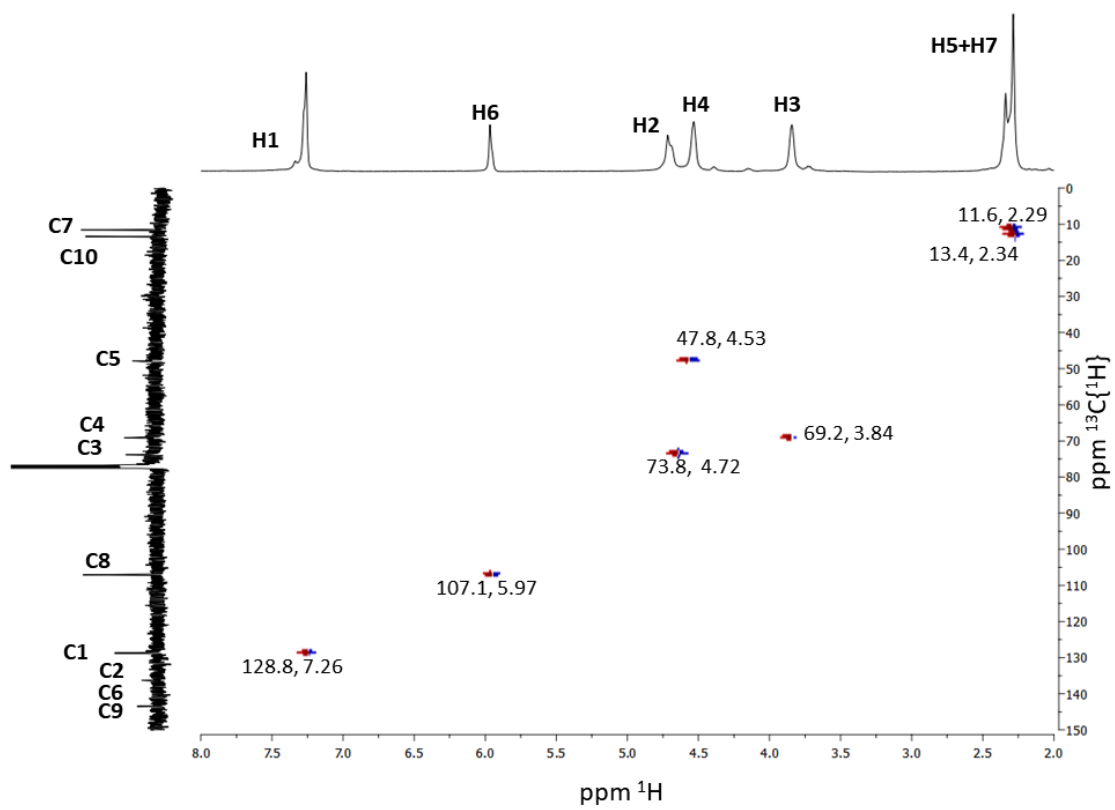


Figure S26. HSQC NMR spectrum of 1 (400 MHz,  $\text{CDCl}_3$ )

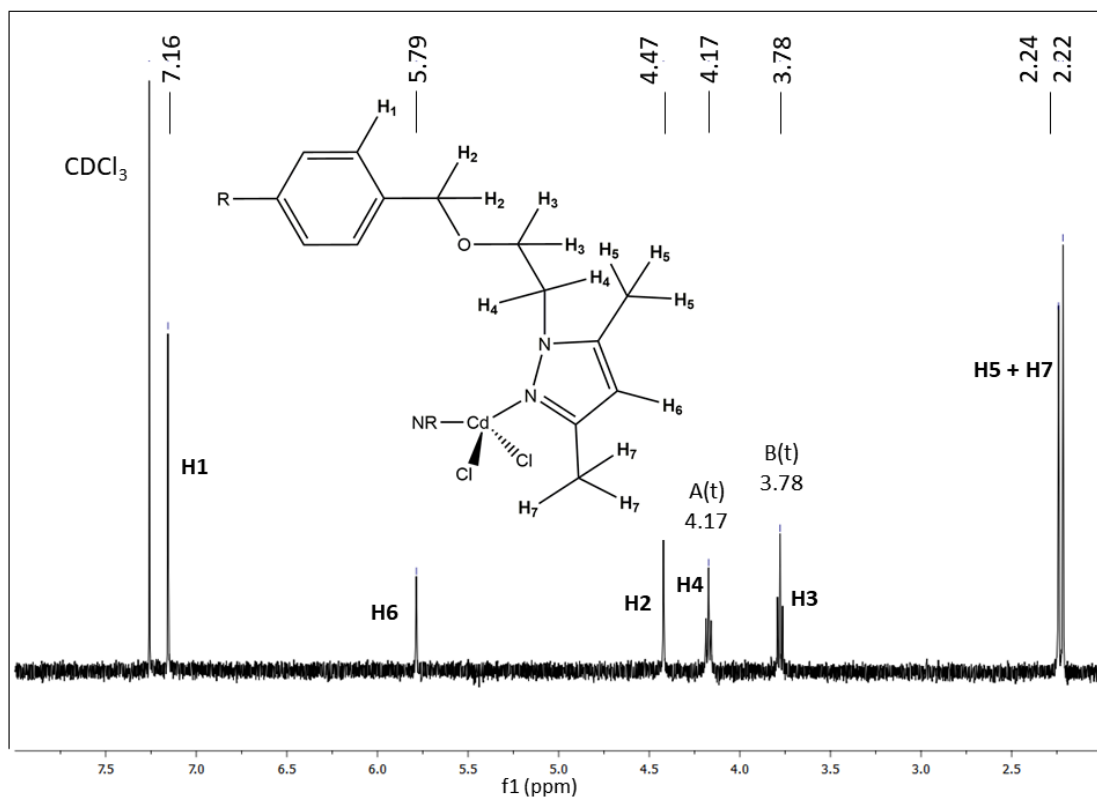


Figure S27.  $^1\text{H}$  NMR spectrum of **2** (400 MHz,  $\text{CDCl}_3$ )

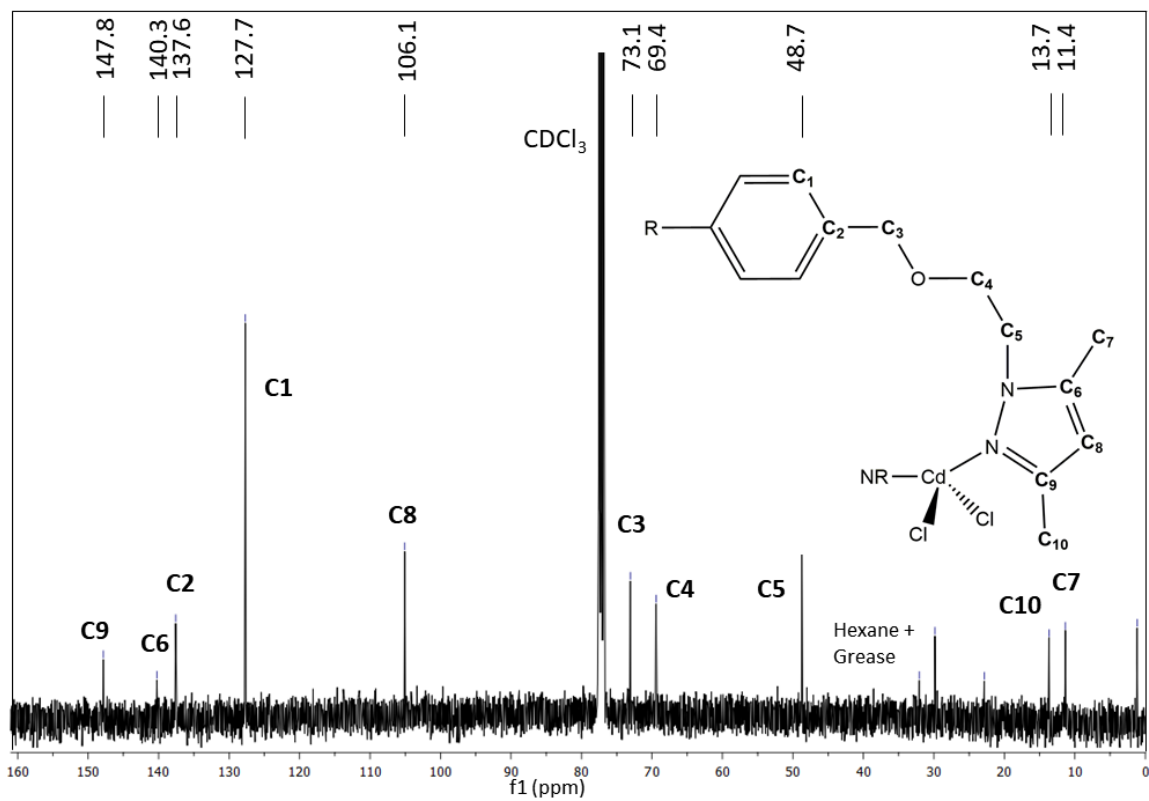


Figure S28.  $^{13}\text{C}\{^1\text{H}\}$  NMR spectrum of **2** (100.6 MHz,  $\text{CDCl}_3$ )

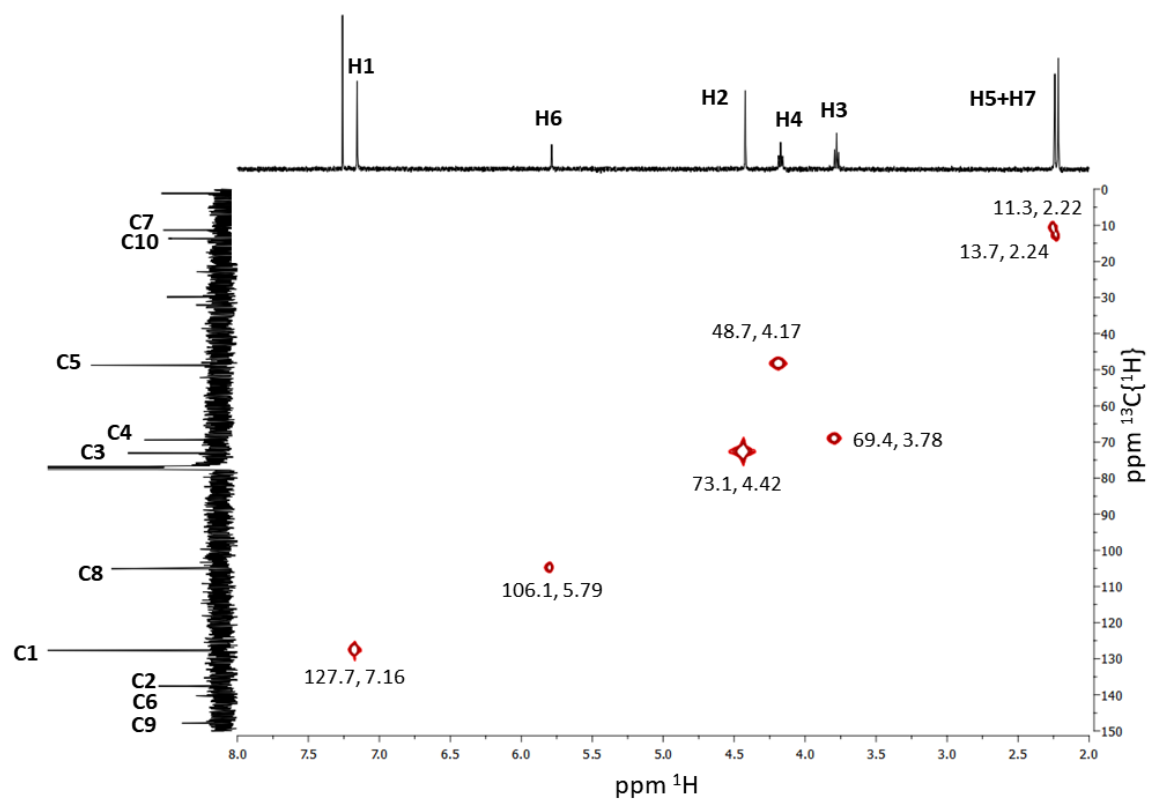
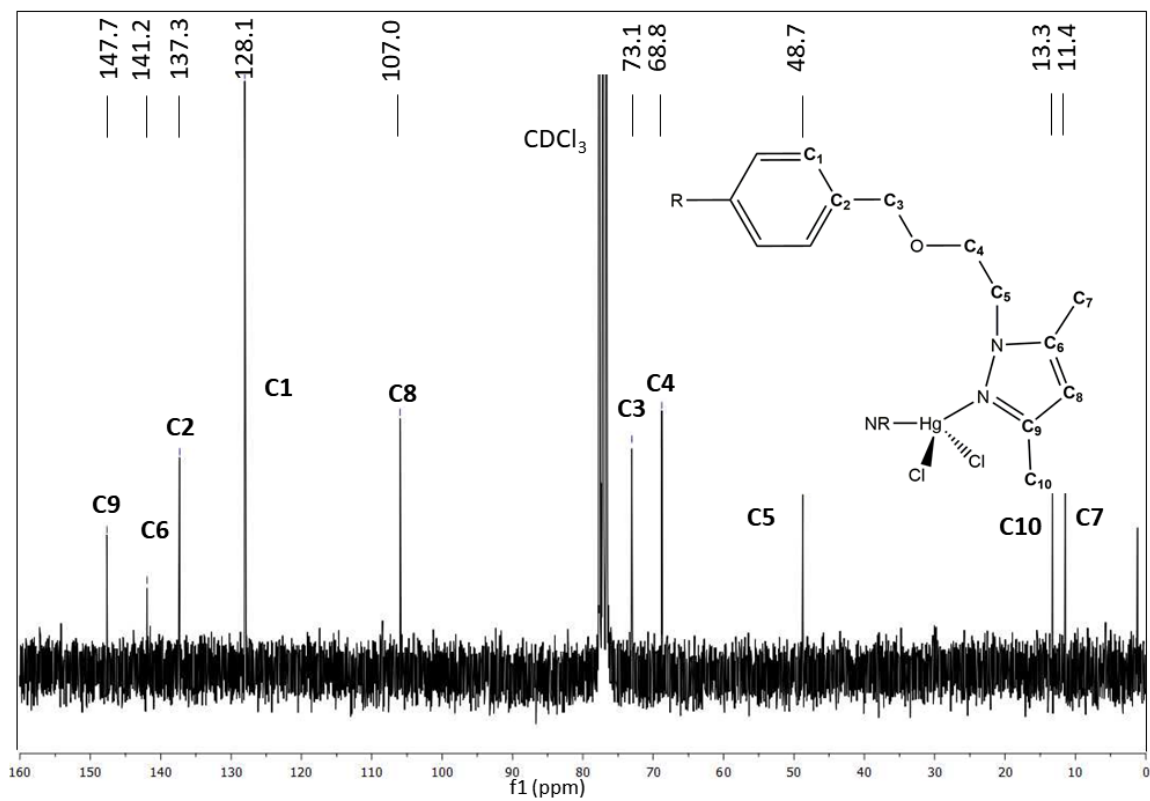
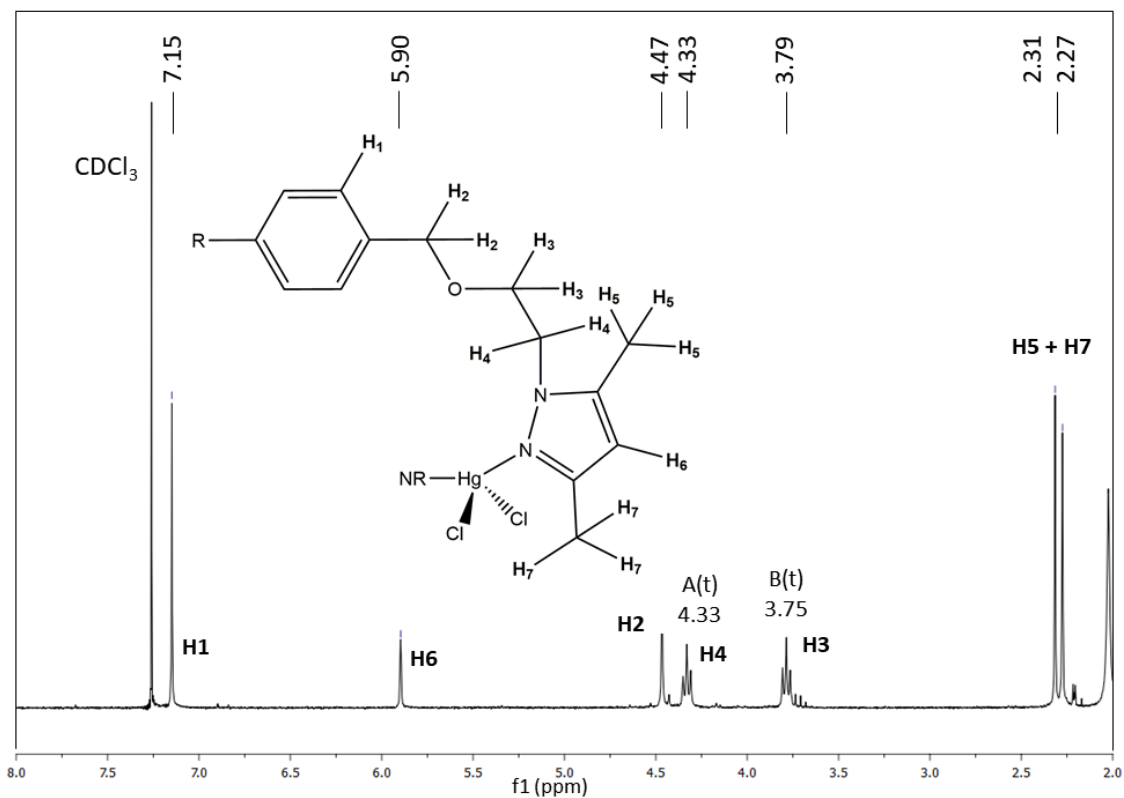
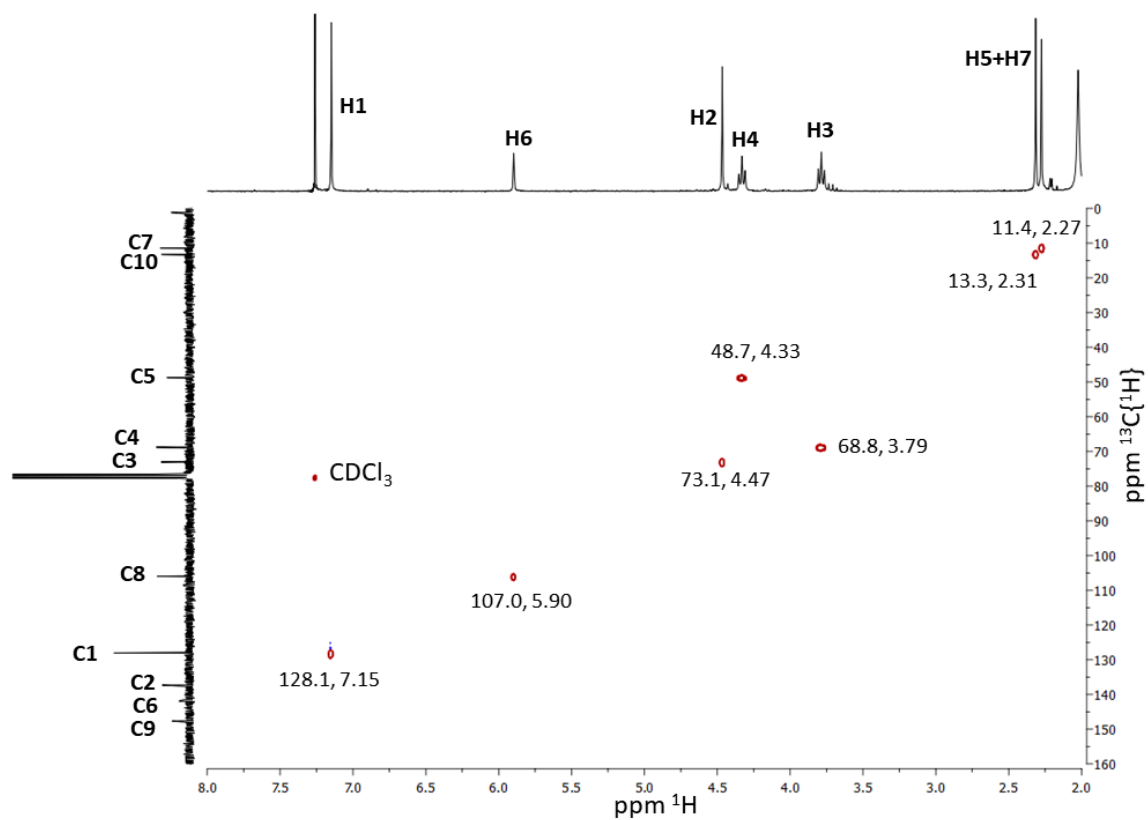


Figure S29. HSQC NMR spectrum of **2** (400 MHz,  $\text{CDCl}_3$ )







**Figure S32.** HSQC NMR spectrum of **3** (400 MHz, CDCl<sub>3</sub>)

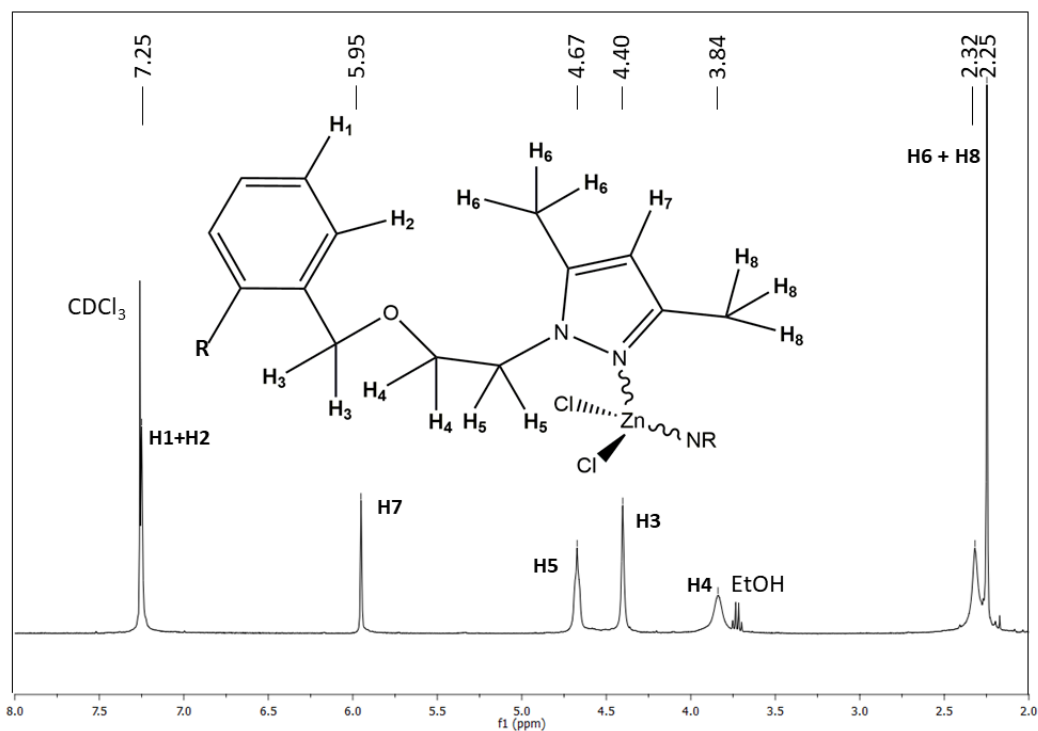


Figure S33.  $^1\text{H}$  NMR spectrum of **4** (400 MHz,  $\text{CDCl}_3$ )

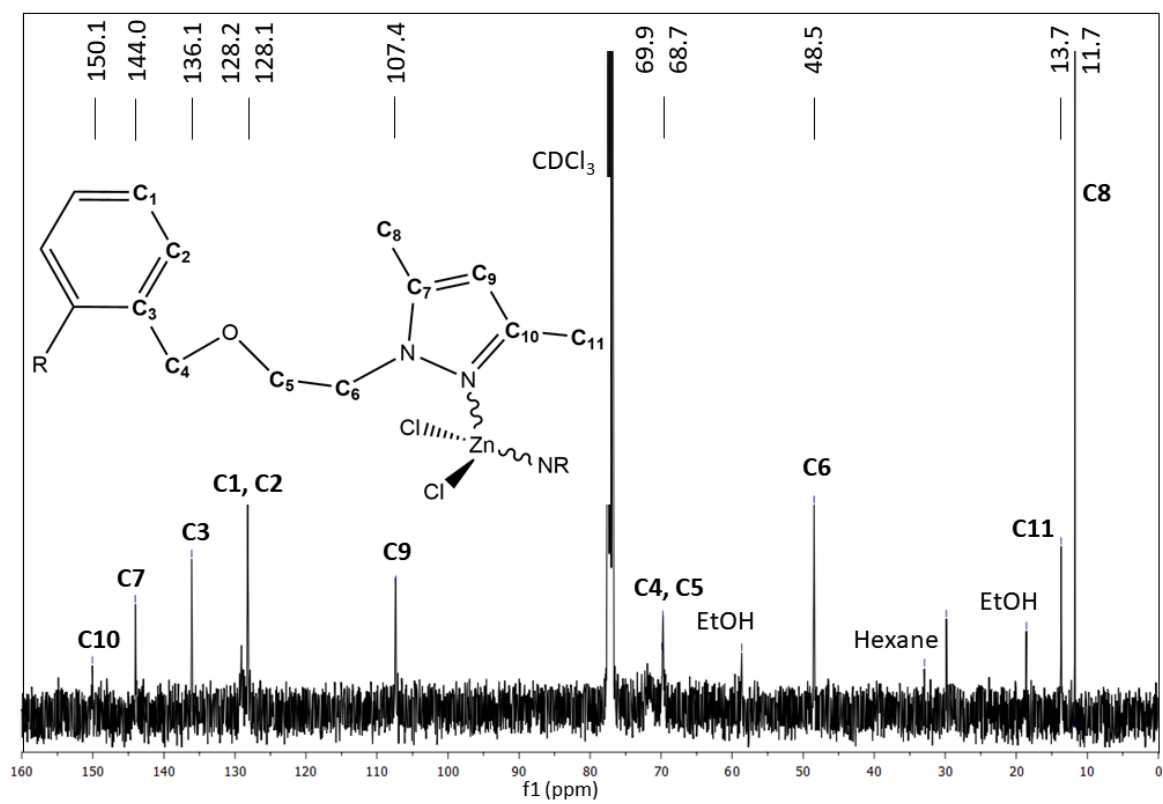


Figure S34.  $^{13}\text{C}\{^1\text{H}\}$  NMR spectrum of **4** (100.6 MHz,  $\text{CDCl}_3$ )

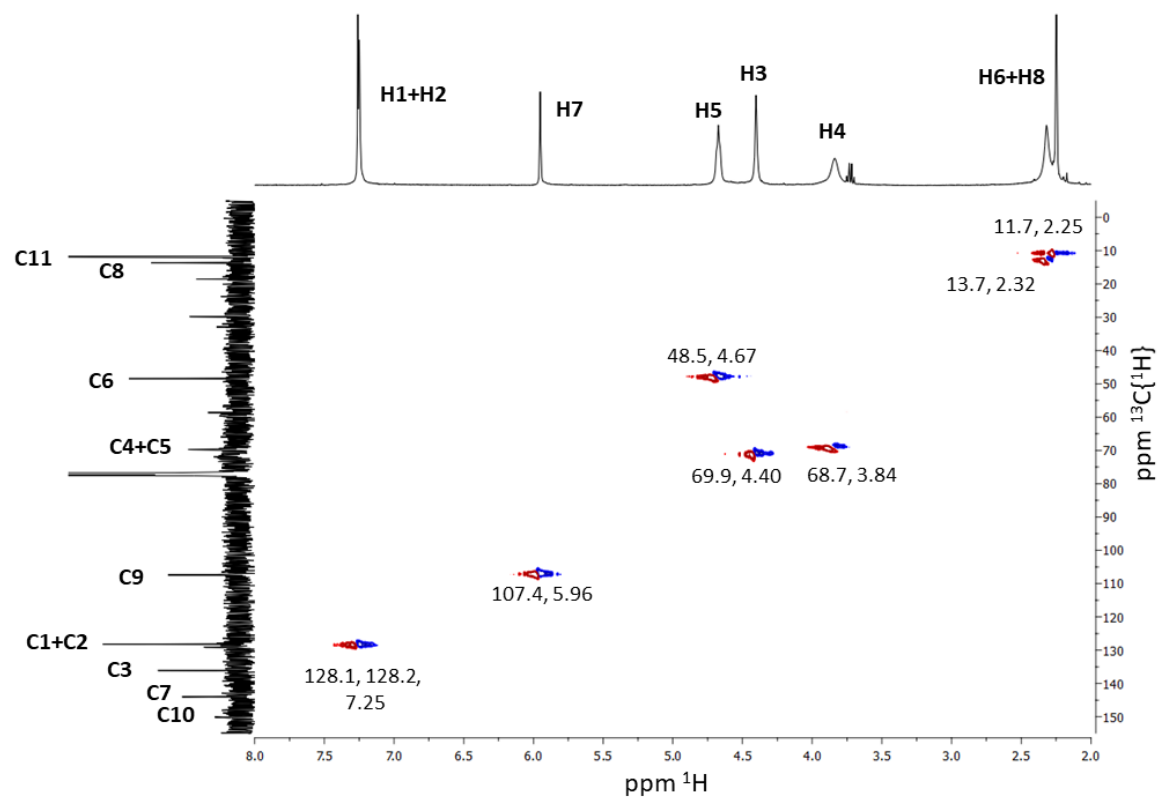


Figure S35. HSQC NMR spectrum of **4** (400 MHz,  $\text{CDCl}_3$ )

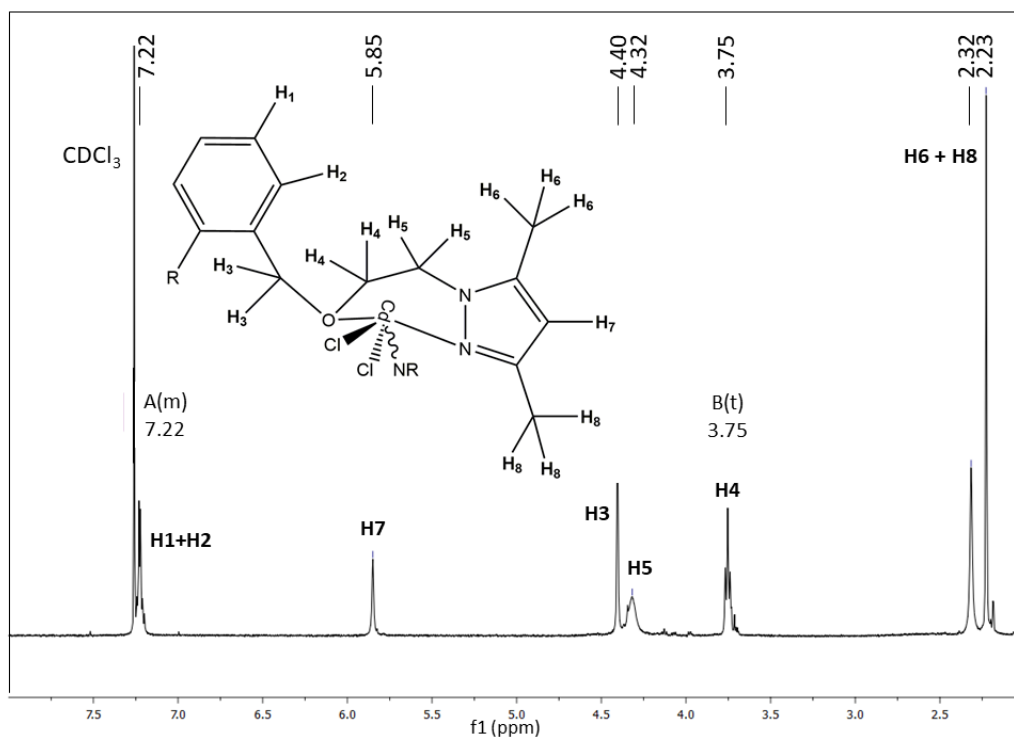


Figure S36.  $^1\text{H}$  NMR spectrum of **5** (400 MHz,  $\text{CDCl}_3$ )

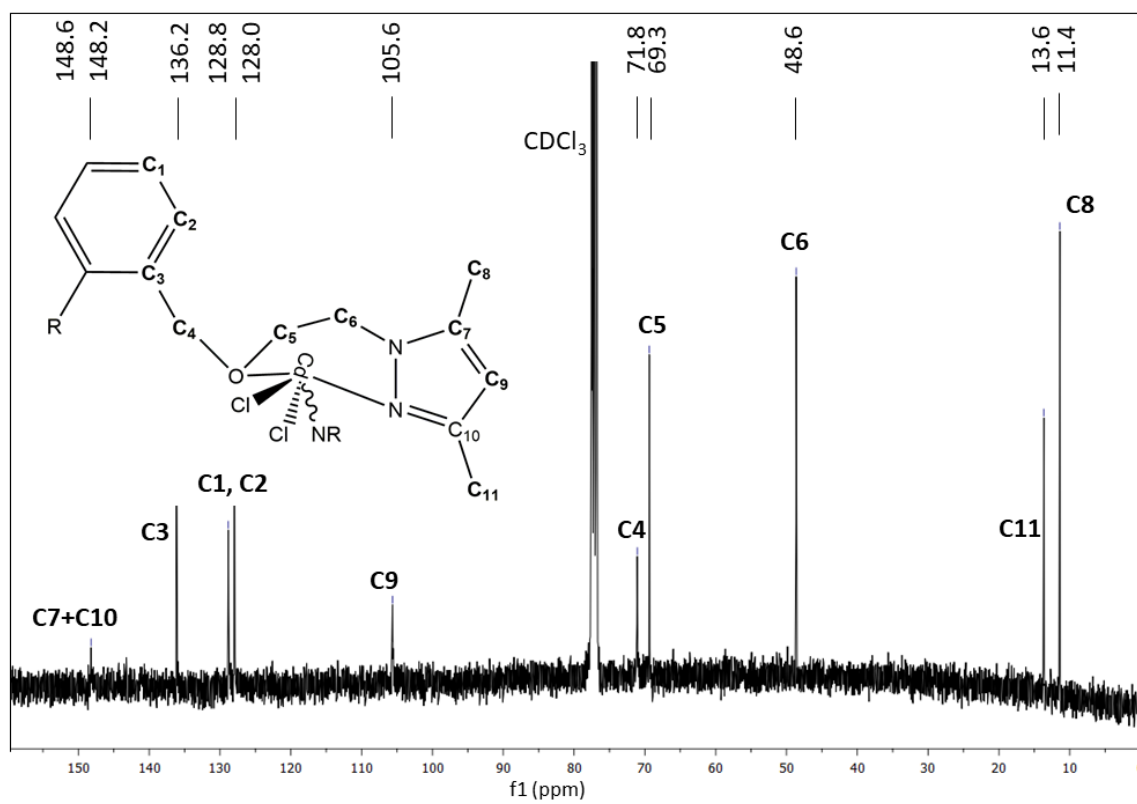
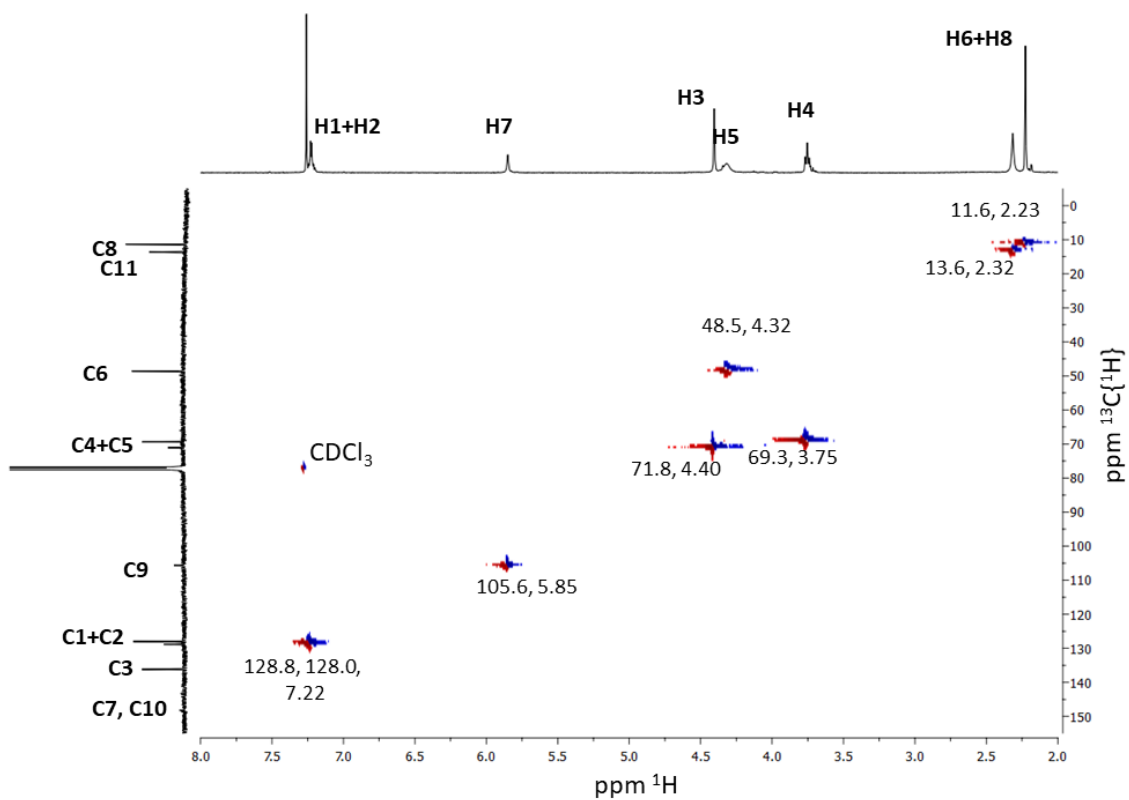


Figure S37.  $^{13}\text{C}\{^1\text{H}\}$  NMR spectrum of **5** (100.6 MHz,  $\text{CDCl}_3$ )



**Figure S38.** HSQC NMR spectrum of **5** (400 MHz, CDCl<sub>3</sub>)

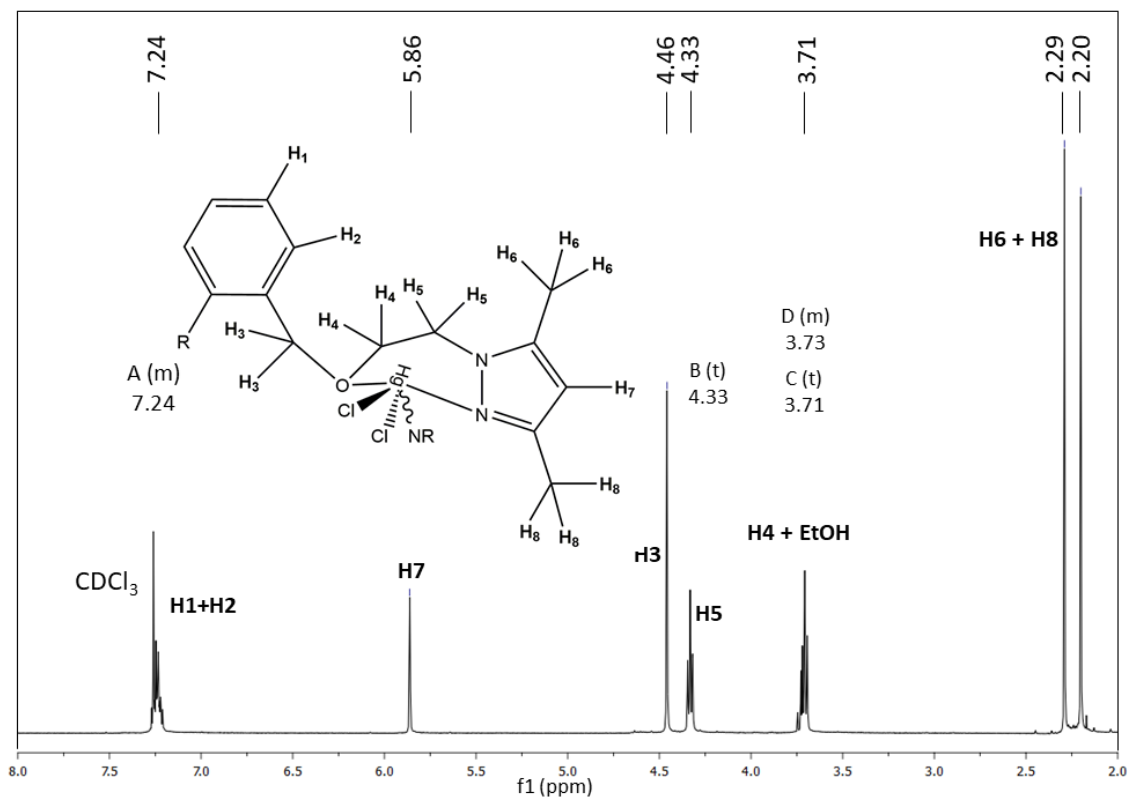


Figure S39.  $^1\text{H}$  NMR spectrum of **6** (400 MHz,  $\text{CDCl}_3$ )

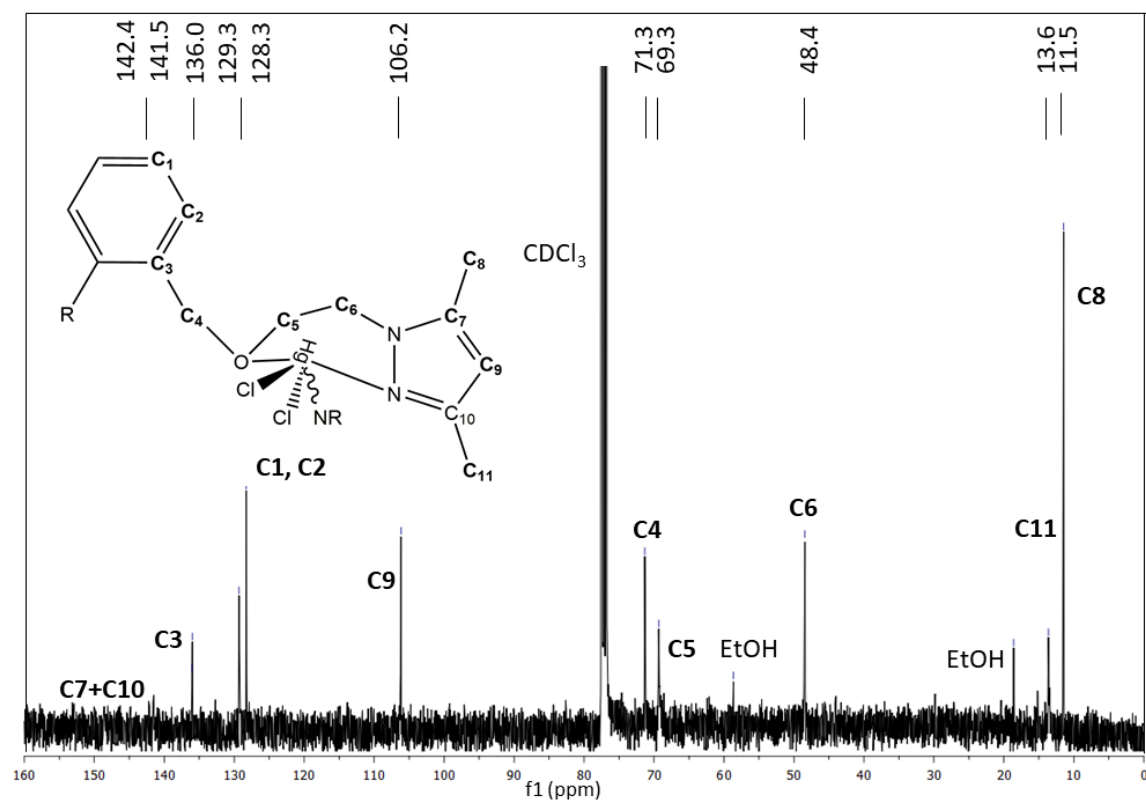
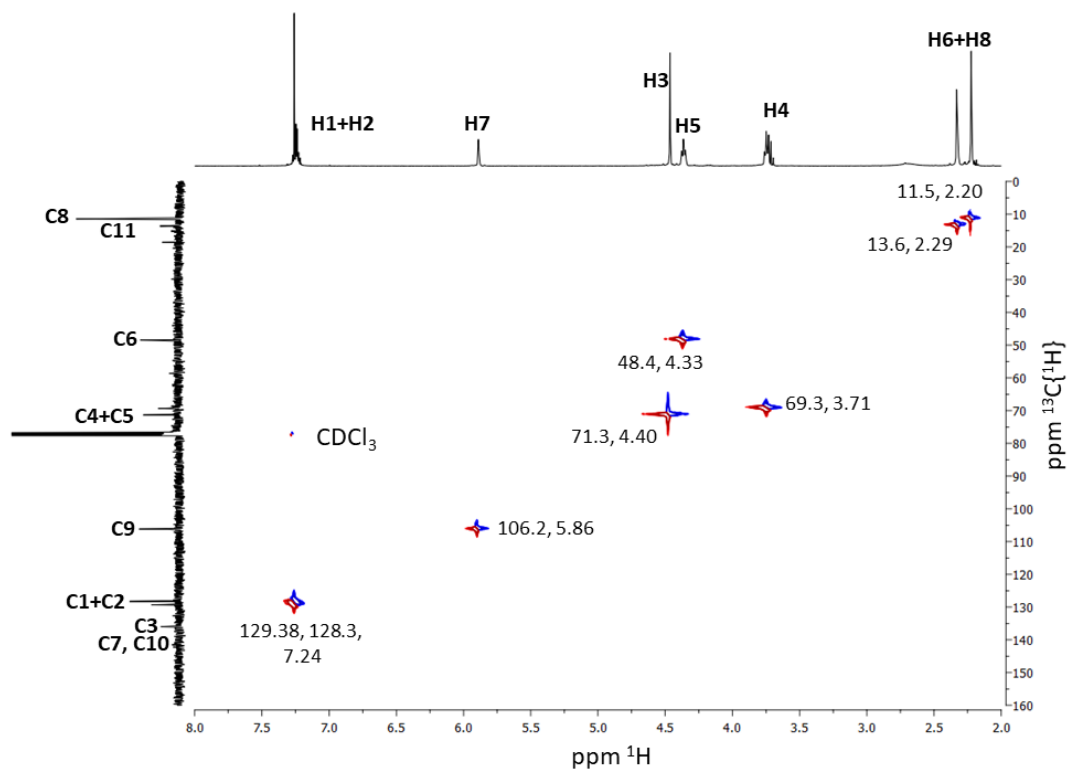
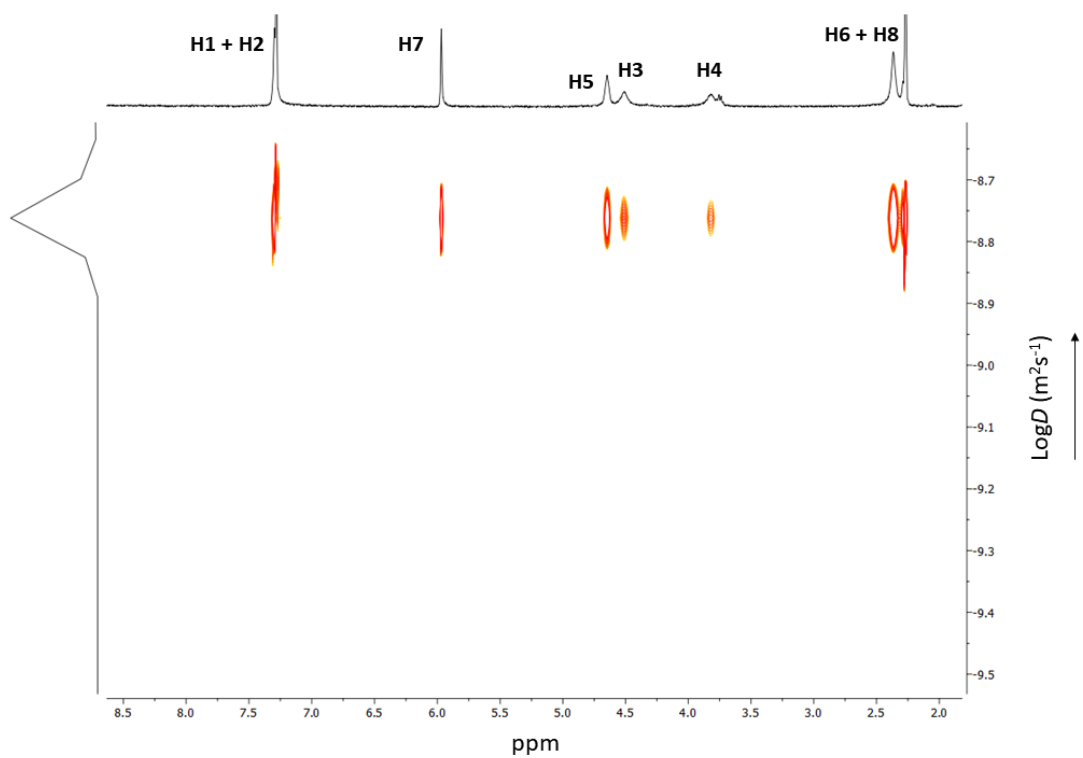


Figure S40.  $^{13}\text{C}\{^1\text{H}\}$  NMR spectrum of **6** (100.6 MHz,  $\text{CDCl}_3$ )



**Figure S41.** HSQC NMR spectrum of **6** (400 MHz,  $\text{CDCl}_3$ )





**Figure S42.** DOSY NMR spectrum of **4** (400 MHz,  $\text{CDCl}_3$ )

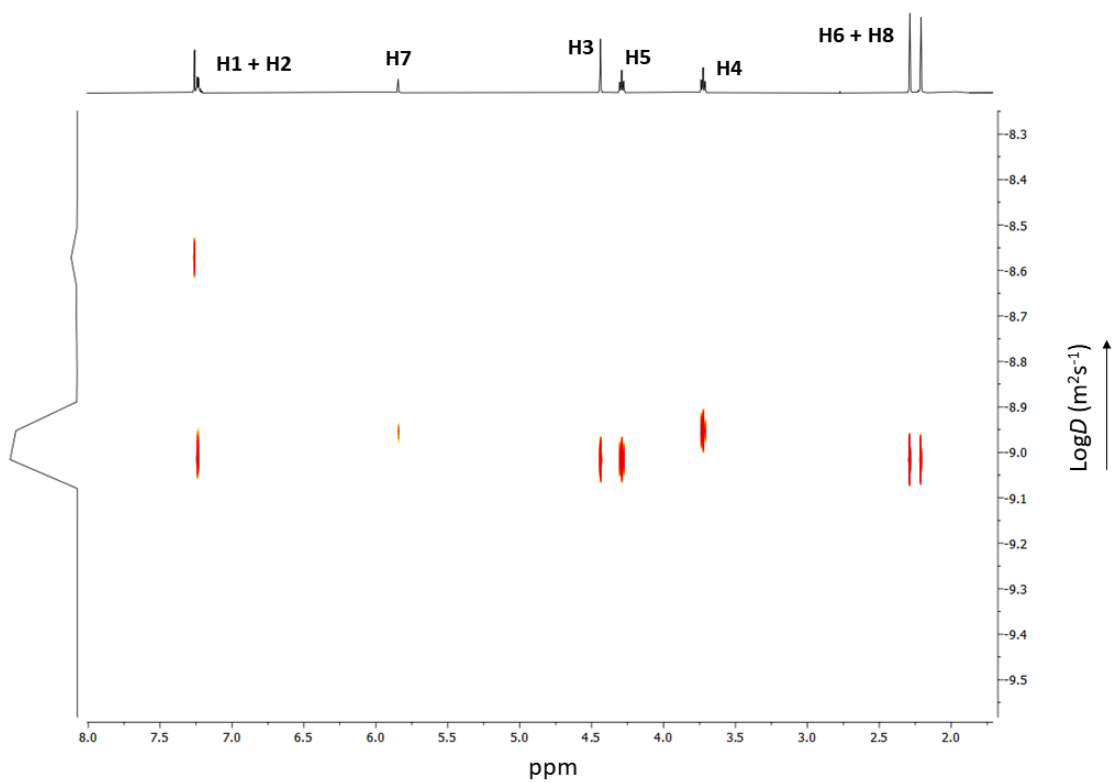


**Figure S43.** DOSY NMR spectrum of **6** (400 MHz,  $\text{CDCl}_3$ )

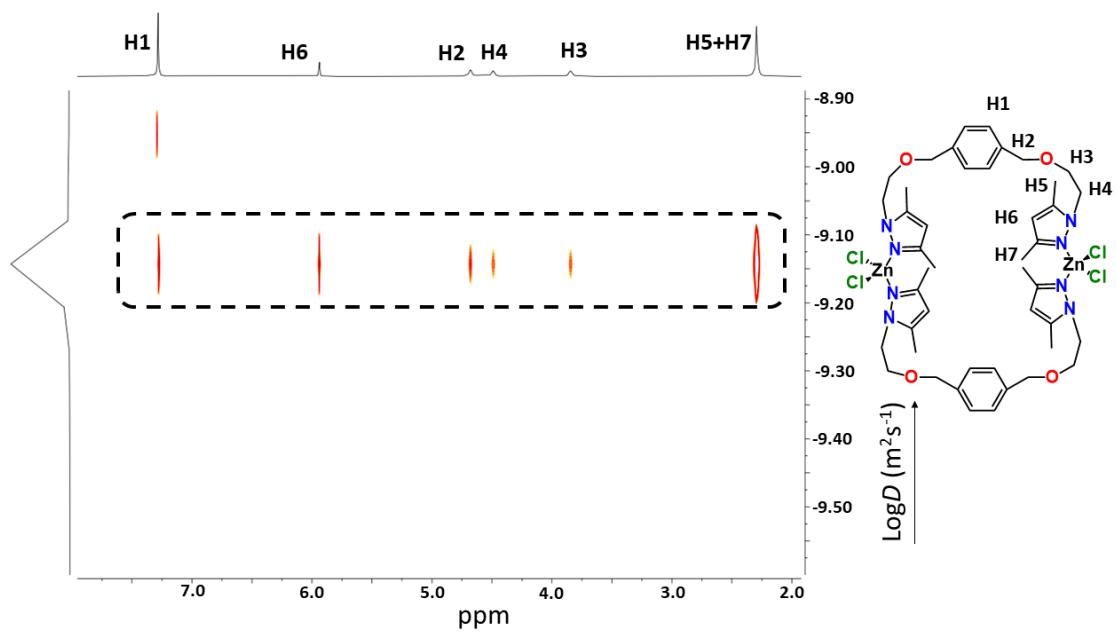


**Figure S44.** DOSY-NMR spectra of **1** (400 MHz,  $\text{CDCl}_3$ )

## UV-Vis Spectra

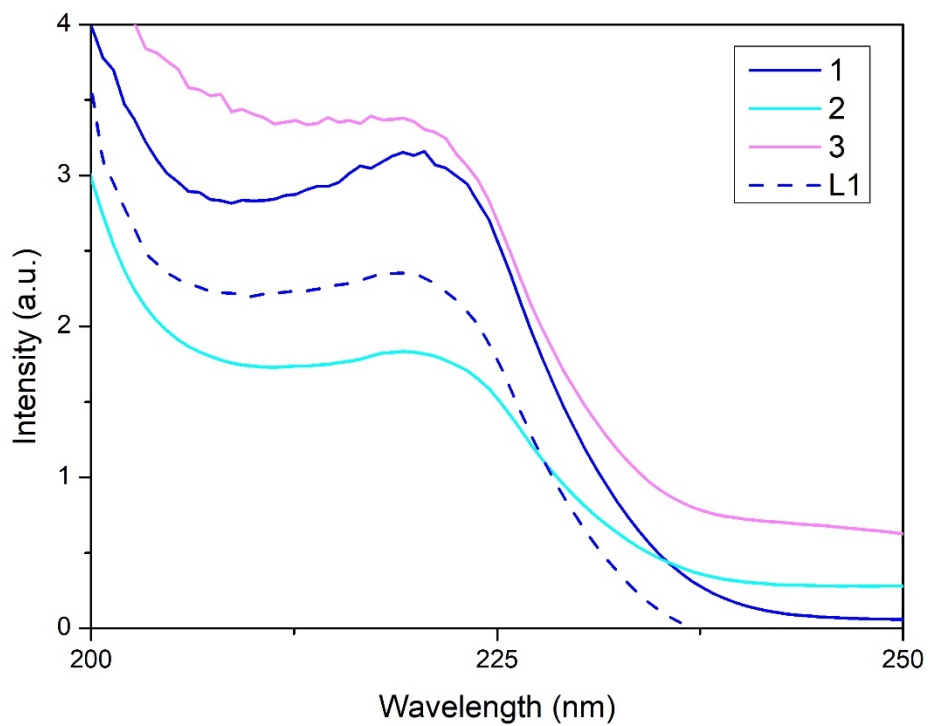


**Figure S45.** UV-Vis spectrum of L1 and 1-3 recorded in CH<sub>3</sub>CN at r.t.

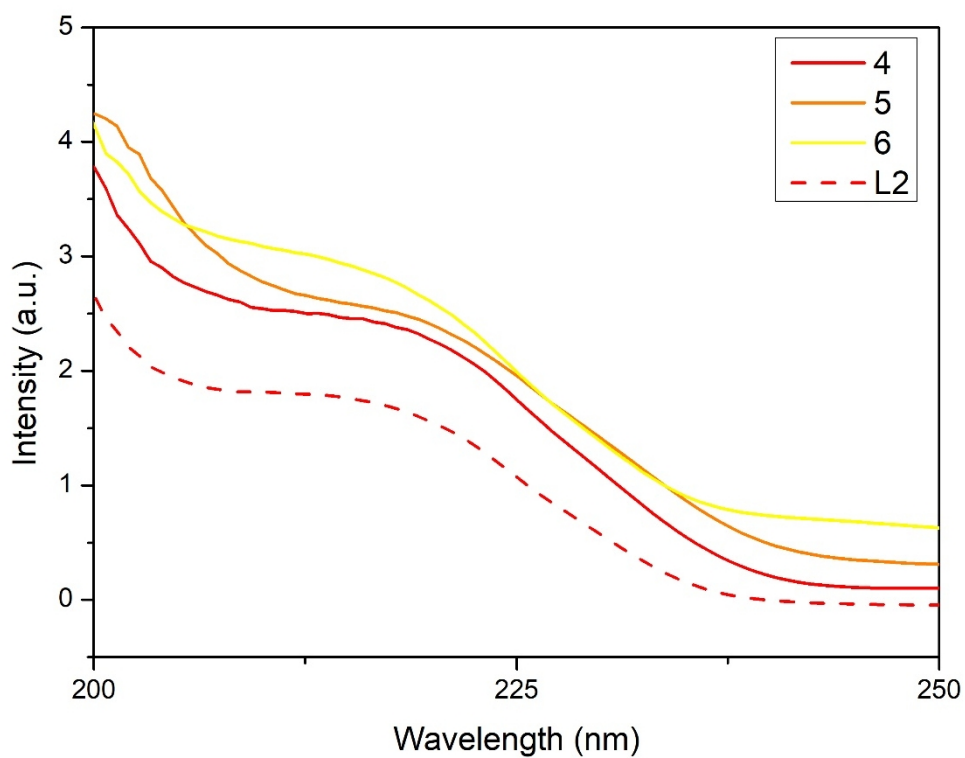


**Figure S46.** UV-Vis spectrum of L2 and 4-6 recorded in CH<sub>3</sub>CN at r.t.